

MICROCOPY RESOLUTION TEST CHART
NATIONAL BUREAU OF STANDARDS 1963-A

AFGL-TR-84-0239

2

AD-A156 062

POLARIZATION DIVERSITY ADDITION TO THE
10 CENTIMETER DOPPLER WEATHER RADAR

James S. Ussailis
Harold L. Bassett

Georgia Institute of Technology
Georgia Tech Research Institute
Atlanta, Georgia 30332

Final Report
1 April 1982 - 31 July 1984

August 1984

Approved for public release; distribution unlimited

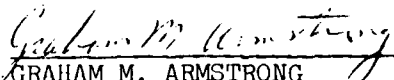
AIR FORCE GEOPHYSICS LABORATORY
AIR FORCE SYSTEMS COMMAND
UNITED STATES AIR FORCE
HANSCOM AFB, MASSACHUSETTS 01731

DTIC FILE COPY

DTIC
ELECTE
JUN 26 1985
S B D

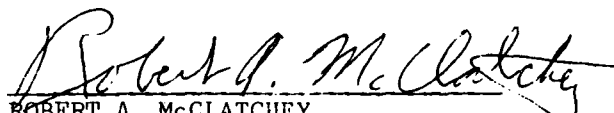
85 06 10 11 8

"This technical report has been reviewed and is approved for publication".


GRAHAM M. ARMSTRONG
Contract Manager


JAMES I. METCALF
Acting Chief, Ground Based Remote Sensing Branch
Atmospheric Sciences Division

FOR THE COMMANDER


ROBERT A. McCLATCHEY
Director, Atmospheric Sciences Division

This report has been reviewed by the ESD Public Affairs Office (PA) and is releasable to the National Technical Information Service (NTIS).

Qualified requestors may obtain additional copies from the Defense Technical Information Center. All others should apply to the National Technical Information Service.

If your address has changed, or if you wish to be removed from the mailing list, or if the addressee is no longer employed by your organization, please notify AFGL/DAA, Hanscom AFB, MA 01731. This will assist us in maintaining a current mailing list.

REPORT DOCUMENTATION PAGE

1a. REPORT SECURITY CLASSIFICATION UNCLASSIFIED		1b. RESTRICTIVE MARKINGS	
2a. SECURITY CLASSIFICATION AUTHORITY		3. DISTRIBUTION/AVAILABILITY OF REPORT Approved for public release; distribution unlimited	
2b. DECLASSIFICATION/DOWNGRADING SCHEDULE			
4. PERFORMING ORGANIZATION REPORT NUMBER(S) A-3226		5. MONITORING ORGANIZATION REPORT NUMBER(S) AFGL-TR-84-0239	
6a. NAME OF PERFORMING ORGANIZATION Georgia Institute of Technology Georgia Tech Research Institute		6b. OFFICE SYMBOL (If applicable) RAIL/MSD	7a. NAME OF MONITORING ORGANIZATION
6c. ADDRESS (City, State and ZIP Code) Atlanta, Georgia 30332		7b. ADDRESS (City, State and ZIP Code)	
8a. NAME OF FUNDING/SPONSORING ORGANIZATION Air Force Geophysics Laboratory	8b. OFFICE SYMBOL (If applicable) LYR	9. PROCUREMENT INSTRUMENT IDENTIFICATION NUMBER F19628-82-K-0038	
8c. ADDRESS (City, State and ZIP Code) HANSCOM AFB, MA 01731 Monitor/Graham Armstrong		10. SOURCE OF FUNDING NOS.	
		PROGRAM ELEMENT NO. 62101F	PROJECT NO. 6670
		TASK NO. 16	WORK UNIT NO. AA
11. TITLE (Include Security Classification) POLARIZATION DIVERSITY ADDITION TO THE 10 cm DOPPLER WEATHER RADAR (U)			
12. PERSONAL AUTHOR(S) USSAILIS, JAMES S. and BASSETT, HAROLD L.			
13a. TYPE OF REPORT Final Technical	13b. TIME COVERED FROM 4/1/82 TO 7/31/84	14. DATE OF REPORT (Yr., Mo., Day) AUGUST 1984	15. PAGE COUNT 80
16. SUPPLEMENTARY NOTATION Mr. J. S. USSAILIS IS NOW ASSOCIATED WITH THE MITRE CORPORATION.			
17. COSATI CODES		18. SUBJECT TERMS (Continue on reverse if necessary and identify by block number)	
FIELD	GROUP	SUB. GR.	POLARIZATION, WEATHER RADAR - ANTENNA TESTING
			POTTER HORN, POLARIZER UNIT, A.I.
19. ABSTRACT (Continue on reverse if necessary and identify by block number)			
<p>The research performed was that of providing antenna modifications for a polarization diversity addition to the AFGL 10 centimeter DOPPLER WEATHER RADAR. Described within are the ANTENNA FEED DESIGN (POTTER HORN), the conversion of the antenna from a prime focus to a Cassegrain Configuration, the results of the feed horn RF measurements, the construction of the POLARIZER ASSEMBLY, and the installation and testing of the antenna system.</p> <p><i>copy included</i></p>			
20. DISTRIBUTION/AVAILABILITY OF ABSTRACT UNCLASSIFIED/UNLIMITED <input type="checkbox"/> SAME AS RPT. <input type="checkbox"/> DTIC USERS <input type="checkbox"/>		21. ABSTRACT SECURITY CLASSIFICATION UNCLASSIFIED	
22a. NAME OF RESPONSIBLE INDIVIDUAL GRAHAM M. ARMSTRONG, AFGL/LYR		22b. TELEPHONE NUMBER (Include Area Code) (617) 861-4405	22c. OFFICE SYMBOL LYR

TABLE OF CONTENTS

<u>SECTION</u>	<u>TITLE</u>	<u>PAGE</u>
1	INTRODUCTION.....	1
2	RADAR MODIFICATION.....	2
2.1	Structural Analysis.....	2
2.2	Conversion to Cassegrain Configuration.....	2
2.3	Fabrication of a Huygens Source Feed.....	2
2.4	Polarizer Assembly.....	8
2.5	Installation.....	8
3	CONCLUSION.....	11
4	PERSONNEL.....	12
5	PREVIOUS CONTRACT AND PUBLICATION.....	13
6	PUBLICATIONS PARTIALLY SPONSORED BY THIS CONTRACT.....	14
7	REFERENCES.....	15
APPENDIX A		
	Paper Presented at 21st Conference on Radar Meteorology.....	46
APPENDIX B		
	Antenna Static and Dynamic Structural Analysis.....	55

Accession For	
NTIS GRA&I	<input checked="" type="checkbox"/>
DTIC TAB	<input type="checkbox"/>
Unannounced	<input type="checkbox"/>
Justification	
By _____	
Distribution/	
Availability Codes	
Dist	Avail and/or Special
A-1	

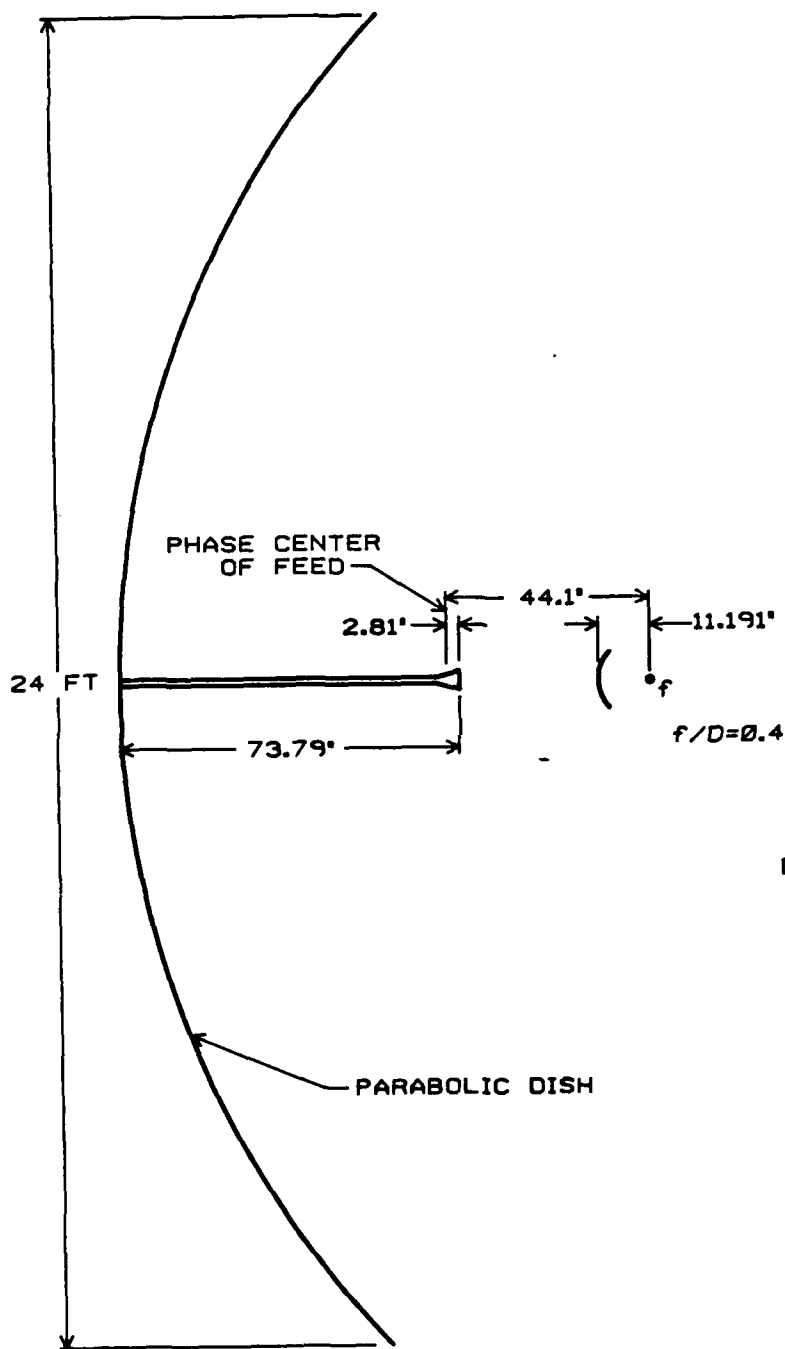


LIST OF ILLUSTRATIONS

<u>FIGURE</u>	<u>TITLE</u>	<u>PAGE</u>
1	H-plane pattern of scaled feed horn, $f = 9.1$ GHz.....	16
2	E-plane pattern of scaled feed horn, $f = 9.1$ GHz.....	17
3	H-plane pattern of scaled feed horn, $f = 9.2$ GHz.....	18
4	E-plane pattern of scaled feed horn, $f = 9.2$ GHz.....	19
5	H-plane pattern of scaled feed horn, $f = 9.3$ GHz.....	20
6	E-plane pattern of scaled feed horn, $f = 9.3$ GHz.....	21
7	H-plane pattern of scaled feed horn, $f = 9.4$ GHz.....	22
8	E-plane pattern of scaled feed horn, $f = 9.4$ GHz.....	23
9	H-plane pattern of scaled feed horn, $f = 9.5$ GHz.....	24
10	E-plane pattern of scaled feed horn, $f = 9.5$ GHz.....	25
11	E-plane pattern of full-size feed in final configuration, $f = 2.70$ GHz.....	26
12	H-plane pattern of full-size feed in final configuration, $f = 2.71$ GHz.....	27
13	E-plane pattern of full-size feed, $f = 2.71$ GHz.....	28
14	E-plane pattern of full-size feed, $f = 2.72$ GHz.....	29
15	E-plane pattern of full-size feed, $f = 2.73$ GHz.....	30
16	E-plane pattern of full-size feed, $f = 2.74$ GHz.....	31
17	E-plane pattern of full-size feed, $f = 2.75$ GHz.....	32
18	E-plane pattern of full-size feed, $f = 2.76$ GHz.....	33
19	E-plane pattern of full-size feed, $f = 2.77$ GHz.....	34
20	E-plane pattern of full-size feed, $f = 2.78$ GHz.....	35
21	E-plane pattern of full-size feed, $f = 2.79$ GHz.....	36
22	E-plane pattern of full-size feed, $f = 2.80$ GHz.....	37
23	VSWR of rectangular-to-circular transition with circular load attached.....	38
24	Normalized impedance of feed horn and of polarizer at 2710 MHz.....	39
25	Input VSWR of polarizer with horn attached to circular port and load attached to unused input.....	40
26	Schematic representation of circular/linear switchable antenna polarizer.....	41
27	Rear mechanical detail of antenna polarizer.....	42
28	VSWR of modified AFGL antenna showing effect of 1-inch diameter VSWR reduction button.....	43
29	VSWR of modified AFGL antenna showing effect of post and disk VSWR reduction method.....	44
30	VSWR of modified AFGL antenna showing effect of differing post length.....	45

LIST OF TABLES

<u>TABLE</u>	<u>TITLE</u>	<u>PAGE</u>
1	Slotted Line Peak and Null Position Data.....	5
2	VSWR of Horn and Transition.....	6
3	VSWR of Polarizer and Transition (Ports Terminated with Matched Loads).....	7



DIAMETER OF SECONDARY REFLECTOR = 2.0 ft.

Positions of feed horn, phase center of feed, and subreflector.

SECTION 1
INTRODUCTION

The objective of this research program was to provide antenna modifications for a polarization diversifying addition to the AFGL 10 cm Doppler weather radar.

This addition, together with a subsequent receiver addition, will allow measurement of the coherent linear or circular monostatic scattering matrix of meteorological phenomena. The observations provided by the modified radar will allow for more direct (rather than inferred) measurement of these phenomena than has been heretofore possible. Examples of these additional observations include measurement of mean particle size, mean particle shape, and thermodynamic phase. The purpose of this report is to discuss the actual antenna modification; the interested reader should review References [1] and [2] to gain insight into the radar measurables as well as the specifications required to attain a reasonable measurement accuracy. Reference [2] is included as Appendix A.

In Section 2 the radar modifications and the installation of the feed horn and associated microwave circuitry are discussed. A conclusion is drawn in Section 3.

SECTION 2
RADAR MODIFICATIONS

2.1 STRUCTURAL ANALYSIS

A structural analysis of the existing reflector together with the proposed subreflector, support span assembly, feed support assembly, and feed horn was performed by Mr. T. Walsh, P.E., of H & W Industries, Inc., Cohasset, Mass. This effort, consisting of both static and dynamic analyses, determined the distortional effects of dead weight, seasonal thermal changes, wind distortion, and inertial loading. The results of these analyses are included as Appendix B.

2.2 CONVERSION TO CASSEGRAIN CONFIGURATION

The antenna was converted from a prime focus configuration to a Cassegrain configuration. This conversion extended the focal length to diameter ratio (f/D) of the main reflector and thus reduced the anticipated linear cross-polarization to acceptable levels. The conversion was accomplished by adding a subreflector and feed support assembly. The existing tripod feed support was replaced with a relocated quadrapod support, not only to provide sufficient latitude to adjust the subreflector, but also to ensure a reduction of both circular and linear cross-polarized levels. The design and fabrication of these items, including the subreflector, was provided by H & W Industries under a Georgia Tech subcontract.

2.3 FABRICATION OF A HUYGENS SOURCE FEED

A Huygens source feed which radiates equal amplitude, TE_{11} and TM_{11} circular waveguide modes (also known as the hybrid or HE_{11} mode) will theoretically induce no cross-polarization when properly illuminating a reflector antenna. All non-Huygens source feeds, including dipoles, magnetic dipoles (slots), and crossed dipoles, will produce off-axis cross-polarization from the reflector. This is true for both linearly and circularly polarized systems.

A few antennas will generate the HE_{11} mode. On this project both a corrugated horn and a multitaper or Potter horn were considered. The Potter horn was chosen on the basis of cost. Because of a lack of design data in the literature, it was decided to construct a scaled feed operating at 9.4 GHz before proceeding with a full sized S-band feed. Five iterations of various tapers and phasing sections were constructed before the final configuration was fabricated. This feed exhibited equal E- and H-plane patterns over a 60-degree angular extent at 9.4 GHz. By symmetry of its circular aperture, it can be said to constitute a Huygens source within this angular domain. Figures 1 through 10 show that it is a functional design from 9.2 to 9.5 GHz and that it is marginally functional at 9.1 GHz.

The dimensions of the successful 9.4 GHz feed were then scaled to 2.735 GHz, the mid-band operating frequency of the radar. Fabrication of the full size feed proceeded with a different mechanical technology; rather than machine a full size horn from a large cylinder of aluminium, the various sections were rolled from thick aluminum stock and machined. This provided a lighter weight, lower cost structure and allowed for modification. This latter benefit was fortunate since the initial full size model did not provide equal E- and H-plane patterns over a reasonable extent, nor did it have a sufficiently low VSWR ($< 1.02:1$) for circular polarimetric operation.

An attempt was made to understand equalization of the patterns by extending the horn's phasing section in three incremental steps of 1/2 inch. This also had little effect on performance. Finally, after an analysis of the unit's characteristics, a front phasing section was added which succeeded in providing equal E- and H-plane patterns at 2.71 GHz. E-plane pattern measurements were recorded from 2.70 to 2.80 GHz for future reference (Figures 11 and 13 through 22). The H-plane pattern at 2.71 GHz is shown in Figure 12, for comparison with Figure 13.

While initial VSWR measurements were undertaken at this time, final VSWR measurements were accomplished during installation. Initially the VSWR of the final feed horn was unacceptably high. An attempt was made to reduce the reflections by use of an iris, but it was decided to limit the effort in this area since the significant VSWR specification was applicable only at the polarizer-horn junction and not between the test equipment-horn junction. VSWR measurements were performed with various sized irises placed between the feed horn and rectangular waveguide to circular waveguide transition. Minimum VSWR was attained with a 2.60 inch iris.

During component installation on the reflector in Sudbury, Mass., the feed VSWR measurements were repeated. This was done to re-establish horn baseline data to: (1) show that no damage occurred in transit from Atlanta and (2) to complete the data package. The following paragraphs summarize the entire set of measurements.

- A. The loss of the rectangular to circular transition was measured so that the actual VSWR at the horn could be determined. The loss was determined by placing a short circuit at the input and then at the output of the transition and by measuring the return loss. The transition was found to have 1.0 dB two-way loss which implies a 0.5 dB one-way loss.
- B. VSWR of the transition was measured. These measurements depended on the reflection from Atlantic Microwave circular load which was attached to the transition. One cannot separate or isolate these reflections from the data. The data may not be useful, but are presented in Figure 23.
- C. Peak and null measurements were made by using a short circuit on a slotted line and a short circuit on a slotted line plus the rectangular to circular transition. These data may be utilized with following measurements to determine the complex value of reflection coefficient. The data are presented as Table 1.
- D. Horn and transition VSWR measurements were made to not only ensure that no electrical damage occurred to the feed horn during shipment but also to acquire complex reflection coefficient data so a scientific approach to VSWR reduction could be performed. The data are presented in Table 2.
- E. VSWR of the polarizer and transition assembly was measured. Only a few data points were taken with this combination to ensure a reasonable conjugate match between the polarizer and horn. The remainder of the data requires completion of the polarizer. These data are required before installation so that the best possible match can be ensured. The available data are presented in Table 3 while the match with the tuning screws in the optimum position is shown in Figure 24. The Smith chart shows the reasonableness of the match between the polarizer and horn. The final match can be improved, but required the final polarizer configuration.
- F. VSWR measurements of the horn plus the polarizer were made with the opposite polarizer port terminated (Figure 25). These measurements established that the horn reasonably matched the incomplete polarizer. The addition of the tuning screws improves the junction match sufficiently to be better than the requirement at 2710 MHz.

TABLE 1. SLOTTED LINE PEAK AND NULL POSITION DATA

FREQUENCY MHz	SLOTTED SECTION		SLOTTED SECTION & TRANSITION	
	PEAK POSITION cm	NULL POSITION cm	PEAK POSITION cm	NULL POSITION cm
2670	13.39	8.97	14.66	10.20
2675	13.30	8.90	14.34	9.90
2680	13.37	8.88	13.96	9.55
2685	13.23	8.77	13.69	9.23
2690	13.14	8.75	13.14	8.95
2695	13.04	8.71	12.87	8.62
2700	13.06	8.75	12.63	8.33
2705	13.04	8.66	12.23	8.05
2710	12.97	8.64	12.15	7.69
2715	12.78	8.60	11.90	7.40
2720	12.67	8.58	11.44	7.14
2725	12.77	8.50	11.02	6.83
2730	12.73	8.44	10.90	6.50
2735	12.46	8.44	10.54	6.20
2740	12.53	8.42	10.19	5.88
2745	12.43	8.36	9.96	5.64
2750	12.41	8.35	9.50	5.35
2755	12.32	8.33	9.05	13.30
2760	12.38	8.22	8.89	12.97
2765	12.48	8.30	8.74	12.72
2770	12.14	8.18	8.42	12.43
2775	12.20	8.21	7.90	12.05
2780	12.20	8.19	7.69	11.81
2785	12.20	8.10	7.45	11.45
2790	11.95	8.09	7.10	11.20
2795	11.87	8.00	6.94	10.98
2800	11.83	7.95	6.53	10.49

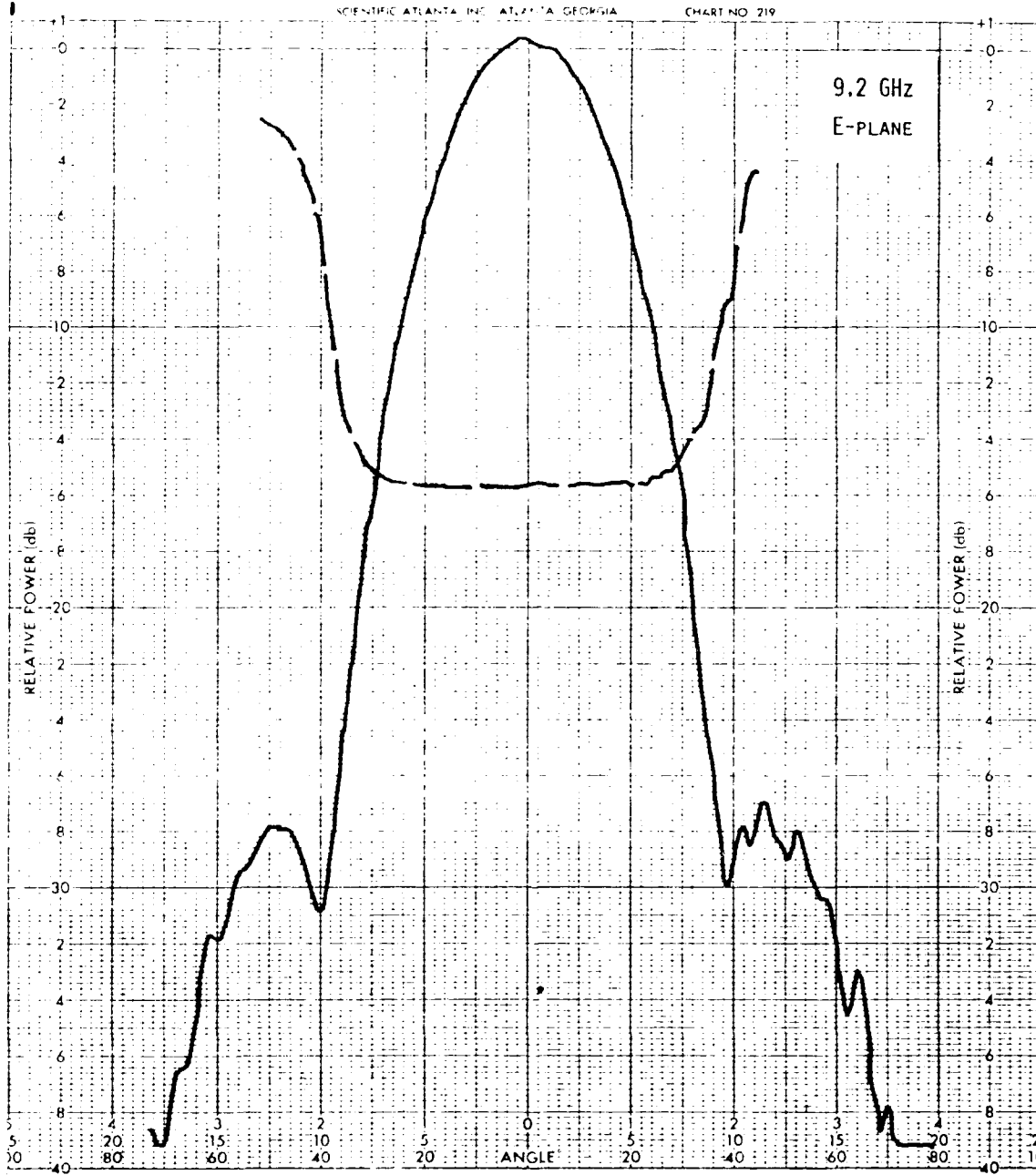


Fig. 10. E-plane pattern of scaled feed horn, $f = 9.2$ GHz

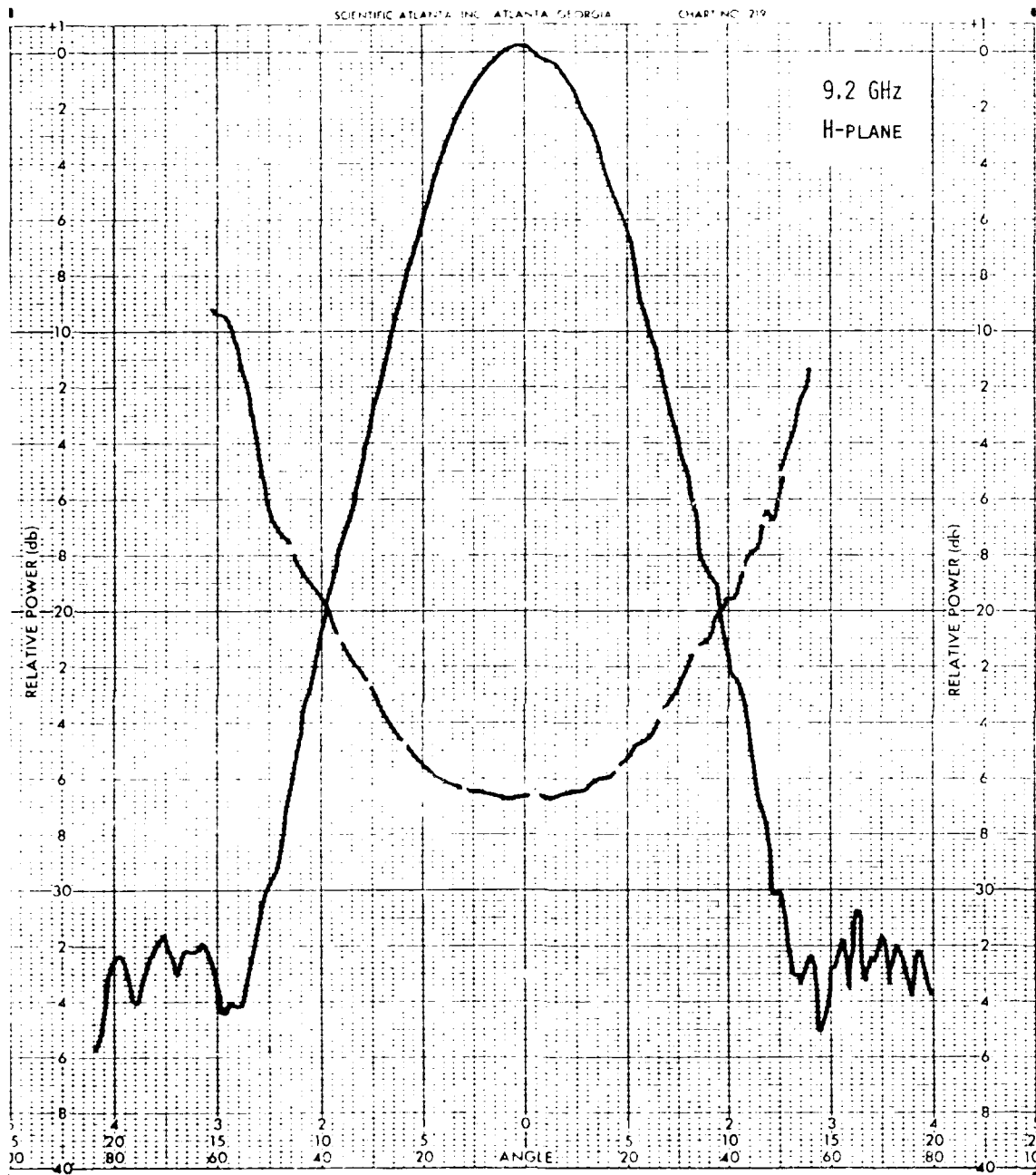


Figure 3. H-plane pattern of antenna feed horn, $f = 9.2$ GHz

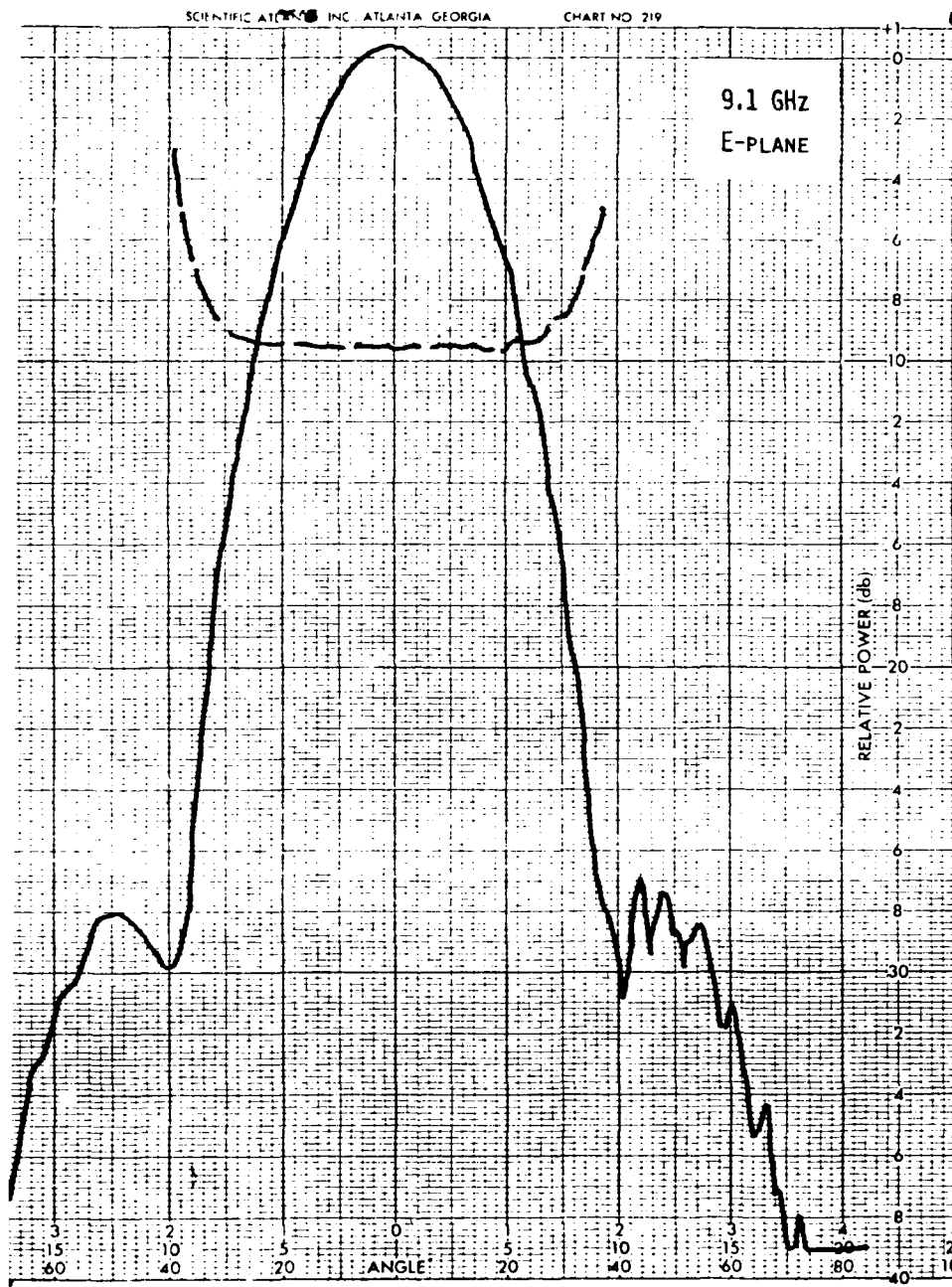


Figure 2. E-plane pattern of scaled feed horn, $f = 9.1$ GHz

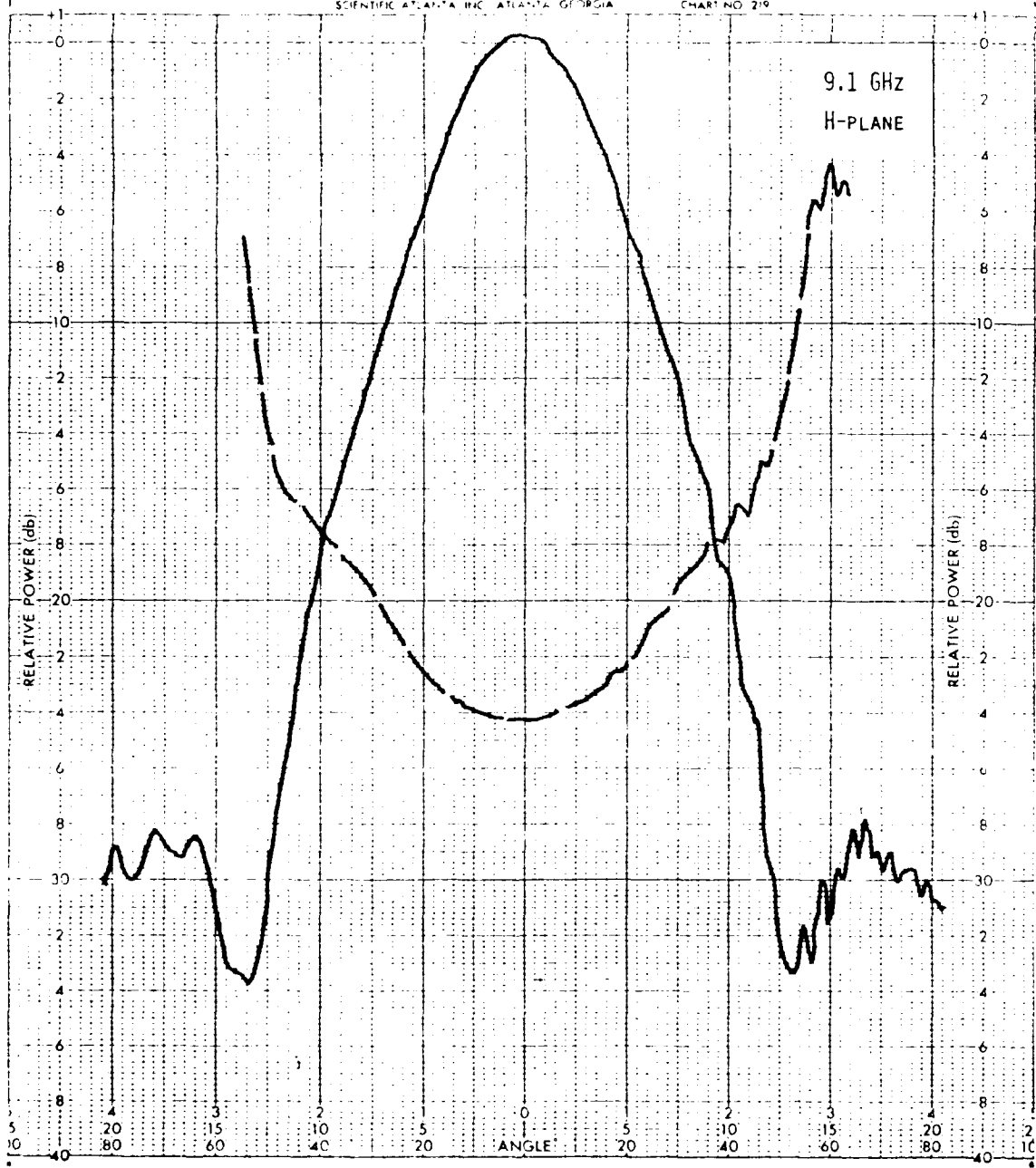


Figure 1 - Main lobe pattern of antenna feed horn, $D = 40$ in.,
range of scan is $\pm 40^\circ$ to 10° (with $\pm 10^\circ$).

SECTION 7
REFERENCES

1. Ussailis, J. S.,
Leiker, L. A.,
Goodman, R. M. IV,
and Metcalf, J. I. "Analysis of a Polarization Diversity
Weather Radar Design, Final Report,
Project A-2807, Georgia Institute of
Technology; AFGL-TR-82-0234, Air Force
Geophysics Laboratory, July 1982.
AD121666.
2. Ussailis, J. S., and
Metcalf, J. I. "Analysis of a Polarization Diversity
Meteorological Radar Design,"
Preprints, 21st Conference on Radar
Meteorology, Edmonton, Alberta, Canada,
19-23 September 1983.
3. Metcalf, J. I., and
Ussailis, J. S. "Radar System Errors in Polarization Diversity
Measurements",
Journal of Atmospheric and Oceanic Technology,
Vol. 1, No. 2, 105-114 (1984).

SECTION 6

PUBLICATIONS PARTIALLY SPONSORED BY THIS CONTRACT

1. "System Errors in Polarimetric Radar Backscatter Measurements", Ussailis, J. S., and Metcalf, J. I., Proceedings of 2nd Workshop on Polarimetric Radar Technology, Redstone Arsenal, AL, 3-5 May 1983.
2. "Radar System Errors in Polarization Diversity Measurements", Metcalf, J. I. and Ussailis, J. S., Preprints, 21st Conference on Radar Meteorology, Edmonton, Alberta, Canada, 19-23 September 1983.
3. "Analysis of a Polarization Diversity Meteorological Radar Design", Ussailis, J. S., and Metcalf, J. I., Preprints, 21st Conference on Radar Meteorology, Edmonton, Alberta, Canada, 19-23 September 1983.
4. "Radar System Errors in Polarization Diversity Measurements:", Metcalf, J. I., and Ussailis, J. S., Journal of Atmospheric and Oceanic Technology, Vol. 1, No. 2, 105-114 (1984).

SECTION 5
PREVIOUS CONTRACT AND PUBLICATION

Previous Related Contract: F19628-81-K-0027

Final Report: "Analysis of a Polarization Diversity Weather Radar Design"; Ussailis, J. S., Leiker, L. A., Goodman, R. M. IV, and Metcalf, J. I., Georgia Institute of Technology, Engineering Experiment Station, Project A-2807, Atlanta, GA, 2 July 1982. Report No. AFGL-TR-82-0234, Air Force Geophysics Laboratory.

SECTION 4
PERSONNEL

The following scientists and engineers contributed to the research reported in this document.

<u>Person</u>	<u>Contribution and Affiliation</u>
James S. Ussailis	Project Director; Georgia Tech
Joseph M. Newton	Electrical Design of Feed Horn; Georgia Tech
Donal Gallentine	Mechanical Design of Feed Horn; Georgia Tech
Keith D. Vaughn	Testing of Feed Horn, Installation; Georgia Tech
Edward Salzberg	Polarizer Design and Manufacture; Atlantic Microwave Corp. Rt. 117, Bolton, Mass. 01740
Robert Dalton	Polarizer Mechanical Design; Atlantic Microwave Corp.
Thomas P. Walsh, PE	Mechanical Analysis of Antenna Design; H & W Industries, Inc. Cohasset, Mass.
James Hayes	Mechanical Design of Antenna; H & W Industries, Inc.
Graham Armstrong	Contract Monitor Air Force Geophysics Laboratory Ground Based Remote Sensing Branch Hanscom AFB, Mass. 01730
Alexander Bishop	Technical Assistance; AFGL
James I. Metcalf	Technical Assistance; AFGL

SECTION 3
CONCLUSION

The antenna of the AFGL S-band Doppler weather radar has been modified for dual polarization operations, and its proper operation has been partially confirmed. Final focusing and overall VSWR reduction are required before cross-polarization levels can be determined. A reduction of the first sidelobe levels is also required before polarimetric measurements are made. Possible methods for accomplishing this include modification of the shape of the subreflector support spars and modification of the illumination of the main reflector by means of microwave absorbing material.

Both devices were inefficient at reducing antenna VSWR (Figures 28, 29, and 30). However, since the post reduced VSWR somewhat, it was left on the subreflector. During the following two weeks, antenna patterns were measured by AFGL personnel. Very high sidelobe levels were noted which were eventually determined to be a result of the VSWR reduction post. The post was removed and replaced by a conical VSWR reduction button of 3-inch diameter.

No further testing was possible in 1983 because of prior commitments of the radar system. Subsequently, it was also discovered that the feed support assembly placed the feed one inch closer to the subreflector than required. This overextension was corrected in August 1984 so that the antenna assembly can be properly focused.

Hardware installation was completed during the period from 22 August to 26 August 1983. After the feed horn was installed, the subreflector and feed horn were mechanically aligned, and initial pattern measurements were performed. Azimuth sidelobes were measured between 18 dB and 19 dB below the main lobe peak at 2.710 GHz and between 16 dB and 17 dB at 2.760 GHz.

During the initial pattern measurements, moderate swings in boresight amplitude were noticed. AFGL believed that the amplitude change was due to shifting of the transmitting antenna. This antenna is a 10 foot prime focus reflector mounted approximately at the 40 foot level of a tower located on Nobscot Hill, at a range of 4.9 miles. Since the owner of the tower (Raytheon Co.) donated the space with the provision that any attachment would employ no welding or drilled holes, a clamping arrangement was devised. Before these tests, the prevailing wind had sufficiently distorted the mount so that the antenna was no longer rigidly held.

Pattern measurements taken by AFGL personnel during the period from 29 August to 12 September indicated that all azimuthal patterns had asymmetrical first nulls. Upon investigation, a drooping of the feed was discovered when the antenna axis was rotated from the vertical to the horizontal. This droop was due to insufficient feed support. H & W Industries then fabricated and assisted in the installation of four feed support spars.

On 17 September 1983, VSWR measurements of the antenna were performed. Two methods were attempted to reduce subreflector VSWR: (1) the addition of a small conically shaped VSWR reduction button at the center of the subreflector and (2) the addition of a post and reactive plate at the same location. The theory of operation of these devices is straightforward. The former attempts to reflect toward the side of the antenna those rays which may otherwise reflect from the subreflector into the feed horn. The latter introduces an out-of-phase component to the electric field to cancel this undesired reflected ray.

2.4 POLARIZER ASSEMBLY

A device, known as a polarizer, was required to generate the various linear and circular polarizations of operation. The unit of choice is a sloped septum polarizer because this device can directly generate each state of circular polarization from a single waveguide input, thus minimizing the number of waveguide junctions in this mode of operation. This is essential, as the circular polarization scattering matrix measurements require the most polarization isolation, and as high polarization isolation implies a minimum VSWR ($\leq 1.02:1$) on all polarizer ports. Minimizing the number of waveguide junctions is necessary to reduce VSWR.

In the less critical linear polarization diversity mode of operation, a topwall hybrid coupler is added to the circuit (Figures 26 and 27). Here the VSWR requirements are $\leq 1.1:1$. However, reconsideration of the differential reflectivity polarization isolation requirements has indicated that a further reduction in the VSWR requirement may be applicable [3].

The polarizer assembly including polarizer, switches, topwall coupler, square waveguide section, square waveguide to circular waveguide section, and assorted waveguide pieces was supplied to Atlantic Microwave Corp., of Bolton, Mass., under a subcontract issued by Georgia Tech.

2.5 INSTALLATION

The final step to the antenna modification was the installation and testing of the antenna system. While the installation proceeded in an orderly fashion, the system tests had to be abbreviated due to prior commitments of the radar.

Georgia Tech began installing the antenna hardware on 9 August 1983. Between 9 August and 18 August the existing feed and tripod support assembly were removed and four reflector panels were drilled, pinned, and removed. Following this, the quadrapod subreflector mount and feed mount were installed, and the modified reflector was assembled. Throughout this operation, Georgia Tech was assisted by a mechanical technician from H & W Industries and by AFGL personnel.

TABLE 3. VSWR OF POLARIZER AND TRANSITION
(PORTS TERMINATED WITH MATCHED LOADS)

FREQUENCY MHz	PEAK POSITION cm	NULL POSITION cm	VSWR
Tuning Screws Out 1 Turn.			
2705.00	13.25	8.69	1.096
2710.02	13.27	8.60	1.095
2715.02	12.80	8.22	1.095
Tuning Screws Out 2 Turns.			
2700.04	13.03	8.36	1.10
2705.01	13.36	8.36	1.095
2710.00	13.04	8.34	1.10
2715.02	12.80	8.24	1.09
Tuning Screws Out 3 Turns.			
2705.00	12.90	8.57	1.10
2710.03	12.90	8.52	1.09
2715.00	12.66	8.25	1.085

TABLE 2. VSWR OF HORN AND TRANSITION

FREQUENCY MHz	PEAK POSITION cm	NULL POSITION cm	VSWR
2670.05	12.44	8.23	1.055
2675.00	12.10	7.13	1.070
2680.03	12.04	7.50	1.030
2685.01	10.27	15.43	1.020
2690.08	9.00	12.88	1.012
2695.09	8.03	11.66	1.025
2700.09	6.70	11.53	1.050
2705.07	6.60	11.06	1.080
2710.06	6.24	10.30	1.095
2715.00	5.70	10.00	1.122
2719.98	5.40	9.80	1.138
2725.00	13.60	9.28	1.155
2730.03	13.25	9.02	1.162
2735.06	12.84	8.60	1.173
2740.02	12.65	8.33	1.157
2745.03	12.05	8.00	1.160
2750.02	11.87	7.69	1.148
2755.04	11.40	7.35	1.135
2759.98	11.27	7.38	1.120
2765.02	10.66	6.68	1.100
2770.02	10.30	6.57	1.095
2775.05	10.20	6.10	1.080
2780.02	10.03	5.80	1.077
2785.01	9.65	13.70	1.073
2790.04	8.98	12.80	1.069
2795.08	8.56	12.74	1.082
2800.00	8.10	11.96	1.090

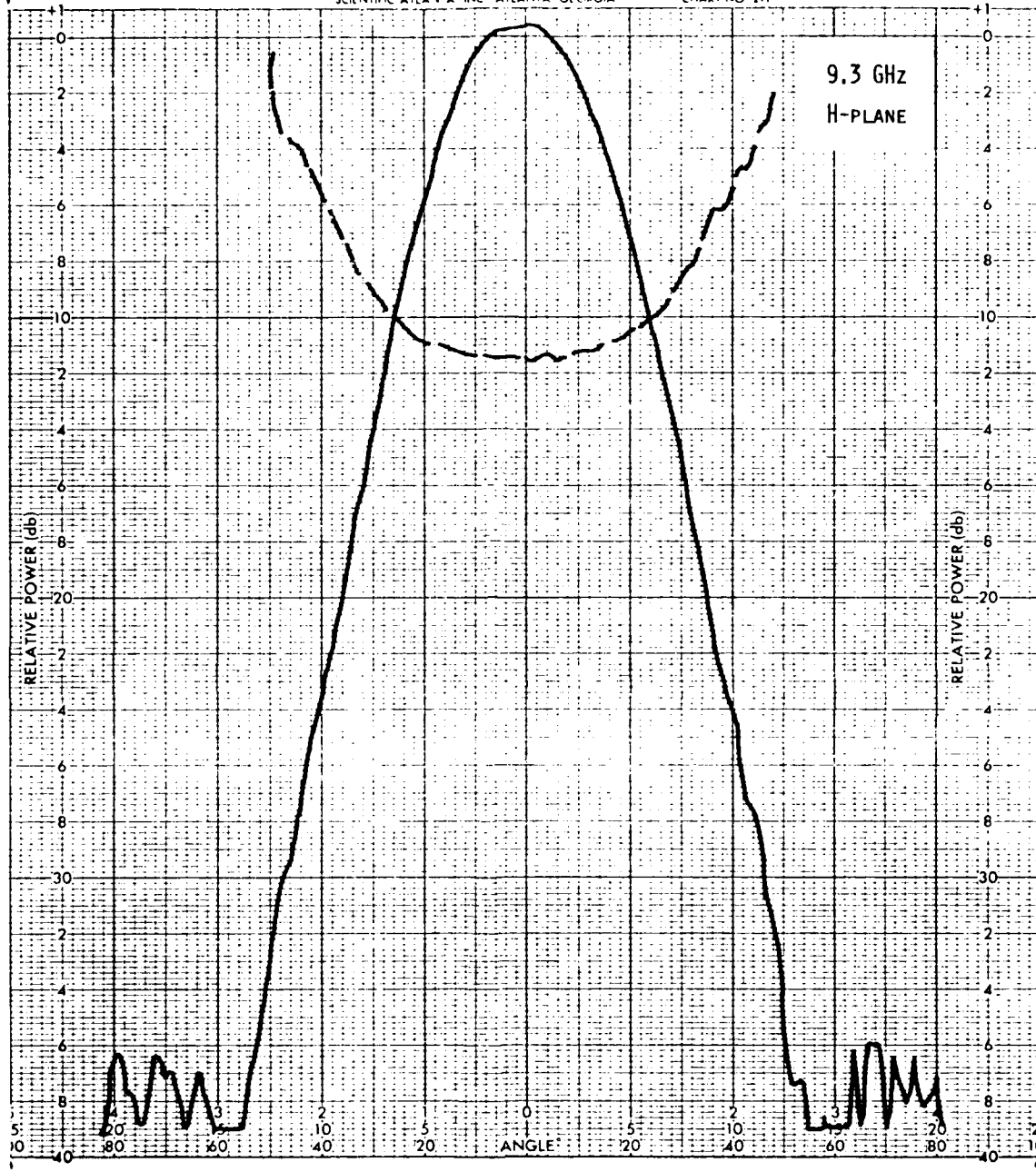


Figure 5. H-plane pattern of sealed feed horn, $f = 9.3$ GHz

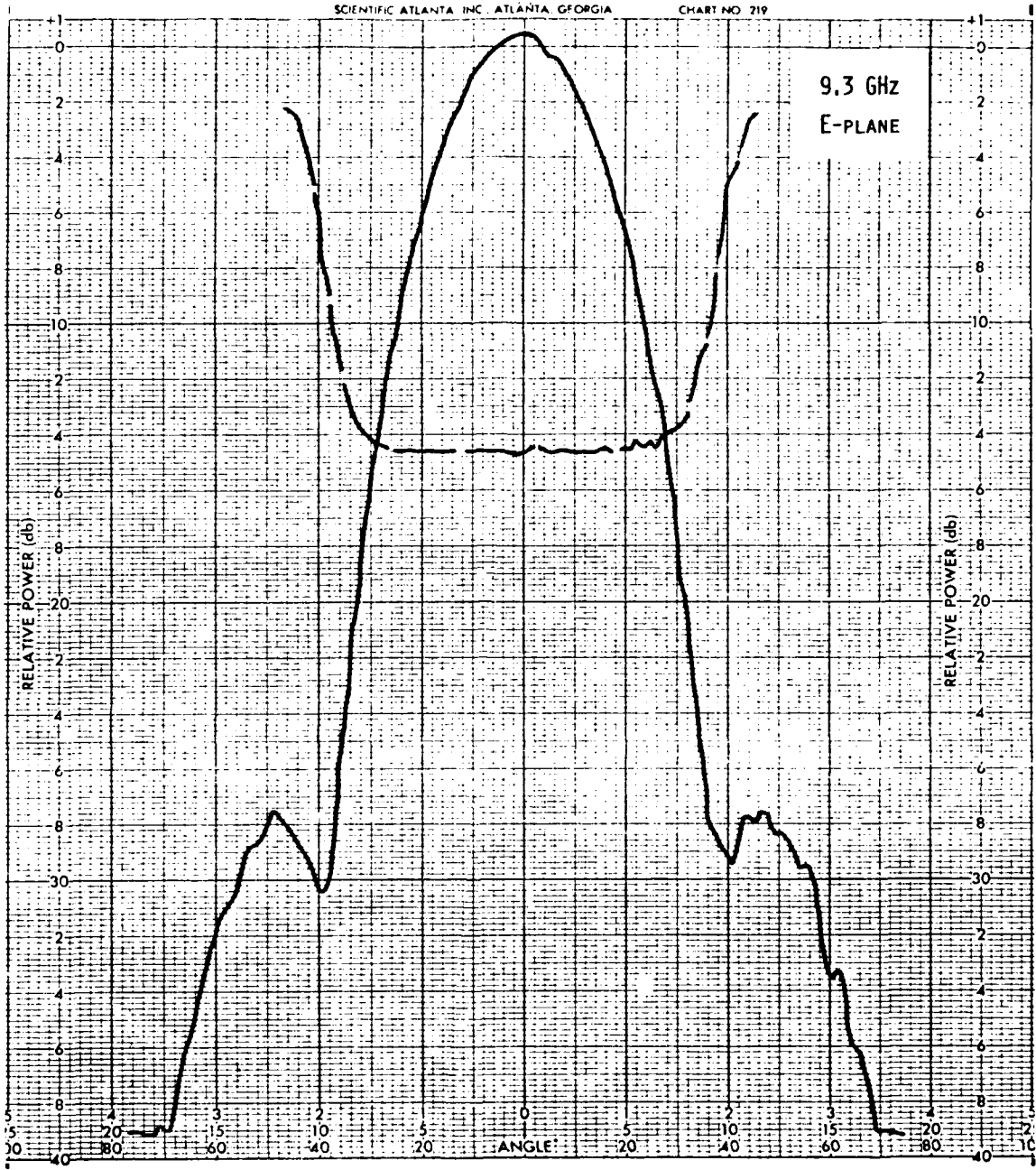


Figure 6. E-plane pattern of scaled feed horn, $f = 9.3$ GHz

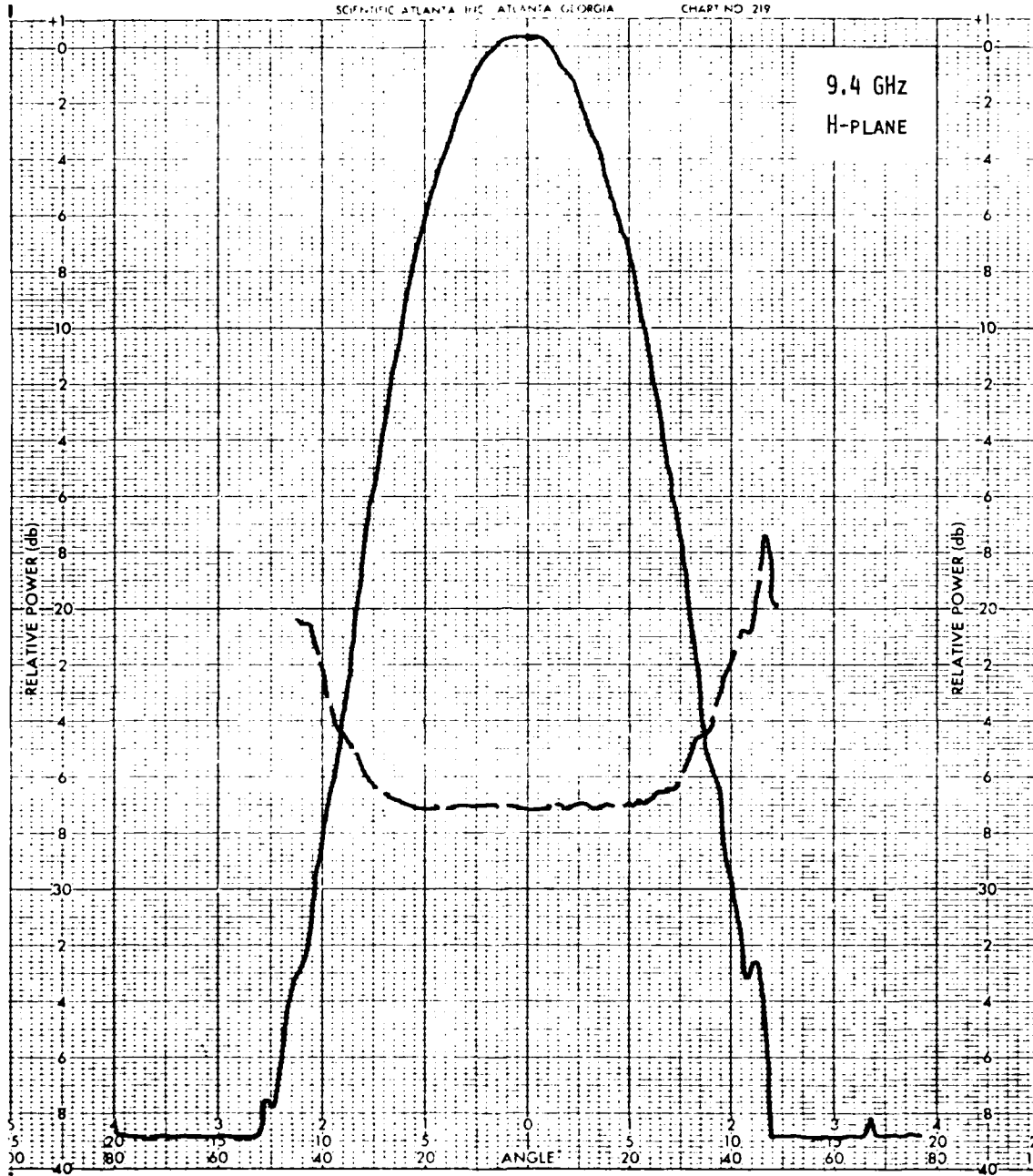


Figure 11. H-plane pattern of sealed feed horn, $f = 9.4$ GHz

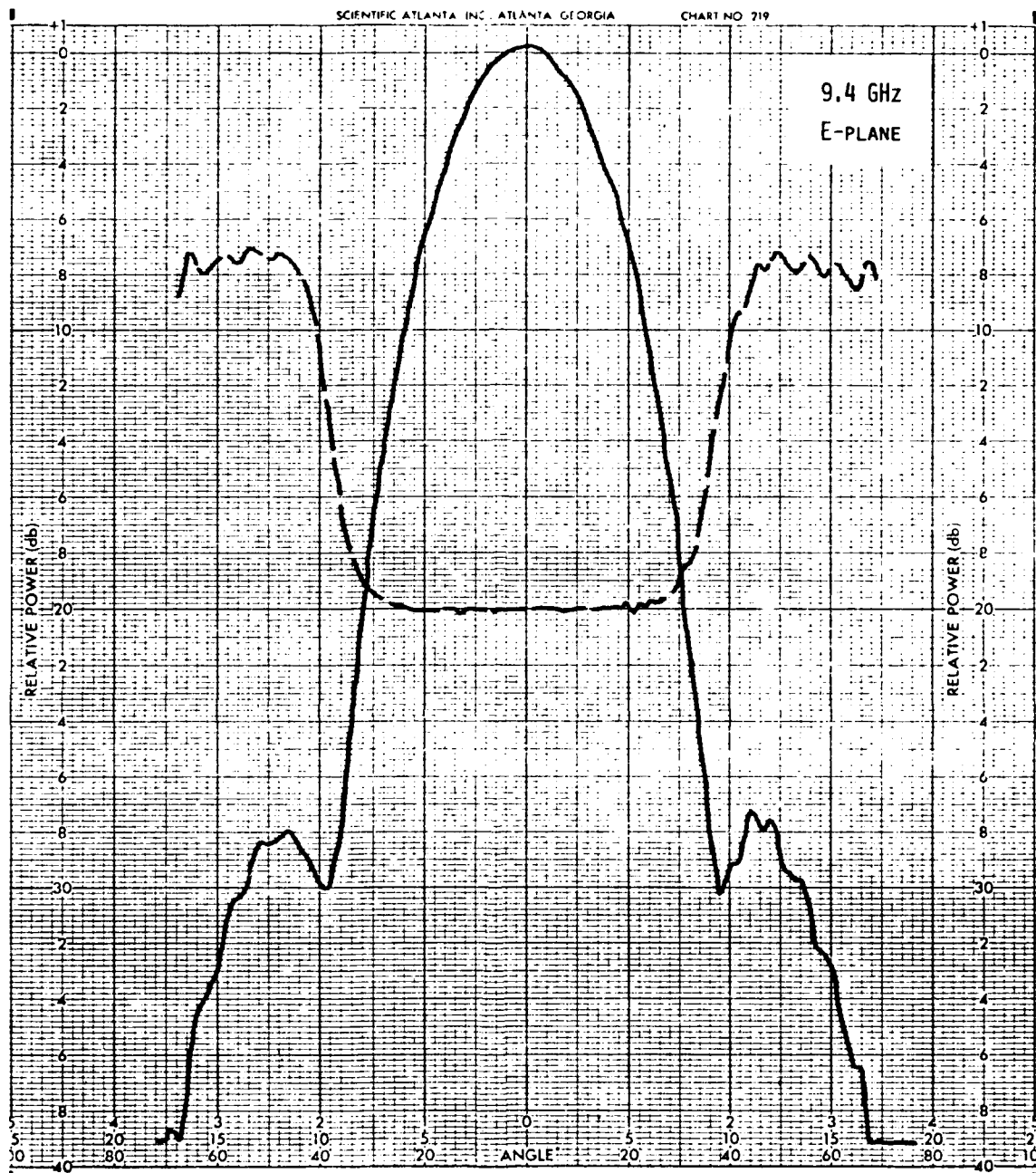


Figure 8. E-plane pattern of scaled feed horn, $f = 9.4$ GHz

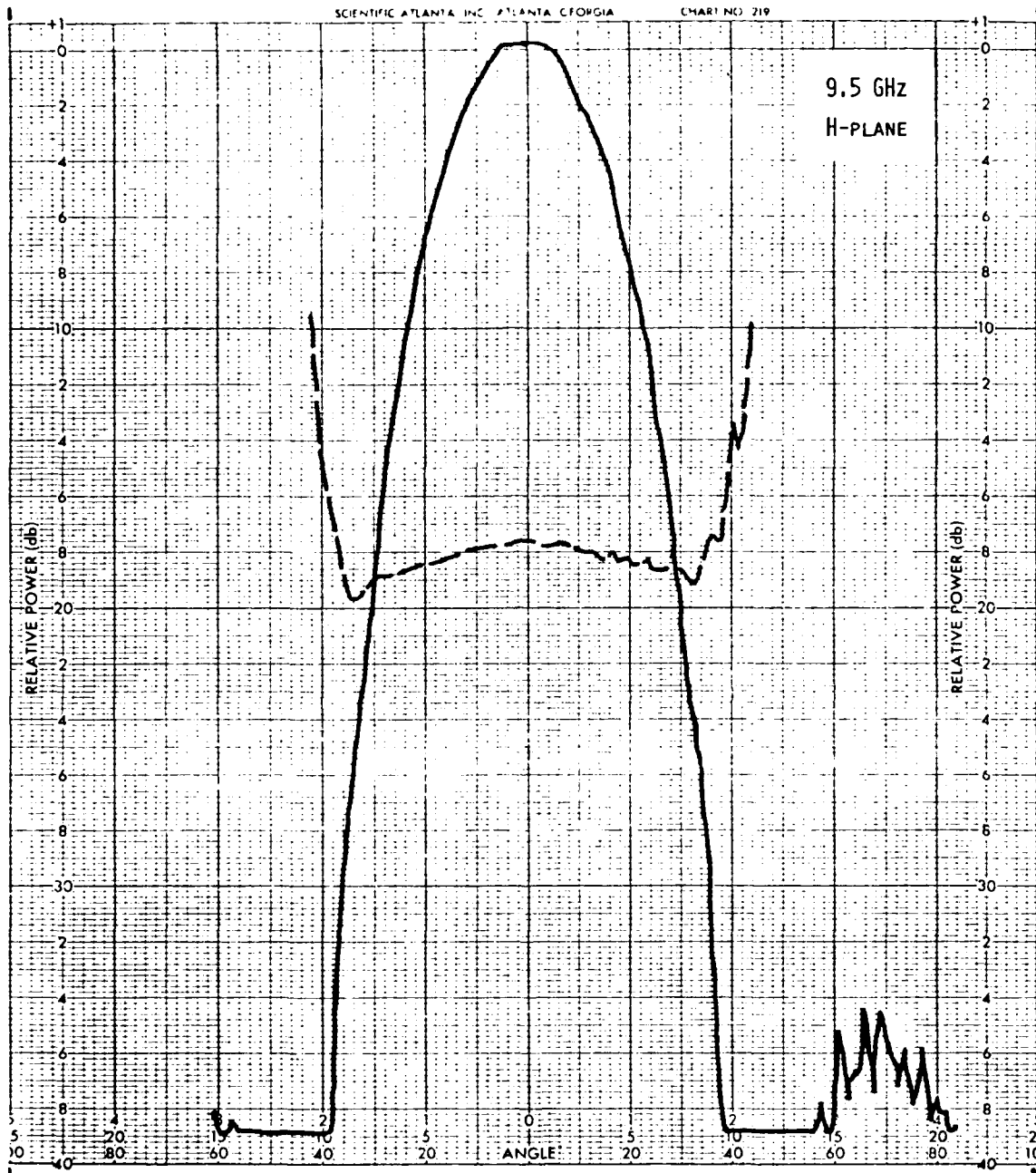


Figure 9. H-plane pattern of scaled feed horn, $f = 9.5$ GHz

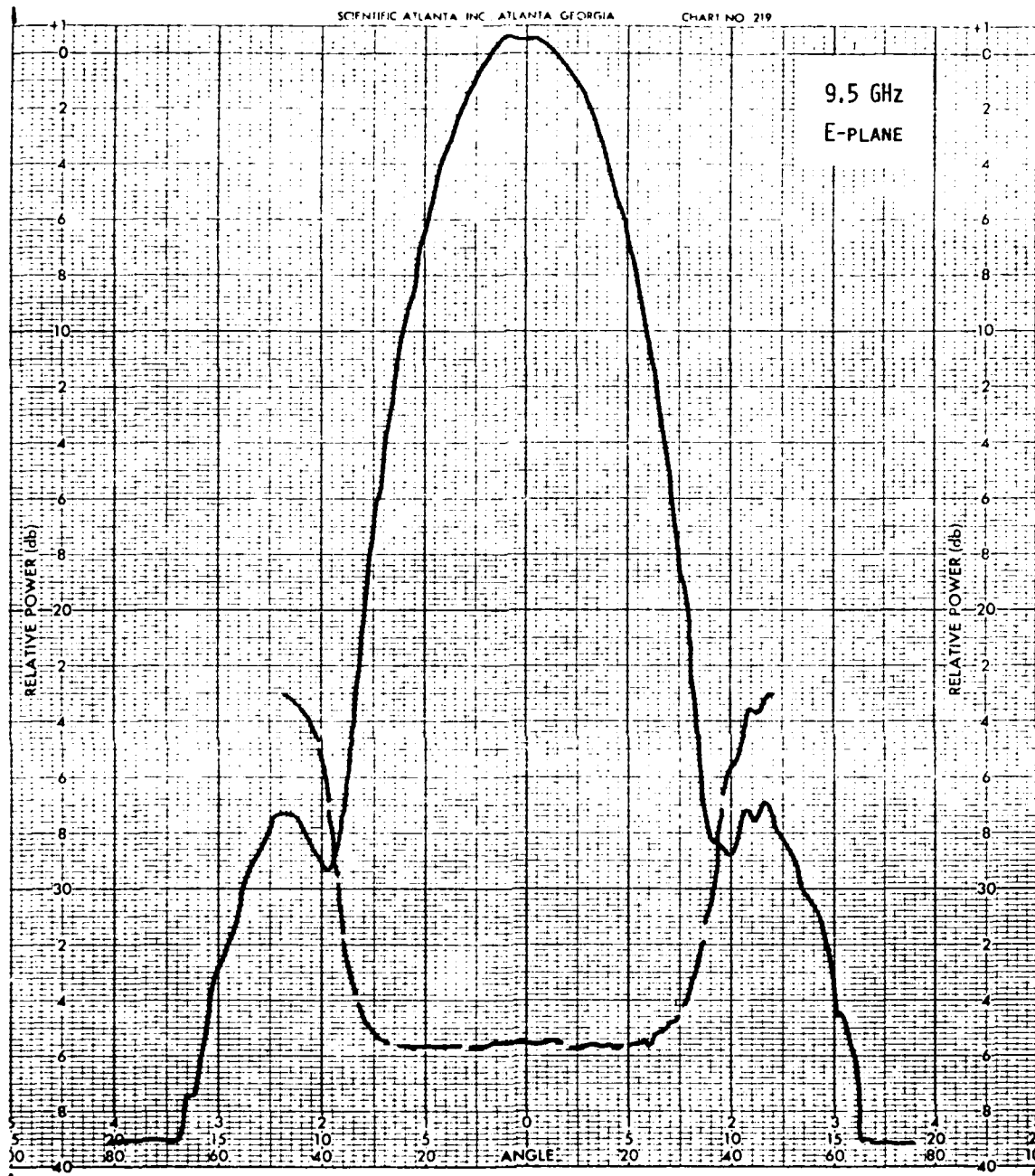


Figure 10. E-plane pattern of sealed feed horn, $f = 9.5$ GHz

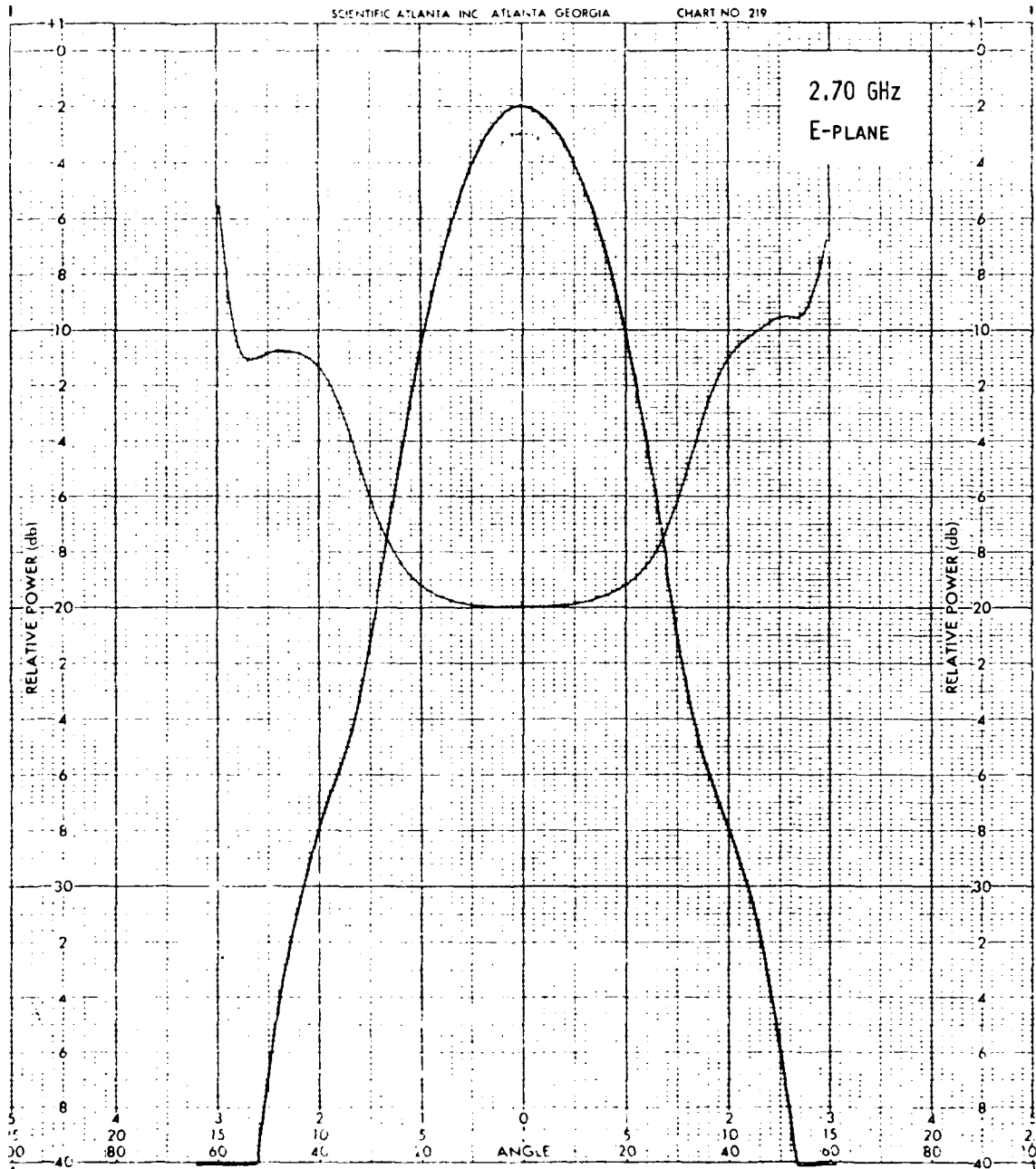


Figure 11. E-plane pattern of full-size feed in final configuration, $f = 2.70$ GHz. Axis of rotation of pattern coincides with E-plane phase center determined at 2.71 GHz (Figure 13). Scale of abscissa is -100° to 100° (bottom scale).

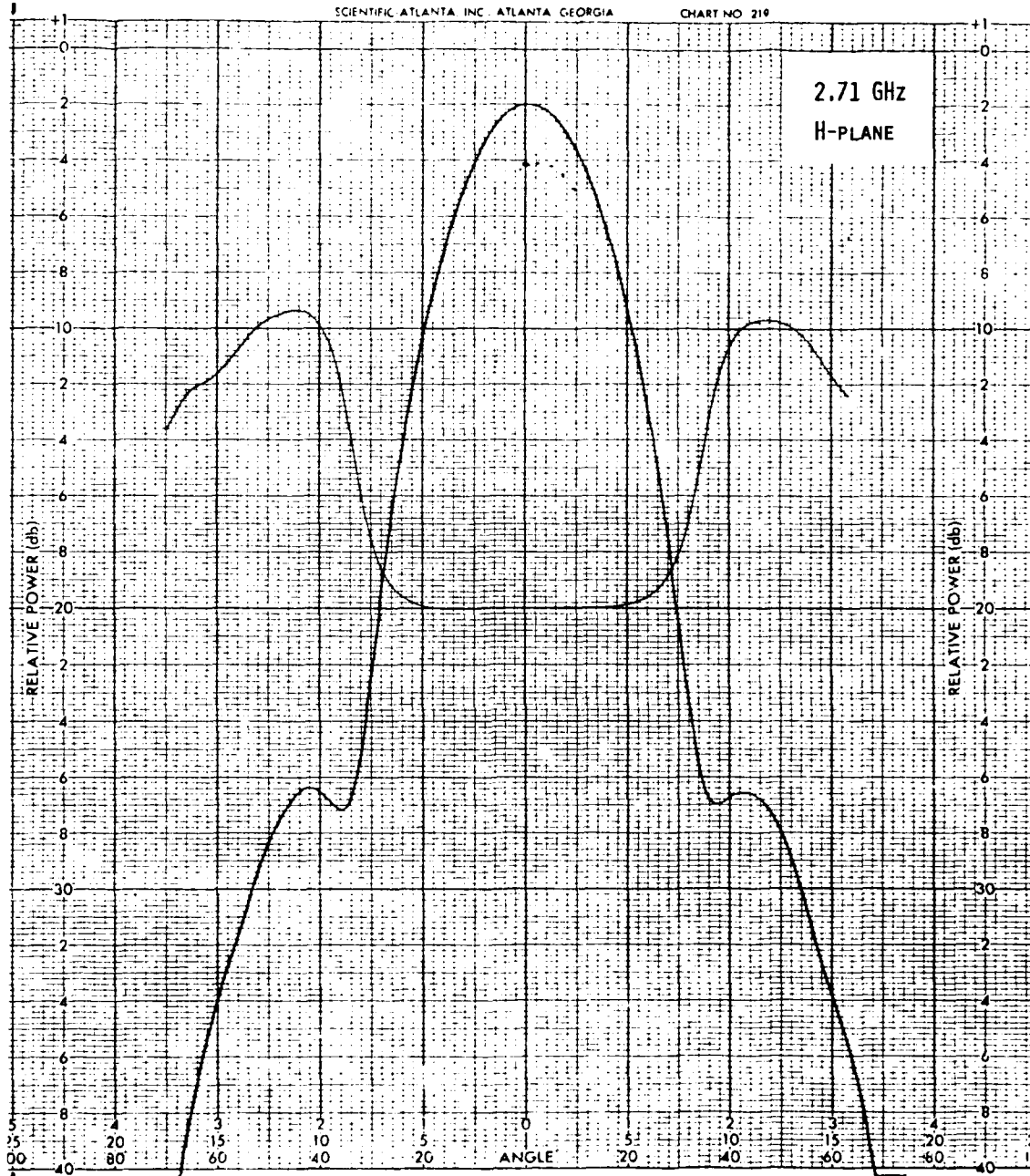


Figure 17. H-plane pattern of full-size feed in final configuration, $f = 2.71$ GHz. Phase center determined to be 2-5/8 inches inside horn aperture. Phase center is axis of rotation of pattern.

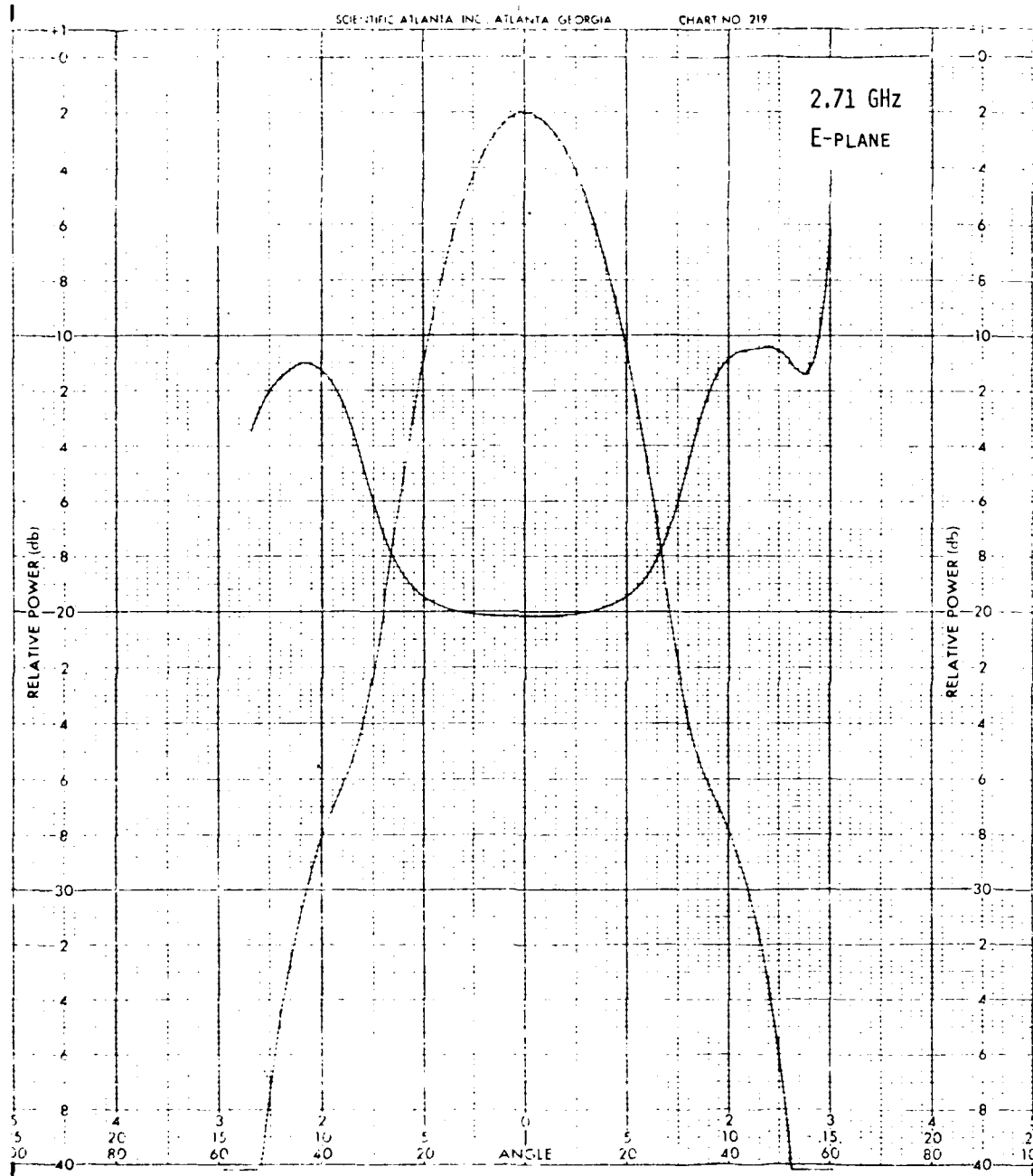


Figure 13. E-plane pattern of full-size feed, $f = 2.71$ GHz. Phase center determined to be $2 \frac{13}{16}$ " inside horn aperture. Phase center is axis of rotation for all E-plane patterns (Figure 11, 14-22).

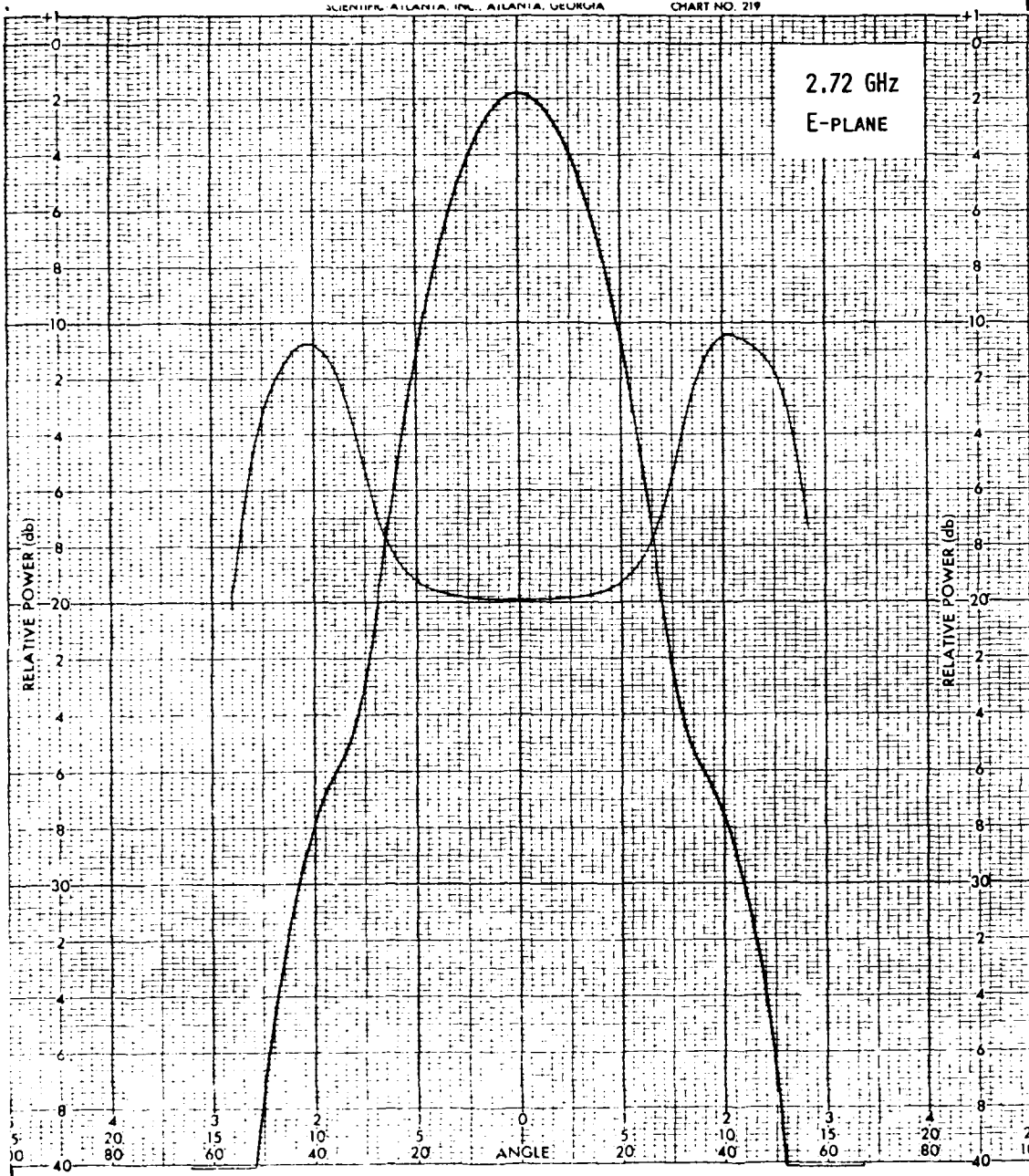


Figure 14. E-plane pattern of full-size feed, $f = 2.72$ GHz. Axis of rotation is same as in Figure 13.

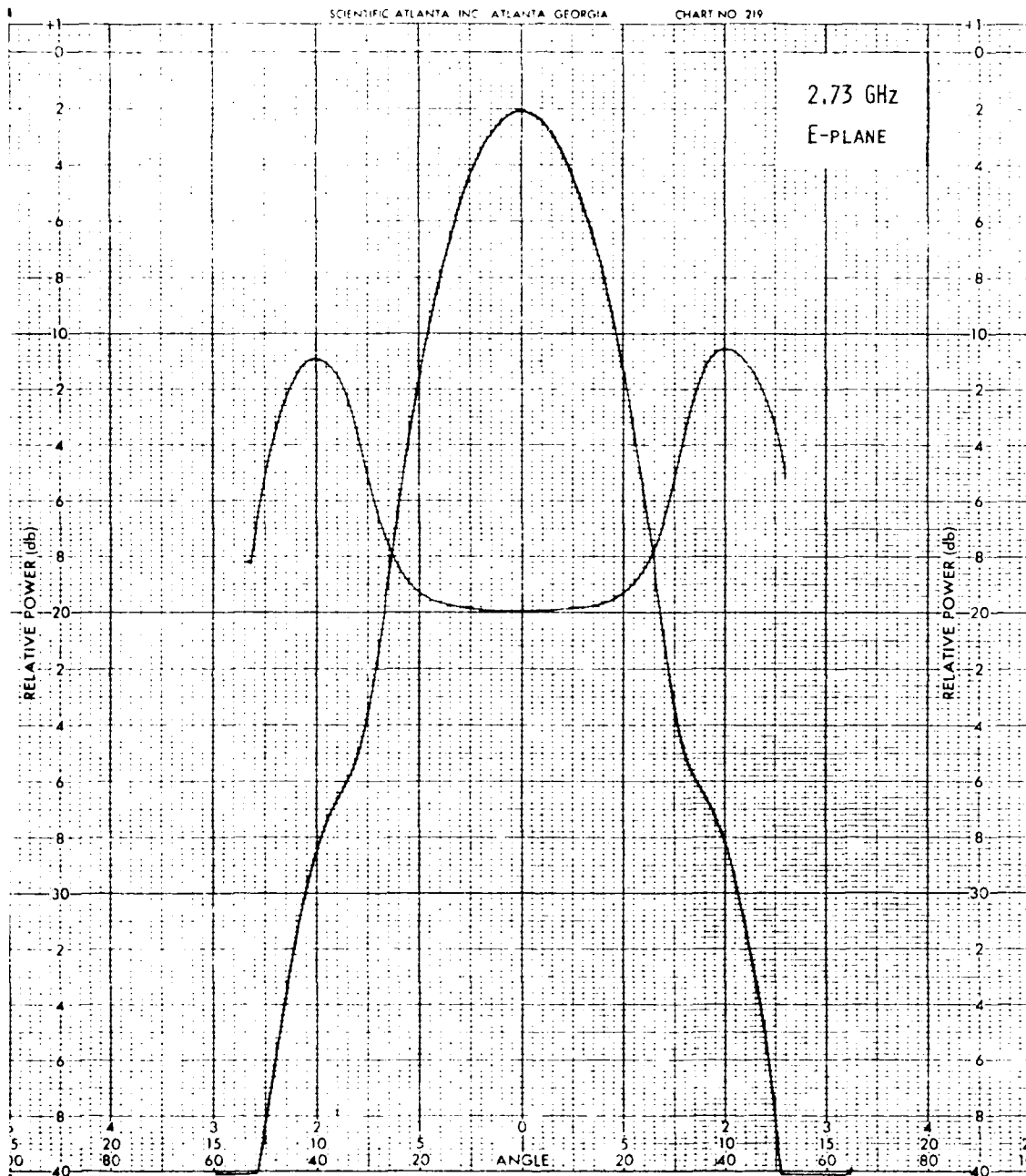


Figure 11. E-plane pattern of 1/4 inch feed, $f = 2.73$ GHz. Axis of rotation is same as in Figure 13.

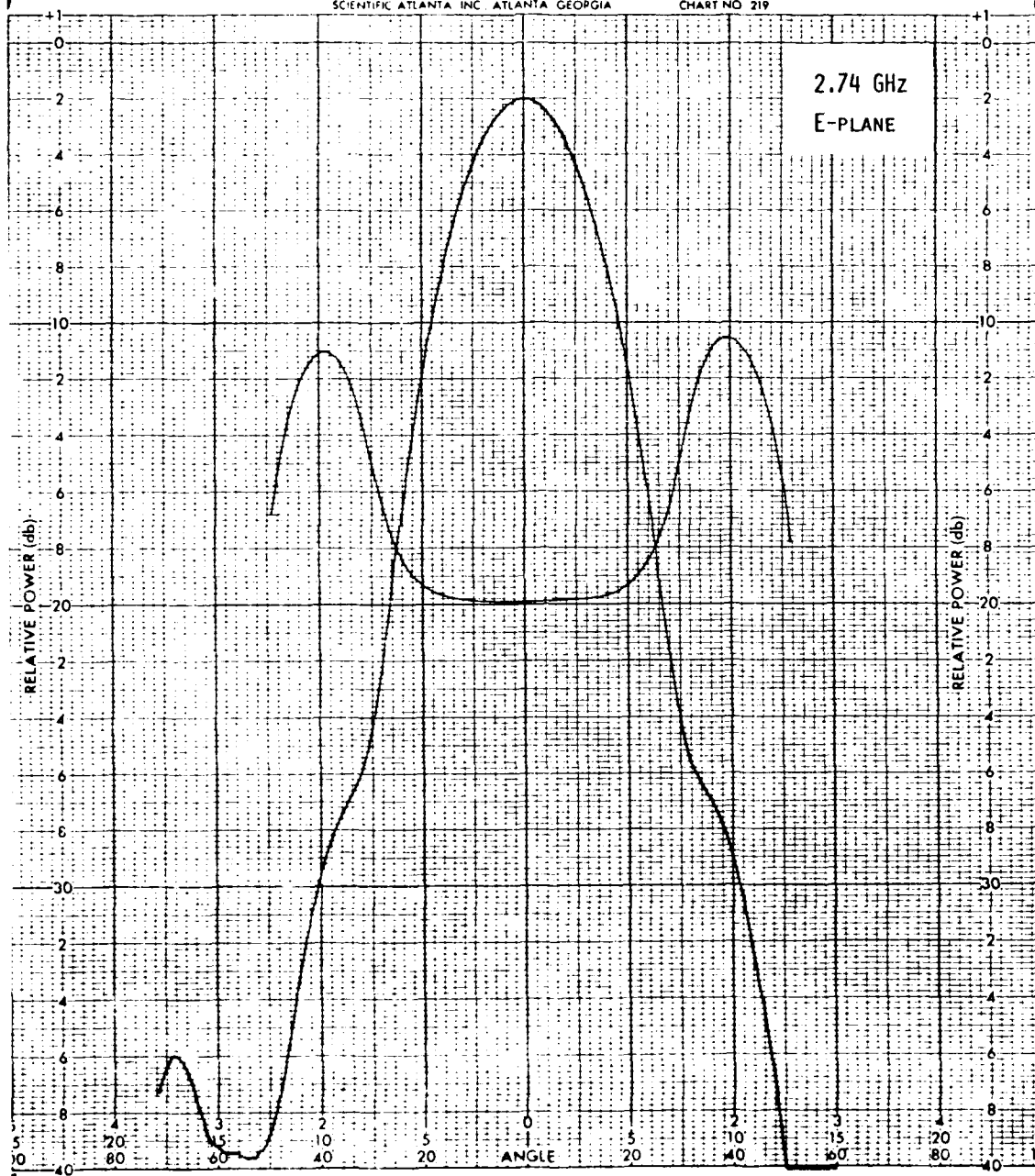


Figure 16. E-plane pattern of full-size feed, $f = 2.74$ GHz. Axis of rotation is same as in Figure 13.

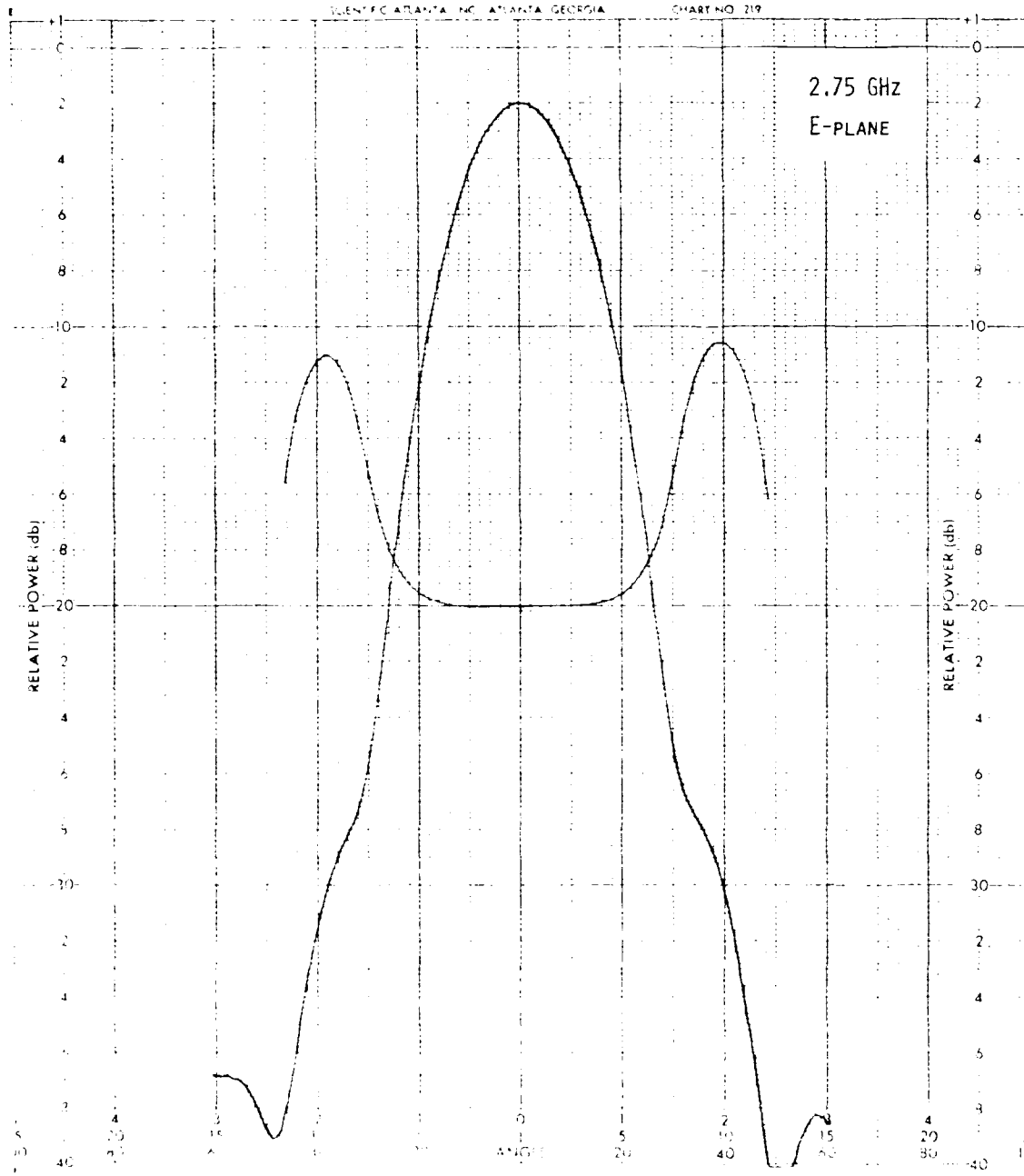


Figure 1. Radiation pattern of horn antenna, $\theta = 10^\circ$ db. Axis of horn antenna is shown in Figure 13.

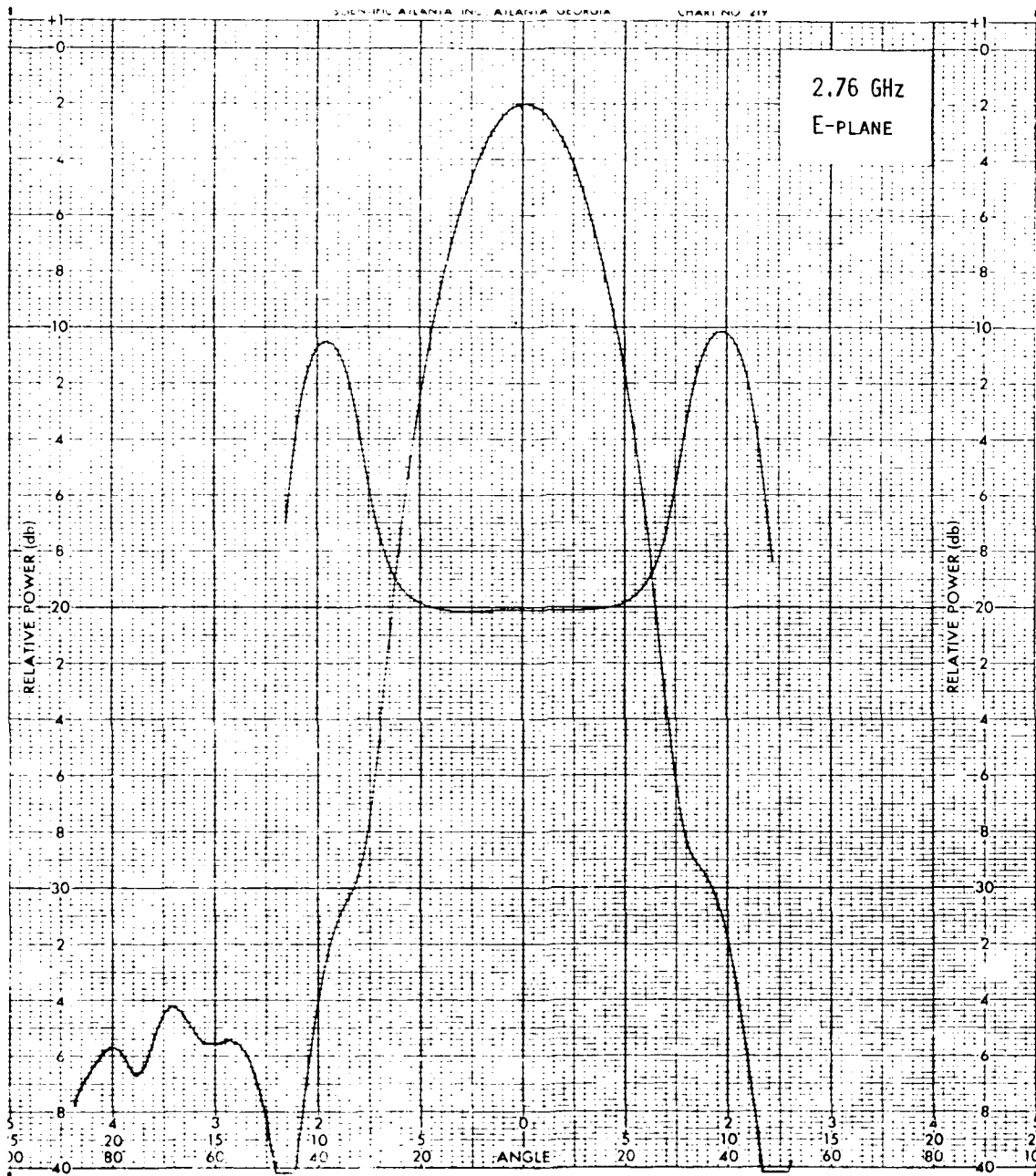


Figure 10. E-plane pattern of full-size feed, $f = 2.76$ GHz. Axis of rotation is same as in Figure 12.

ANALYSIS OF A POLARIZATION DIVERSITY
METEOROLOGICAL RADAR DESIGN

James S. Ussailis
Engineering Experiment Station
Georgia Institute of Technology
Atlanta, Georgia, USA

James I. Metcalf
Ground Based Remote Sensing Branch
Air Force Geophysics Laboratory
Hanscom AFB, Massachusetts, USA

1. INTRODUCTION

This work describes an ongoing design and modification to provide a polarization diversity addition for the Air Force Geophysics Laboratory (AFGL) 10 cm coherent weather radar. The unmodified radar is documented in Glover et al. (1981). Much of the information contained herein will be of interest as it is applicable to polarimetric radars in general.

In the fall of 1980, the Radar and Instrumentation Laboratory of the Engineering Experiment Station of the Georgia Institute of Technology received a contract from AFGL to perform a design study for this polarization diversity addition. The constraints of this effort were to retain, as much as possible, the present equipment and operating features, such as the antenna reflector, transmitters, microwave circuitry, and receivers while supplying a constructable design for the modification. The modified radar is to be ultimately capable of coherent operation in both the circular depolarization ratio (CDR) and differential reflectivity (Z_{DR}) modes. The radar is to provide significant new research information by exceeding the measurement capability of current systems.

One of the difficulties we encountered at the outset was the lack of uniformity of nomenclature between the radar engineering community and the meteorological community. To avoid possible misunderstandings, we present definitions of cross-polarization ratio terms in Table 1. Fundamental differences exist between the measurements performed by and the equipment required for CDR and Z_{DR} radars. Specifications for measurement of these parameters are given in Table 2, which includes traditional values as well as design goals for the AFGL radar. Some of the elements which determine these specifications, such as polarization isolation of the radio frequency (RF) switch or polarizer, are slightly beyond today's technology and require reasonable development efforts to attain, while other elements such as the effect

TABLE 1. DEFINITIONS OF CROSS-POLARIZATION RATIO TERMS

ICR_1	One-way integrated cancellation ratio: equal to the integrated cross-polarized energy radiated by a circular polarized antenna divided by the integrated co-polarized energy of the same antenna. Limits of integration are theoretically over 4π , in practice integration to the 1st null of the co-polarized beam suffices.
ICR_2	Two-way integrated cancellation ratio: defined as above for transmission and reception through the same antenna.
ICR_{LP}	One-way integrated cross-polarization ratio: as ICR_1 , but for linear polarization only.
ICR_{LP2}	Two-way integrated cross-polarization ratio: as ICR_2 , but for linear polarization only.

of reflector surface errors, polarization isolation, or radome induced cross-polarization are at present not understood and will require a substantial development effort.

TABLE 2. CDR, Z_{DR} , AND AFGL RADAR SPECIFICATIONS

Specification	CDR		Z_{DR}		AFGL	
	Trad.	Calc.	Trad.	Calc.	Composite	Goal
ICR_2	-40 dB	---	---	---	-35 dB	-37 dB
Error in ICR_2 Measurement	---	3 dB	---	---	3 dB	< 3 dB
$ICPR_2$	---	>-20 dB	>-26 dB	-26 dB	-30 dB	---
Power Ratio Accuracy 0.1 dB	---	0.1-0.3 dB	---	0.2 dB	0.1 dB	---
Amplitude Tracking Uncertainty	1.0 dB	< 0.23 dB	---	---	0.2 dB	< 1.1 dB
Receiver Phase Tracking Uncertainty	< 1.5°	---	---	---	< 1.5°	1.0°
Polarization Isolation	>-40 dB	---	>-20 dB	>-26 dB	-37 dB	-40 dB (P) -26 dB (R) -30 dB (LP)

2. ANTENNA MODIFICATION

2.1 CROSS POLARIZATION OF REFLECTOR ANTENNAS,
A REVIEW OF THE LITERATURE

A study of the literature of linear and circular cross-polarization of axisymmetric reflectors was undertaken that chronologically covered the past forty years. From this effort, it was initially determined that the cross-polarization pattern for linearly polarized antennas has maxima which lie in 45° planes between the principal axis of the antenna. These maxima consist of a set of pencil-beam lobes on each arm of these planes, with the first maxima occurring approximately at the first null of the co-polarized beam (Silver, 1949). Jones (1954) determined an exact solution for cross-polarization characteristics of the front fed paraboloid using an electric dipole, magnetic dipole, and Huygens or plane wave feed antenna. Here the results for the characteristics of a paraboloid excited by a short electric dipole or magnetic dipole were shown to be identical, with the sole exception that the E and H plane antenna patterns are to be interchanged when the dipoles are interchanged. Finally, for a plane wave feed chosen such that the E and H plane patterns are identical, he determined that the cross-polarized components of the fields are equal in magnitude and of opposite sign within each of the paraboloid quadrants so that, "it is noticed that the far zone field has no cross polarized radiation fields."

Watson and Ghobrial (1972) presented results which disagreed with the preceding

APPENDIX A

PAPER PRESENTED AT
21ST CONFERENCE ON
RADAR METEOROLOGY

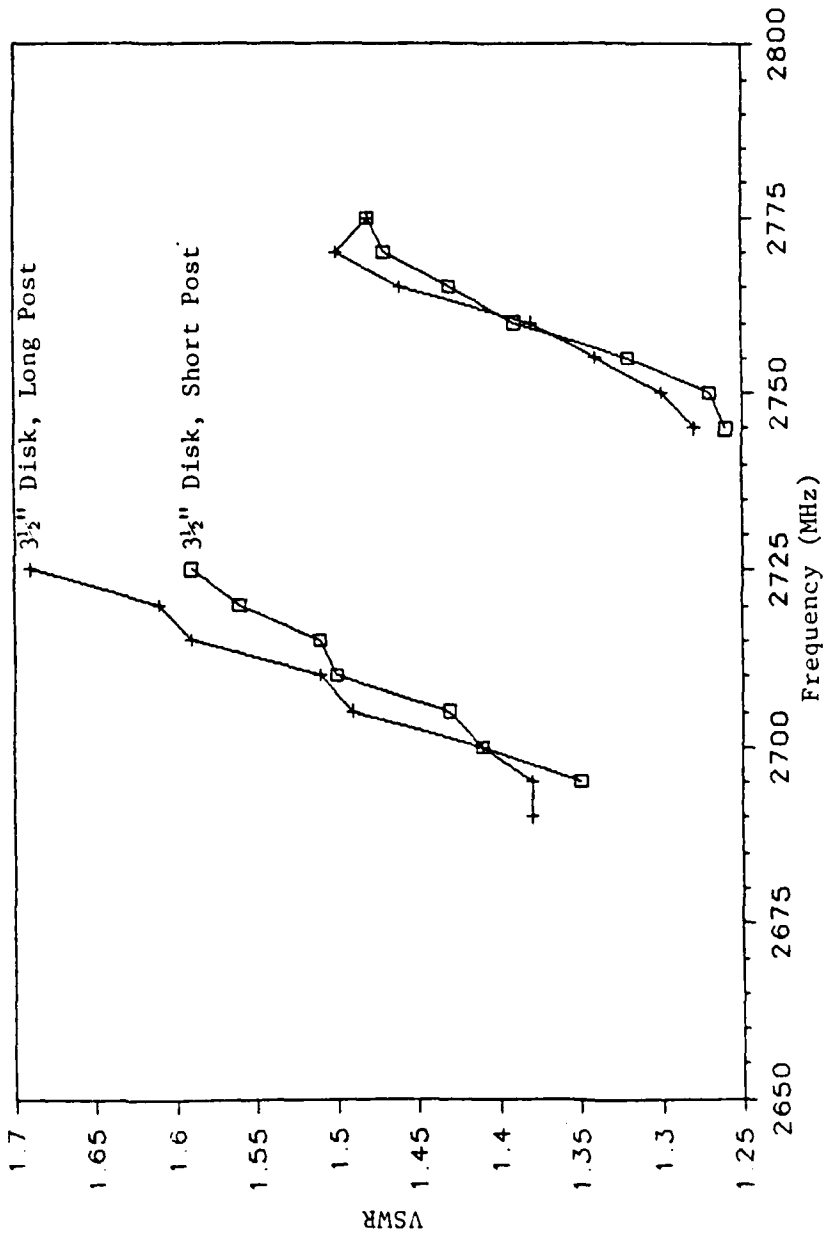


Figure 30. VSWR of modified AFGL antenna showing effect of differing post length.

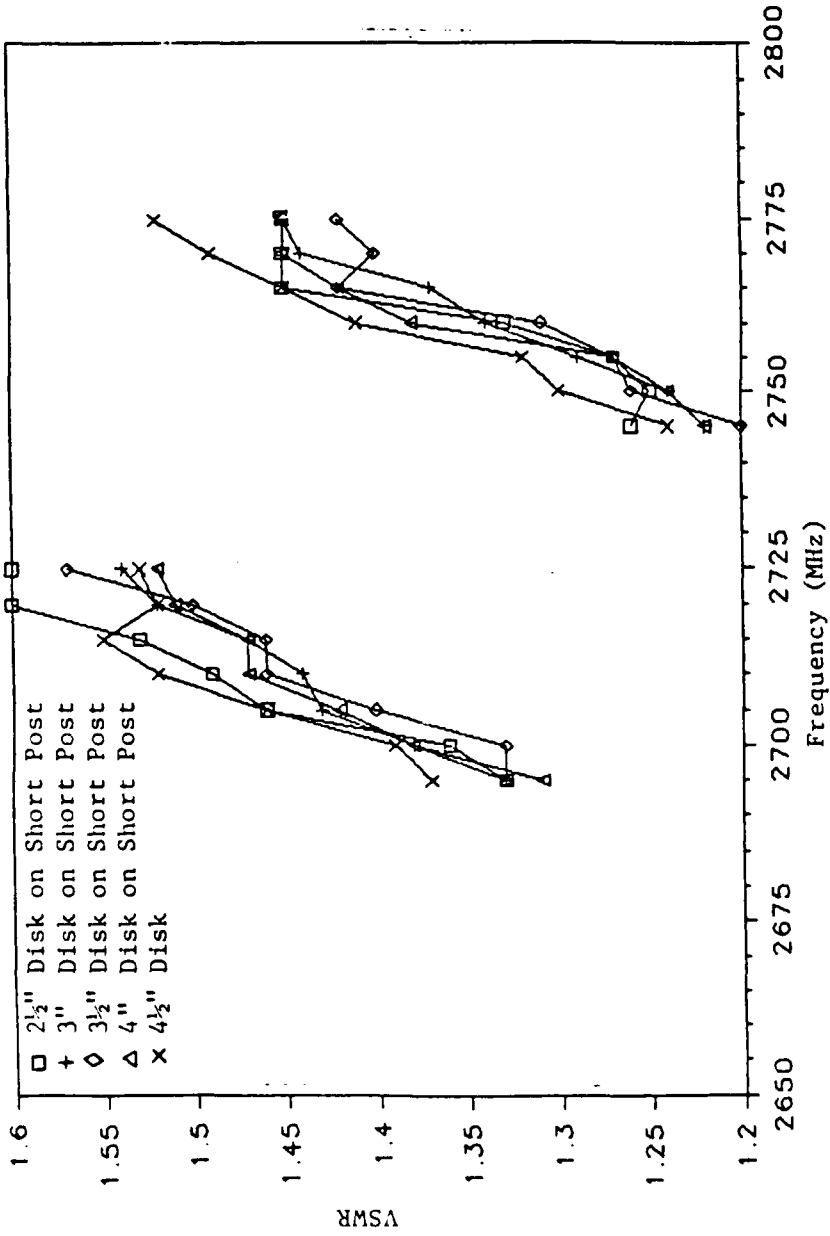


Figure 29. VSWR of modified AFGL antenna showing effect of post and disk VSWR reduction method.

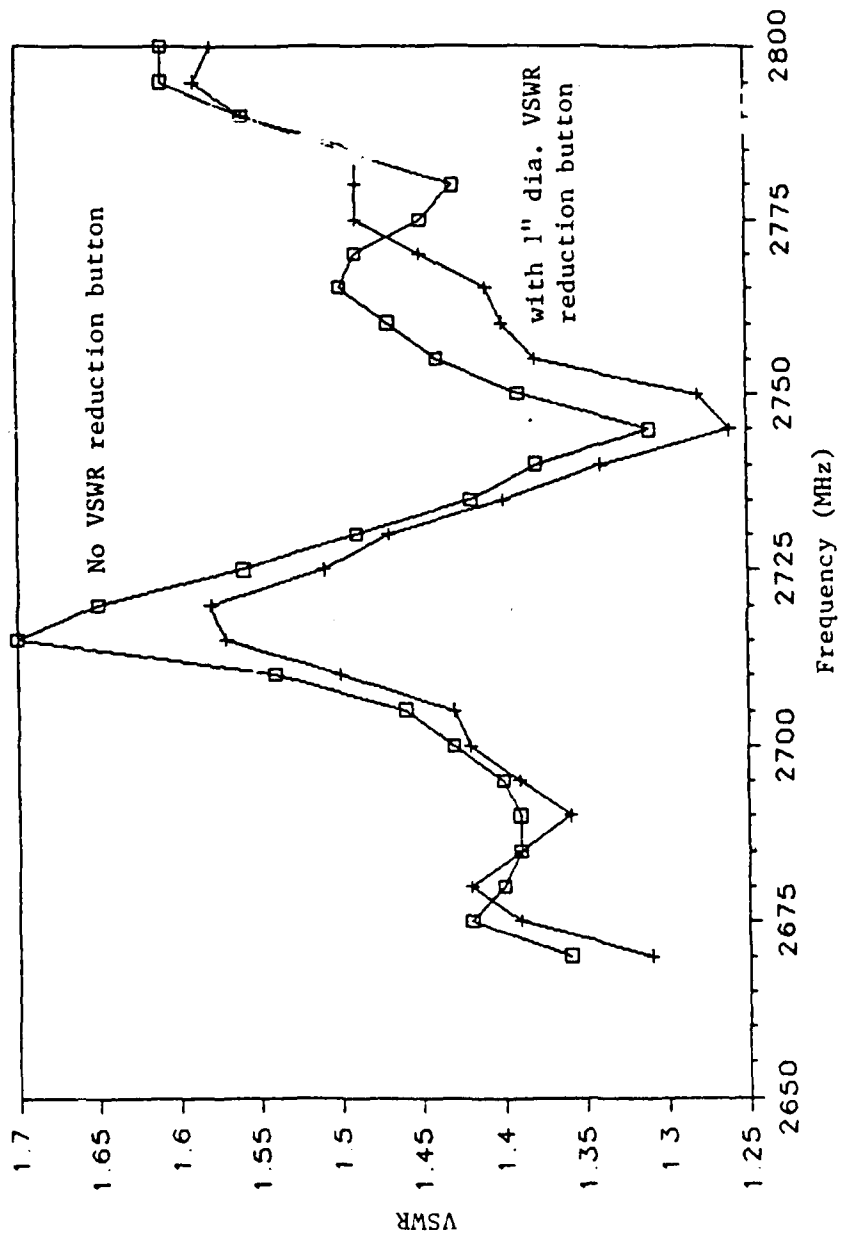


Figure 28. VSWR of modified AFGL antenna showing effect of 1-inch diameter VSWR reduction button.

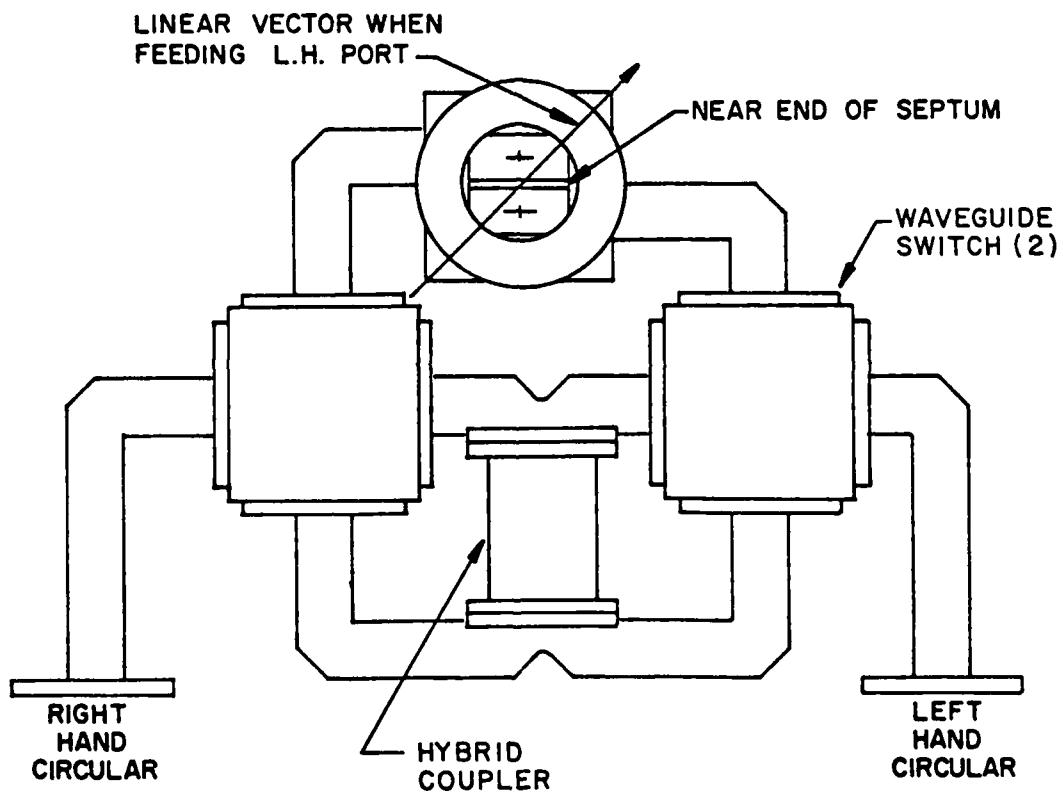


Figure 27. Rear mechanical detail of antenna polarizer.

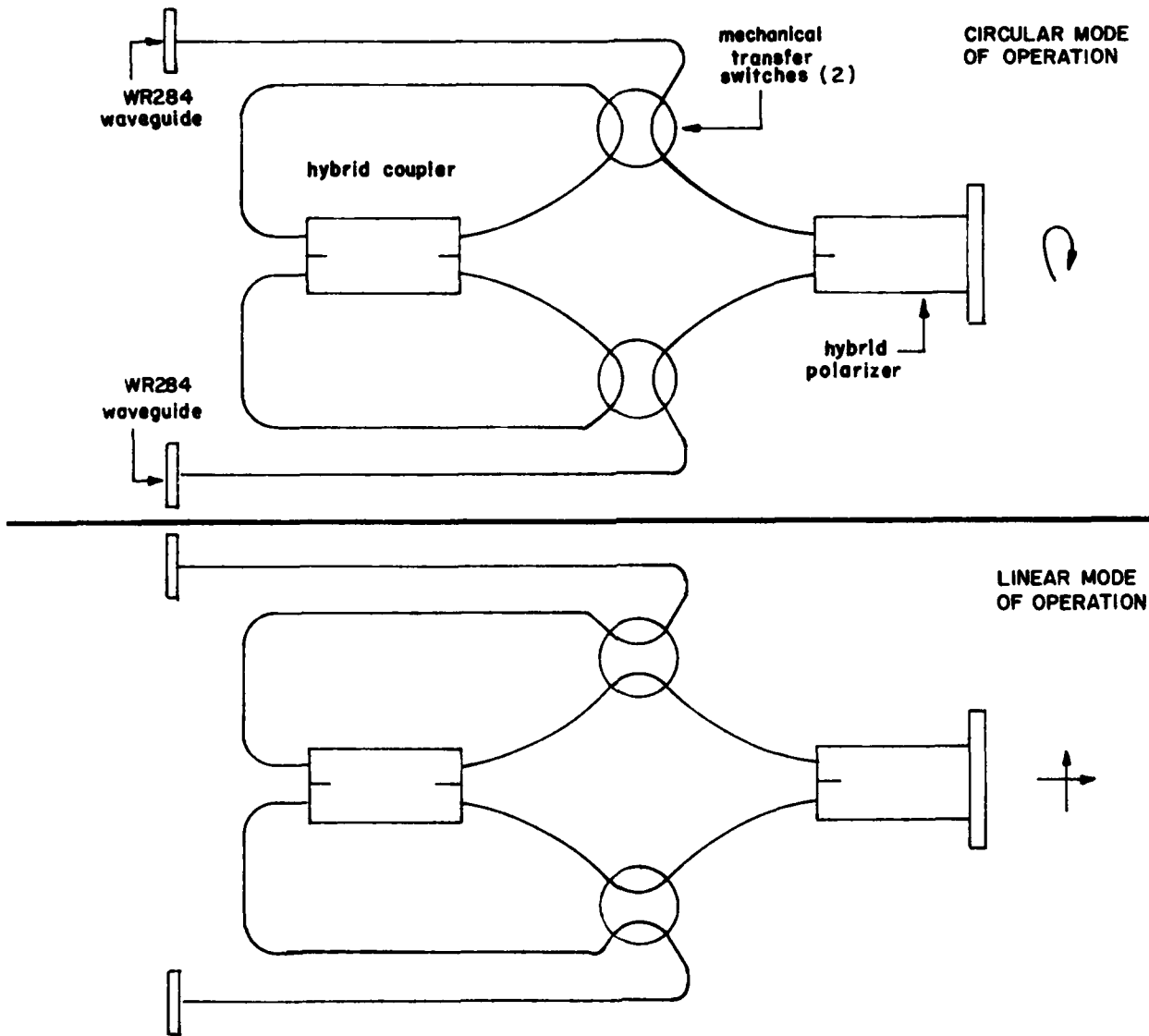


Figure 26. Schematic representation of circular/linear switchable antenna polarizer.

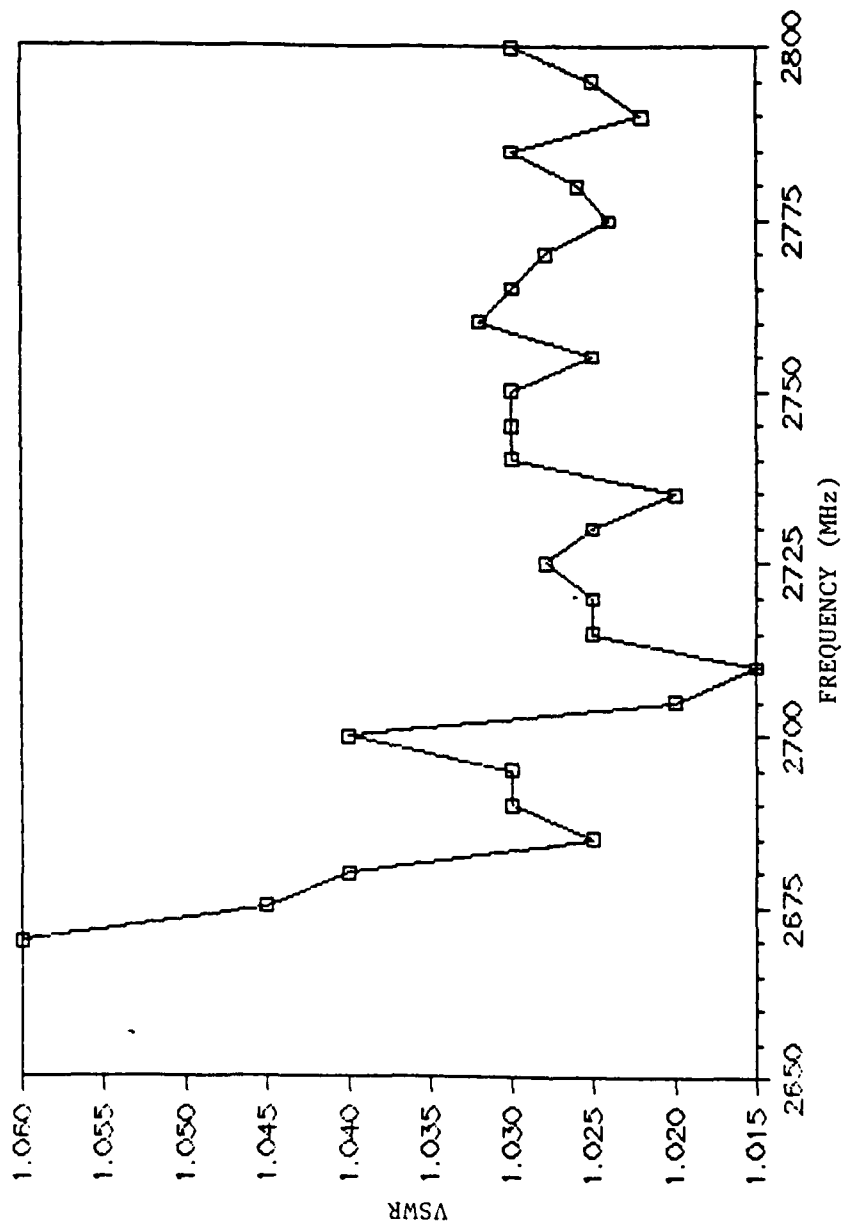


Figure 25. Input VSWR of polarizer with horn attached to circular port and load attached to unused input port.

NAME	TITLE	DWG. NO.
SMITH CHART FORM 02 SPR '2-40	RAY ELECTRIC COMPANY, PINE BROOK, N.J. ©1949 PRINTED IN U.S.A.	DATE

IMPEDANCE OR ADMITTANCE COORDINATES

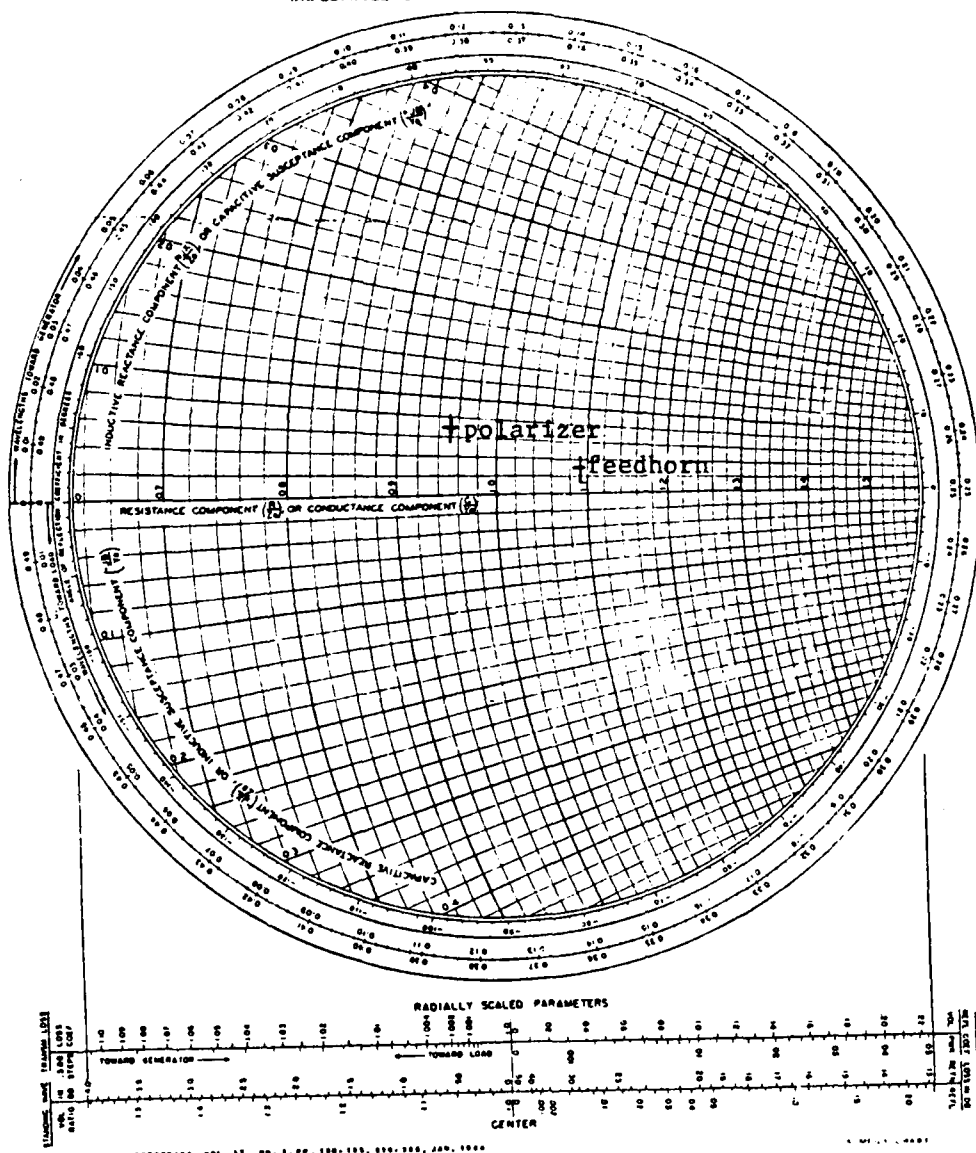


Figure 24. Normalized impedance of feed horn and of polarizer at 2710 MHz.

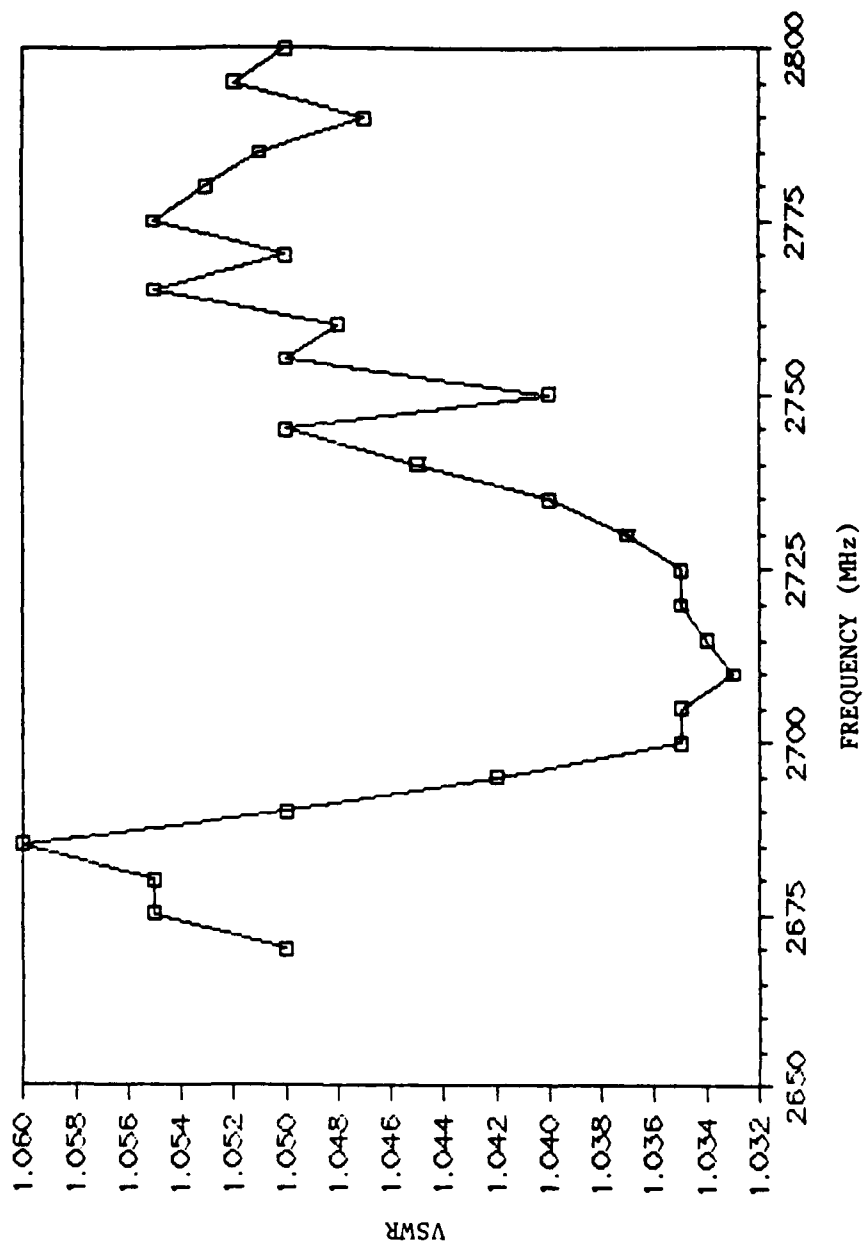


Figure 23. VSWR of rectangular-to-circular transition with circular load attached.

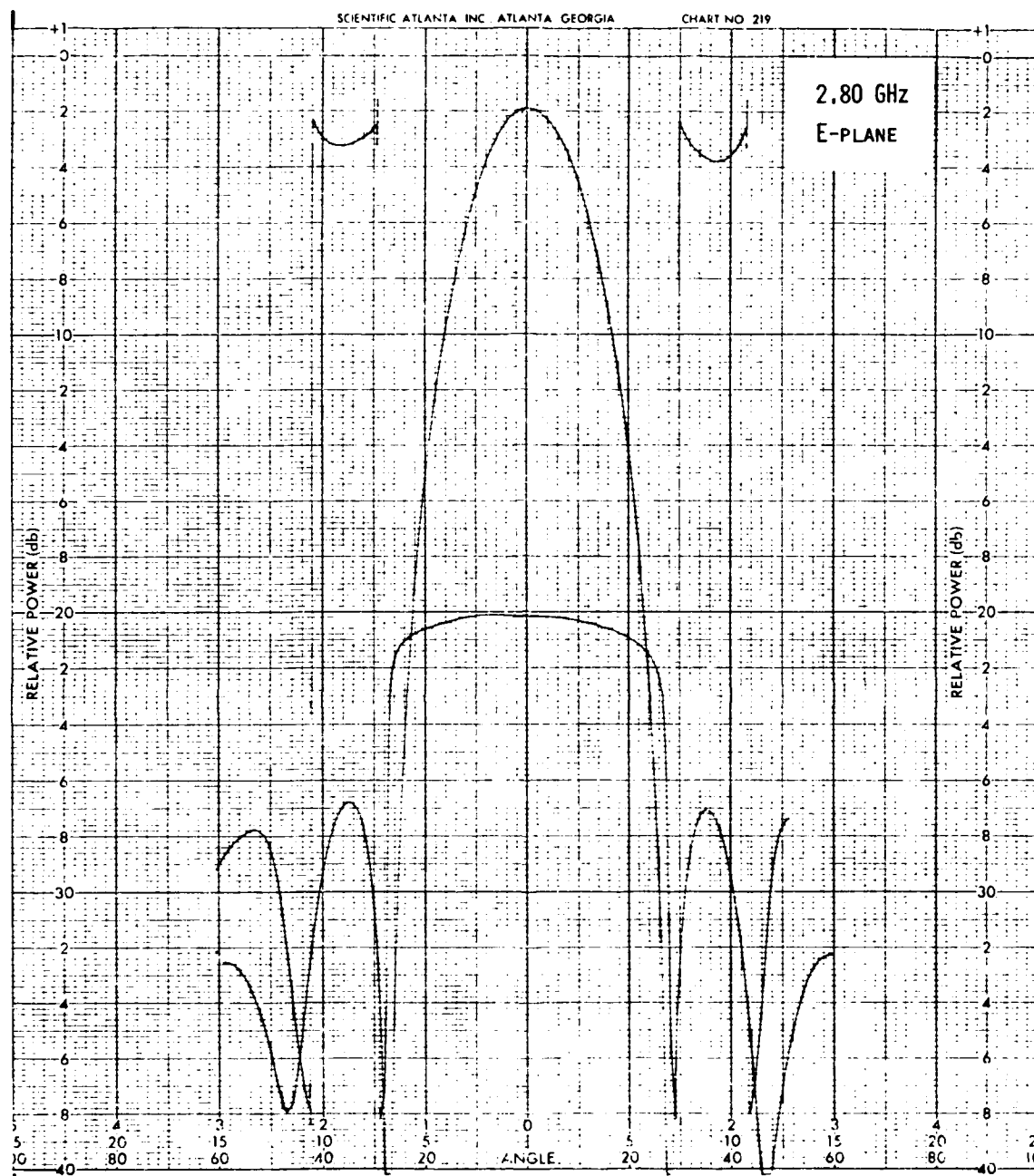


Figure 22. E-plane pattern of full-size feed, $f = 2.80$ GHz. Axis of rotation is same as in Figure 13.

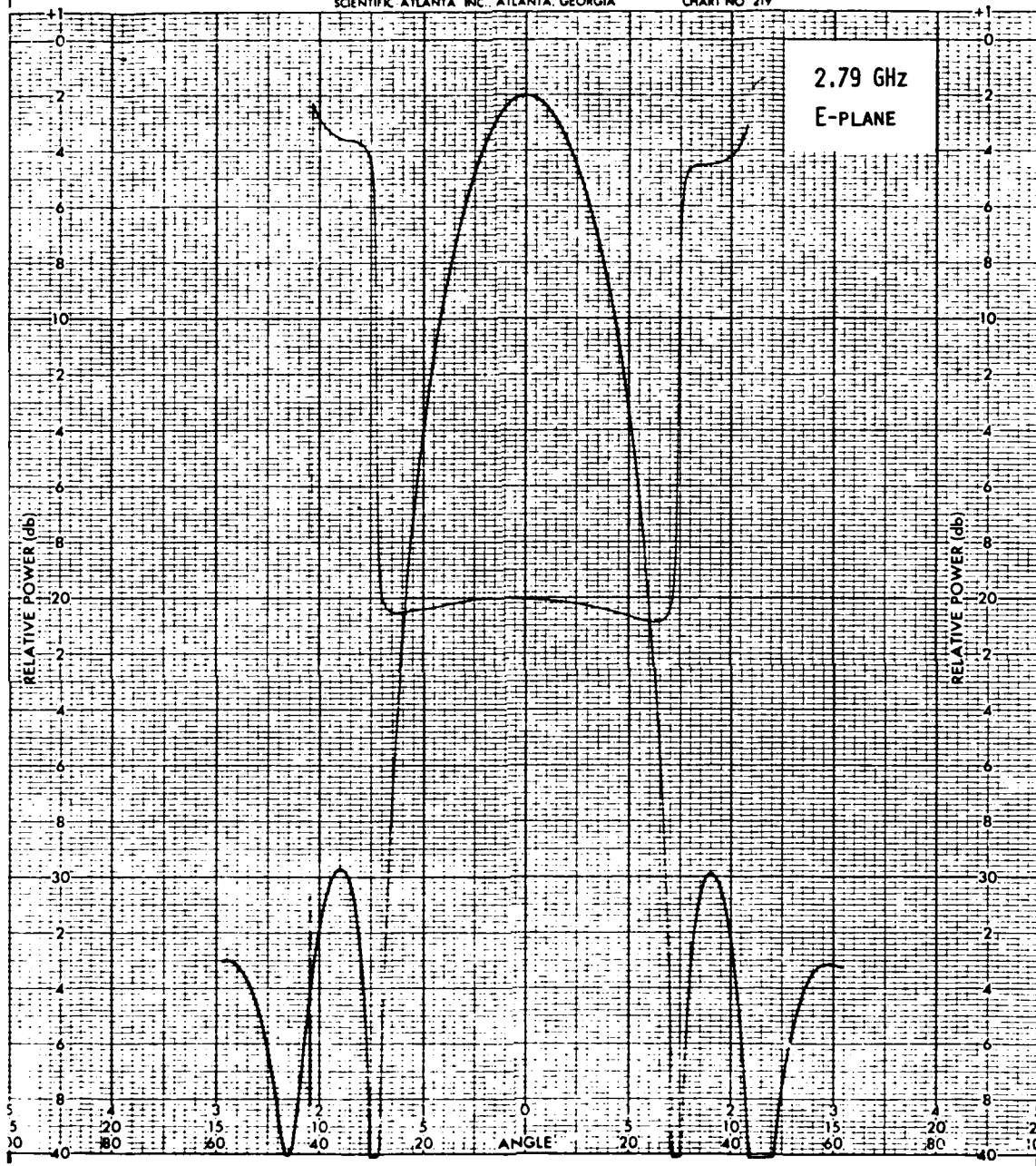


Figure 21. E-plane pattern of full-size feed $f = 2.79$ GHz. Axis of rotation is same as in Figure 15.

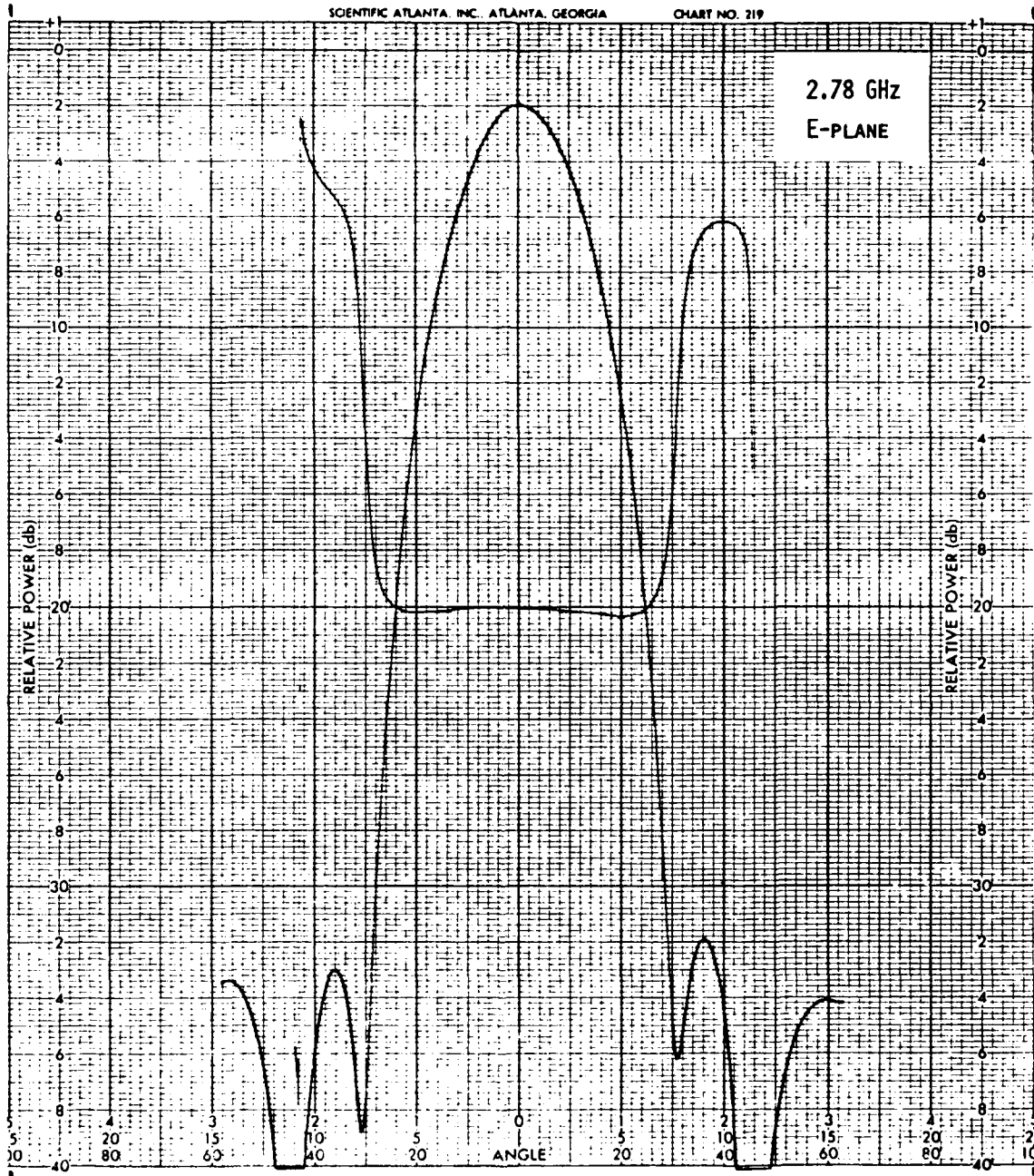


Figure 20. E-plane pattern of full-size feed, $f = 2.78$ GHz. Axis of rotation is same as in Figure 13.

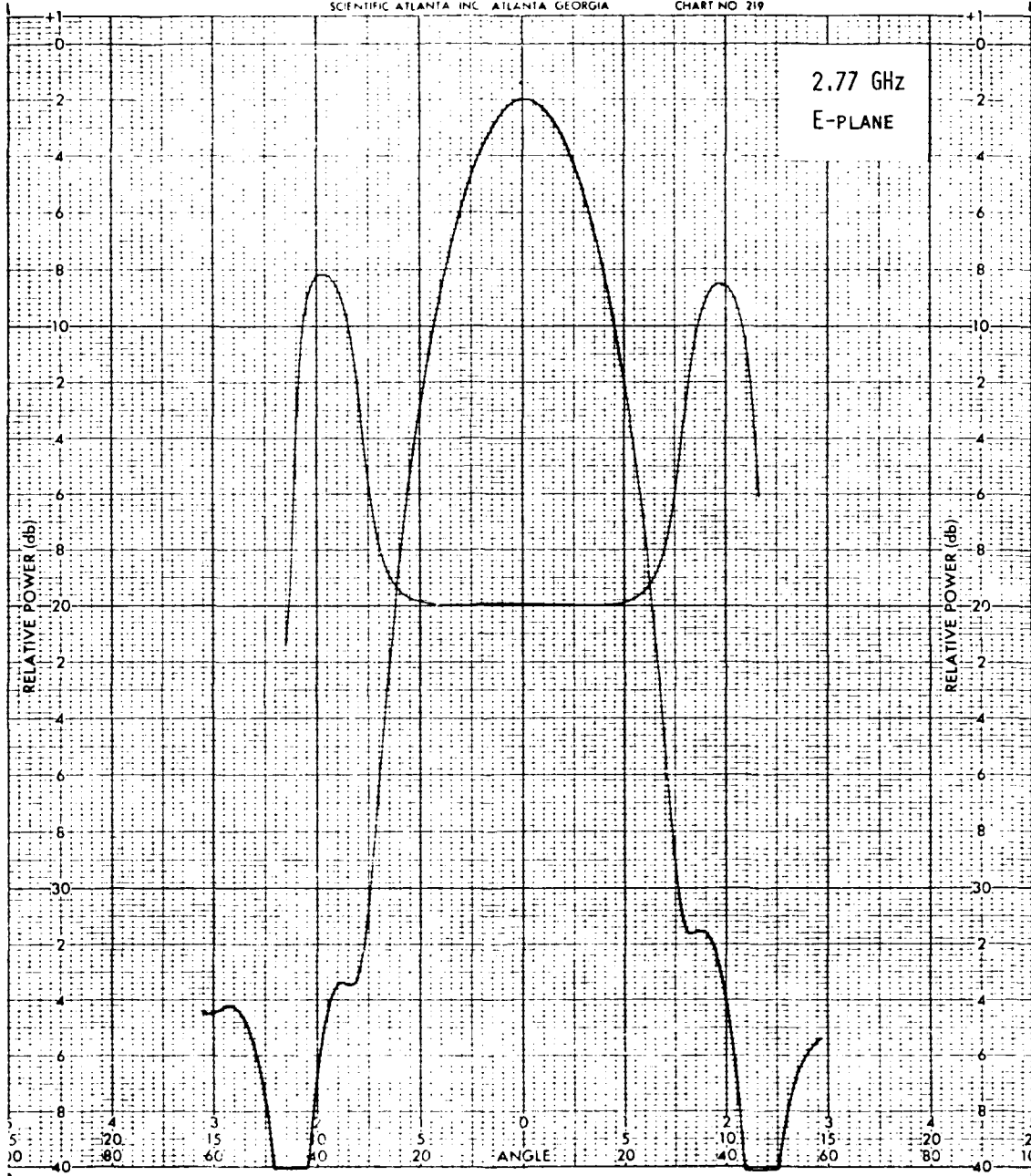


Figure 19. E-plane pattern of full-size feed, $f = 2.77$ GHz. Axis of rotation is same as in Figure 13.

profound statement by Jones and with future work by others including Ghobrial. In this paper it was shown that cross-polarization is a function of the electric field, the magnitude of the first cross-polarization lobe is far greater than that given by Jones, and the off-axis cross-polarization behavior of a Cassegrain antenna is superior to that of a front fed antenna, "due to the fact that the convex subreflector compensates to a high degree for cross-polarization caused by the concave main reflector." Later, Ghobrial and Futuh (1976) contradicted the last statement by showing that the polarization properties of Cassegrain antennas are identical to those of front fed antennas of equivalent focal length.

Prior to this, Ludwig (1973) presented three differing definitions of cross-polarization. According to the third definition, zero cross-polarization will result with a Huygens source feed (a physically circular feed with equal E and H amplitude patterns in all planes). Furthermore, he argued that the cross-polarization currents on a paraboloid illuminated by an infinitesimal electric dipole are often incorrectly attributed to reflector curvature. The electric dipole itself generates cross-polarization where it is viewed off axis by the reflector. Cross-polarization is then reduced by increasing the focal length of the paraboloid so that the reflector views less off-axis dipole energy.

We next examined the results of Dijk, et al. (1974). Here not only do the results for a short electric dipole feed agree with those of Jones, but also a practical example using an approximation of a Huygens source is given. Finally, polarization loss efficiency factor curves are presented for both open waveguide and electric dipole feeds as a function of subtended half-angle between the feed and the reflector. Polarization efficiency is defined as the ratio of total co-polarized antenna gain to the antenna gain if the cross-polarized energy were zero everywhere. This definition is in accordance with Potter (1967) and can be related to ICPR. Calculated examples were presented of polarization loss efficiency factor versus subtended half-angle for an electric dipole feed employed in a front fed paraboloid, Cassegrain antenna of various magnification factors, and a front fed paraboloid excited by an open waveguide structure operating in the TE_{10} mode. In the final example, it was shown that a Huygens source could not be attained with a rectangular or square aperture.

Finally, our investigation of linearly polarized reflector antennas continued to the effort of Ghobrial (1979) for an approximation to the cross-polarization calculations of Jones. Not only is there good agreement between these calculations, but also he derives an expression for peak cross-polarization which is related to the overall polarization efficiency, η ,

$$\text{peak cross polarization (dB)} = 10 \text{ LOG}_{10} \left| 0.29 \left(\frac{1}{\eta} - 1 \right) \right|. \quad (1)$$

Our conclusion is that, for a theoretical

axisymmetric reflector antenna without a feed support structure, the ICPR may be determined from a measurement of the level of one of the cross-polarization lobes.

Thus far, we have investigated reflector antennas with linearly polarized feeds. We conclude our review of the literature with an examination of a text by P. J. Wood (1980) which develops insight into the cross-polarization properties of reflector antennas with circularly polarized feeds. Wood has shown by his vector diffraction analysis method that circular cross-polarization lobes exist in phase quadrature with the co-polarized lobes and they have an absolute peak level of 8 dB_i independent of reflector diameter. Obviously, these lobes vanish in the optical limit, $\lambda/D \rightarrow 0$. For the AFGL antenna, the amplitude of the peak lobe then is approximately 35 dB below the main beam.

2.2 ANTENNA CONFIGURATION CONSIDERATIONS

2.2.1 Waveguide Location

While consideration was given to the merits of the various antenna geometries, equal consideration must be given to the equipment configuration imposed by those geometries. If the AFGL front fed antenna configuration were retained, then either two phase matched waveguide runs from the back of the reflector to the polarizer and feed horn assembly would be required, or the entire assembly consisting of RF switch, microwave circuit, and receiver would have to be located at the prime focus. Obviously, the latter is impractical as it would impose severe antenna blockage. Less obvious is the impossibility of placing only the feed horn at the focus with the polarizer behind the main reflector, as this configuration would place unrealistic voltage standing wave ratio (VSWR) requirements and thermal requirements upon the waveguide connections. These constraints dictate the use of a Cassegrain antenna configuration so that these components may be contained in a relatively small, environmentally controlled package located behind the reflector.

2.2.2 Minimum Focal Length

During this effort we determined that $ICPR_1$ must be less than -32 dB. Employing Equation (1) in conjunction with the efforts of Dijk and Ghobrial for both an open WR-284 waveguide feed and an electric dipole feed, we considered the focal length to diameter ratio (f/D) required to achieve this value of $ICPR_1$. The results of this calculation are presented in Figure 1, together with the results of $ICPR_1$ determined by the Georgia Tech reflector antenna program, a computer program developed to calculate the co- and cross-polarized pattern performance of single reflector and double reflector antennas. This program has been validated over the past several years not only with data Georgia Tech has obtained, but also with other data that have appeared in the literature. The program was utilized to analyze the amount of anticipated cross-polarization as a function of various reflector focal lengths. The results show that, while a -20 dB $ICPR_1$ can be obtained with the existing AFGL reflector, which has an f/D of 0.4 further improvement requires a

reflector with a longer focal length. Again, we are led toward a Cassegrain configuration as the focal length of the existing reflector can only be extended by employing a Cassegrain geometry.

2.2.3 Blockage and Unsymmetric Diffraction

Depending upon the feed arrangement and the choice of theory, the circular cross-polarization lobes should disappear or become almost insignificant; usually this is not the case. Experimentally, it can be shown that excessive aperture blockage will contribute diffracting surfaces which will increase cross-polarization as well as reduce overall antenna efficiency. Should a Cassegrain configuration be employed, reduction in antenna efficiency due to subreflector blockage can, in this instance, be discounted as it is given by the ratio of the square of the reflector diameters and for this antenna provides an almost unmeasurable effect on the total antenna gain. Diffraction from the main reflector edge, subreflector edge, feed horn edge, and support structure edges, on the other hand, can contribute energy into both the cross-polarized and co-polarized sidelobes. This diffraction contribution can be reduced by various methods, some of which are: (1) elimination of edges, (2) occultation of edges, and (3) employment of a symmetrical design. For the AFGL radar, the feed support will consist of a shroud wrapped around and behind the feed to occlude polarizer and feed reflecting surfaces. In the case of the latter consideration, detailed attention must be given to the overall axial symmetry of the entire antenna structure.

2.2.4 Antenna Configuration

Having considered the antenna geometries, we concluded that a Cassegrain affords the best compromise between focal length, feed location, blockage, and symmetry to produce favorable co-polarized and cross-polarized sidelobe architecture. We considered a third configuration, offset Cassegrain, as a possible geometry to eliminate illuminator blockage and further reduce these unwanted lobes.

In an axisymmetric antenna with a dipole feed, cross-polarization is generated in the aperture electric field by off-axis observation of the feed antenna; thus, cross-polarization has the property that it is oppositely directed in adjacent quadrants. Then by symmetry, cross-polarization cannot exist in the principal planes of the antenna, but does achieve a maximum value in the planes located midway between the principal planes. If a feed is constructed such that equal electric and magnetic dipole patterns are placed on the reflecting surface (Huygen's source), a second set of cross-polarized electric field vectors is generated by the magnetic field in the aperture which, in the case of axisymmetric reflectors, are equal and opposite to those generated by the electric field. In the case of an asymmetric reflector, an asymmetry exists because the distance between the subreflector and the upper main reflector quadrants is greater than the distance between the subreflector and the lower main reflector quadrants. In theory, this

distance variation can be ameliorated by an offset subreflector. The best achievement of such an arrangement has yielded an antenna with two -34 dB cross-polarized lobes (relative to the main beam) symmetrically displaced from the antenna's principal axis (Wilkinson and Burdine, 1980). The virtue of such an antenna is its capacity for a great reduction in the near co-polarized sidelobes; for this example, a 17 dB improvement was achieved, compared to the level expected for a conventional axisymmetric Cassegrain antenna.

In light of these achievements, this geometry was considered, but the cost of an appropriate development program quickly dispelled further attention.

2.3 SUBREFLECTOR MOUNTING STRUCTURE

Although not a direct consideration of the specific antenna geometry, the feed and subreflector mounting structure has a significant influence upon the sidelobe and cross-polarization lobe integrity. Maintenance of overall antenna symmetry is the foremost requirement of cross-polarization reduction if the proper feed assembly is used. Because of the quadrapole nature of the cross-polarized antenna pattern, symmetry cannot be preserved with a tripod secondary reflector mount or with the existing tripod feed mount. Either a bipod with support wires or a quadrapod structure is required. Furthermore, the attachment points for the mount must be located as close to the rim of the main reflector as possible. This reduces lobe structure by reducing blockage from the spars and, when a reasonable illumination taper is employed, by reducing the scattered energy level from the attachment points.

No special spar cross-section has been shown to reduce cross-polarization backscatter from the support spars; however, the location of the quadrapod structure does affect the cross-polarized sidelobe structure. Since the cross-polarized lobes are located in planes rotated by $\pi/4$ with respect to the horizontal and vertical planes, the spars should be positioned in the horizontal and vertical planes to minimize scattering of the cross-polarized energy. When considering ICPR however, this attention to spar location may not be necessary.

2.4 SUBREFLECTOR

While the specific detail of design for the hyperbolic subreflector is not a subject of this paper, an interesting addition to the subreflector shape was provided by Wilkinson. The center of the subreflector employed in circularly polarized earth station antennas is conically shaped so that a "hole" exists in the reflected pattern. This "hole" prevents reflected energy from re-entering the feed by radiating that energy beyond the rim of the main reflector. This is an important consideration in the design of circularly polarized reflector antennas. Should a mismatch exist within the polarizer, any energy reflected into the polarizer from the feed will be reflected at the mismatch and retransmitted with the opposite polarization sense.

This conical section should have a smooth taper into the hyperbolic subsection of the subreflector to prevent diffraction effects. The use of absorbing material in place of the conical section cannot be considered as it would provide an additional diffracting edge. In other instances, this conical section is replaced by a button located at the center of the subreflector. This button serves the same purpose of scattering rather than returning energy into the feed.

2.5 POLARIZER ASSEMBLY

Three polarizers were considered for this modification: (1) short slot hybrid coupler, orthomode transducer combination, (2) lossless power divider with an orthomode transducer, and (3) sloped septum hybrid. Each concept (Figure 2) employs attending phase shifting devices and attenuators to accommodate both linearly or circularly polarized transmission as well as reception of the transmitted and orthogonal polarizations. The selection criteria were based upon the requirement of a minimum -37 dB isolation between polarizations for circular polarization and -26 dB isolation between polarizations for linear polarization.

Thus far, the general design has not shown ICR_2 to be bounded to less than -40 dB. However, if consideration is given to the VSWR of the components attached to the hybrid junction within any polarizer configuration and to the equivalence of hybrid junction isolation with ICR_2 , then -40 dB isolation is most likely unachievable without VSWR improvement circuitry, while isolations of -35 dB to -37 dB are realistic, difficult-to-achieve anticipations. The validity of this realization exists because of the one-to-one mapping of VSWR and isolation of a hybrid junction (Riblet, 1952). A -40 dB polarizer isolation requires a VSWR < 1.02:1 on all ports of the hybrid, which is generally unachievable for microwave components operating over any reasonable bandwidth.

In analyzing each polarizer configuration we assumed an attached corrugated or multitaper feed horn with a VSWR of 1.025:1, required a minimum isolation of -35 dB for circular polarization, and determined that the components attached to the polarizer input ports must have a VSWR of 1.05:1 or less.

2.5.1 Short Slot Hybrid and Orthomode Transducer Polarizer

The minimum achievable VSWR for the transducer ports of this polarizer (Figure 2a) is insufficient to provide better than -30 dB polarization isolation. Although the combined transducer, phase shifter, waveguide flanges, bends, and transfer switch VSWR may be significantly reduced by an appropriate choice and location of matching hardware, such a design would present a formidable construction task and, in the end, might have insufficient high-isolation bandwidth as well as excessive phase dispersion across the signal bandpass.

2.5.2 Lossless Power Divider and Orthomode Transducer Polarizer

The input E and H arms of the magic tee in

the lossless power divider (Figure 2b) do not suffer the same isolation constraints as a hybrid junction unless the reflections from the colinear arms are in quadrature. The divider can certainly be constructed so that the reflections are in phase over a small bandwidth. However, taken as an entity, the lossless power divider exhibits the equivalent isolation and VSWR characteristics as the single hybrid junction, so that the same requirements are also enforced for the microwave components between the power divider and the orthomode transducer. If less isolation could be tolerated, then this polarizer does offer the flexibility of transmission in any elliptical polarization and reception of that polarization and the orthogonal polarization.

2.5.3 Sloped Septum Polarizer

Obviously, the polarizer of choice, when operating in a circular mode, should involve as few microwave components as possible between the transmitter and the feed antenna so that full advantage of the low VSWR of the feed could be utilized. Therefore, such a device must be capable of directly generating the proper circular polarization from each waveguide input. A sloped septum polarizer (Figure 2c) is such a device. It is described in Chen and Tsandoulas (1973) and in Saltzberg (1978). The polarizer is a true hybrid coupler with two input ports and a common output port; exciting one input port causes the excitation voltage to be equally divided with one division receiving a 90° phase lag prior to entering the square output port; radiation exiting this port is circularly polarized. This device also obeys the VSWR versus isolation rule of the previous polarizers such that a minimum of attached components must exist in the high isolation circular polarization mode, while more attached components are tolerated in the less demanding linear polarization mode. Linear polarization is achieved by adding a hybrid coupler between the source and the polarizer to provide an appropriate 90° phase shift and allow equal amplitude excitation of the input ports (Figure 2c). Since transfer switches with a VSWR of less than 1.05:1 are obtainable, the possibility of constructing a -37 dB isolation feed assembly exists if a very low VSWR horn feed antenna is employed.

2.6 FEED ANTENNA

Various horn antennas were candidate feeds for this modification. The first consideration, a pyramidal horn, can be easily attached to the polarizer, requires no square-to-circular waveguide transition, and is inexpensive to manufacture. However, this feed can be shown to be equivalent to an orthogonal pair of magnetic dipoles and will give rise to high off-axis cross-polarization (Nelson, 1972). This effect has also been noted experimentally by Wilkinson. The second feed under consideration was a circular multitaper horn which can be designed with equal E and H plane patterns but only for a relatively narrow bandwidth. Since the third feed considered, a corrugated horn, can meet all the requirements of this design, but at a relatively high cost, the multitapered

design was chosen for further investigation. An experimental multitaper horn was successfully constructed for 9.4 GHz in April 1983. Over a large portion of its pattern, it represents the attributes of a true Huygens source with equal E and H patterns in all planes.

2.7 ANTENNA SUMMARY

Using -32 dB as the ICPR₁ requirement, a minimum focal length of 230 inches is required ($f/D = 0.8$). This is based upon linear polarization considerations only; cross-polarization in the circularly polarized mode is only the result of antenna, feed and polarizer imperfections; it is independent of focal length.

A quadrapod mounting structure consisting of cylindrical spars attached near the reflector rim offers the optimal sidelobe and cross-polarization reduction condition. Furthermore, no structure visible to the subreflector should be employed to support the feed assembly as such a support would encourage scattering and might detract from overall symmetry. This requires the feed support be wholly contained within a shroud that is, with respect to the secondary reflector, occluded by the feed horn.

For high isolation in the circular mode and respectable isolation in linear polarization a sloped septum polarizer with a hybrid coupler or magic tee to provide linear polarization is the polarizer of choice. Finally, to maintain costs within reasonable bounds, for a relatively narrow high-isolation frequency band (± 200 MHz at 9.4 GHz) a multitaper horn is the feed of choice. Specific recommendations for the antenna modification are presented in Table 3.

TABLE 3. RECOMMENDATIONS FOR ANTENNA MODIFICATION OF AFGL RADAR

Requirement	Recommendation
Antenna Configuration	Cassegrain with $f/D > 0.8$
Number of Support Spars	4
Support Spar Cross-Section	Circular
Feed/Polarizer Supports	Entire assembly must be covered by axisymmetric shroud
Secondary Reflector	Hyperbola with center half-conical section or VSWR button
Secondary Reflector Pattern Taper	About -10 dB on reflector edges
Feed Antenna	Multitaper horn or corrugated horn
Feed Antenna VSWR	$< 1.025:1$
Polarizer	Sloped septum
VSWR at Polarizer Input Ports	$< 1.05:1$
Anticipated ICPR ₂	> -35 dB
Anticipated ICPR ₁	> -26 dB

3 MICROWAVE PACKAGE

3.1 THERMAL REQUIREMENTS

The microwave package contains those components which interface with the transmitter, receiver, and polarizer and, as such, must be capable of operating at the transmitter power level as well as be able to withstand heating due to losses. These components must critically maintain polarization isolation phase, and amplitude balance during transmission and reception. This can only be accomplished if the microwave package and non-video portions of the receiver are thermally stabilized and located as close as possible to the antenna feed

assembly. In this instance, the operating temperature is dictated by the phase stability of the most unstable component. We believe that component to be the transmit-receive circulator and we have performed a cursory phase versus temperature experiment on the existing unit. The temperature at which the minimum phase change was observed was between 42.5°C and 45°C. Since this temperature is close to the expected maximum summer ambient temperature inside the radome, we recommend a complete heat exchanger system for the microwave package and receiver enclosure.

3.2 POLARIZATION ISOLATION IMPROVEMENT NETWORK

In an attempt to improve the polarization isolation, an improvement network has been conceptually included in the design. Various candidate VSWR reduction schemes are possible for the interconnections of the various microwave components, but the final choice of the specific solution will depend upon the achieved characteristics of the RF switch, polarizer, and feed antenna. One scheme under consideration (Hollis et al., 1980) is employed in the K_u-band radar at the National Research Council of Canada. We have confirmed that this scheme can be constructed to be effective over the required bandwidth; however, when the transmitter power of the AFGL radar was considered, little isolation improvement could be realized with reasonable component values.

VSWR improvement is also realizable by adding reactive devices into the microwave package. However, the magnitude and location of those devices can only be ascertained after the complex reflection values of the microwave components have been determined. The isolation improvement network, then, remains a concept; its necessity will be determined after the interconnected microwave components such as the antenna including the polarizer and high speed polarization switch are evaluated.

3.3 HIGH POWER RADIO FREQUENCY SWITCH

The RF polarization switch is the only other device currently thought to limit the polarization isolation performance of the modified radar. The basic high speed waveguide switch employs a configuration of phase shifters, magic tee, and short slot hybrid. Switching transmitted energy between output ports is achieved by appropriate setting of the phase shifters. Although reception of backscatter is available at orthogonal polarizations in the E and H arms of the magic tee, the polarization isolation at these ports may not be as great as that achieved upon transmission. In a more conservative design, backscatter is received through circulators located in each of the arms between the RF switch and polarizer.

Two designs have been proposed to realize the isolation requirement of the RF switch: (1) three switches connected in a series-parallel configuration and (2) a variation of a previously successful approach wherein a logic-based update network sampled the main and isolated ports and adjusted the current in each of the phase shifters to correct for isolation

deficiency. Since all variations employ a hybrid coupler in their design, the isolation limitation is a function of VSWR, both external and internal to the switch. The VSWR presented to each port of the switch must be carefully controlled.

A mechanical switch was also considered. Of the varieties that exist, none can approach the switching time or other performance characteristics of an electronic device. Shutter switches are available with switching speeds in the 10 millisecond region, rotary switches are an order of magnitude slower, and the ingenious fast rotating devices employed on differential reflectivity radars do not afford the liberty of variable PRF and cannot attain the low VSWR demanded by the polarizer for circularly polarized modes.

4. RECEIVER

The general requirements of the receiver were considered up to, but not including, the processor. Of these, three unique critical requirements exist: phase tracking, amplitude tracking, and inter-channel isolation. Gross phase and amplitude balance will be maintained throughout by careful component selection, thermal control, and phase/amplitude trimmer assemblies inserted at strategic locations. Critical phase and amplitude tracking errors will be eliminated in software via a look-up table. While the object of this design was to retain a maximum of present components as well as present operating features, some existing hardware must be altered to maintain phase and amplitude tracking and to improve inter-channel isolation.

4.1 INTER-CHANNEL ISOLATION

To realize the full 37 dB isolation offered by the antenna feed assembly, the minimum receiver inter-channel isolation must be greater than 45 dB, a value confirmed by McCormick (1981). Furthermore, McCormick has suggested that to avoid a conspicuous data error, a minimum 55 dB isolation is necessary. Three paths which affect intra-channel isolation must be considered: (1) cross coupling in the local oscillator channel, (2) coupling via receiver coaxial cables, and (3) coupling via the DC power supply lines. The last two mechanisms can be reduced to insignificant levels by employing good engineering practices and, in the case of the RF signal path, employing copper semi-rigid cables. Cross-coupling via the local oscillator channel can be reduced by minimizing the VSWR seen by the hybrid couplers employed as power dividers and by the use of isolators prior to each of the mixers.

4.2 SENSITIVITY

Noise figure is a measure of overall system sensitivity. A low system noise figure is as important as an increase in transmitter power; an improvement in noise figure provides the same overall performance improvement as a likewise increase in transmitter power, but at a considerably reduced cost.

The noise power level presented to antenna terminals of an ideal receiver is related to the source temperature, T_s , and the receiver effective temperature, T_{eff} , such that, for situations where $T_s = O(T_{eff})$, improvements in noise figure will yield slightly better improvements in overall sensitivity than would be expected from the noise figure improvement alone. In this design, for example, utilizing an overall 5 dB noise figure will result in a noise floor -109.2 dBm/MHz during observation of -40°C (223°K) ice clouds. Under the same conditions, however, a 3 dB improvement in overall noise figure will result in a 3.5 dB improvement in noise floor so that an observational sensitivity of approximately -112.7 dBm/MHz will be realized.

Another factor which will contribute to sensitivity degradation in the superheterodyne receiver is reception of the unwanted mixer sideband which contributes 3 dB of noise. This sideband can be suppressed either by a preselector, located either prior to the front-end low noise amplifier (LNA) or between the LNA and the mixer, or by a sideband suppression mixer. If a preselector is located prior to the LNA, it adds a front-end insertion loss which is equivalent to an increase in noise figure by the value of the insertion loss. Usually, however, the preselector loss is only on the order of 1 dB, so that an overall improvement results. On the other hand, if a preselecting filter is placed between the LNA and the mixer, little sensitivity degradation will result. While this location is appealing on the basis of sensitivity considerations, it does not preselect out-of-band signals from the LNA. Likewise, a sideband suppression mixer does not offer LNA preselection. Since intense out-of-band signals that would require LNA preselection do not normally exist at the site of the AFGL radar, post LNA preselection was chosen to simplify the design.

4.3 DYNAMIC RANGE

Two definitions of receiver dynamic range exist: (1) overall dynamic range, defined as the operating range of the receiver from the noise floor to the 1 dB signal compression point, and (2) the spurious free dynamic range (SFDR), defined as the operating range from the noise floor up to a power level at which spurious signals are processible.

The 1 dB compression point is an order of magnitude more coarse than our requirement. As a rule of thumb, the 0.1 dB compression point (the linearity requirement for this modification), is approximately 10 dB less than the 1 dB compression point. Furthermore, most amplifier manufacturers define the 1 dB compression point as an output value; the system designer must be careful to subtract the amplifier gain so that the 1 dB or 0.1 dB compression point is referenced to the amplifier input. From a calculation of the expected return energy from each form of hydrometeor, assuming a minimum radar range of 1 kilometer and using a transmitter level of +88 dBm with a two-way antenna gain of +84 dB, the maximum expected signal at the receiver input was

determined to be -8 dBm. This design then requires a dynamic range of approximately 109 dB, which is impossible to achieve with present logarithmic amplifiers so an alternate method must be used to expand the receiver's dynamic range.

In most receivers, a form of automatic gain control (AGC) is available to reduce the RF and intermediate frequency (IF) amplifier gain as the return signal level is increased. However, AGC removes the power level measurement capabilities of the receiver unless the AGC voltage is carefully calibrated and monitored. Another method to increase overall dynamic range is to minimize the RF amplifier gain and electronically remove the IF preamplifier when the expected return approaches receiver compression; the computer, cognizant of this condition, adjusts its processing accordingly. We have chosen this latter method in conjunction with a logarithmic amplifier capable of a 90 dB dynamic range.

The dynamic range of a receiver is also limited by spurious responses which are accepted by the processor. These spurious responses, known as intermodulation products (IMP), are internally generated in the low noise amplifier and mixer from external sources. The frequencies of these products are given by (McVay, 1967)

$$F_{\text{spur}} = \pm nf_1 \pm mf_2, \quad (2)$$

where n,m are integers.

In this design, only those values where $n + m = 3$ are of concern as the resultant signals are close to frequencies which can be received and converted to the intermediate frequency by the mixer. However, for these signals to be processible by the receiver of a pulsed radar, they must be the product of continuous carrier sources, in which case they may be characterized as such and reduced or eliminated.

Because of the dual transmitters employed in this radar (2710 MHz and 2760 MHz), a possible corruption of power channel data by velocity channel data, and vice versa, does exist, as the spurious frequency sideband energy generated from one channel is in the nearby spectrum receivable by the other channel. While this is a valid argument for LNA preselection, at present, only IF filtering has been considered for the elimination of this cross-channel IMP.

4.4 IF FILTER

The IF filter fulfills two missions: it determines the overall system noise floor and it provides the required selectivity. Exact choice of an IF filter is not a trivial task, as the filter and the RF amplifier essentially determine the receiver performance.

For optimum signal-to-noise receiver performance of a pulse modulated signal, the IF half-power bandwidth must be approximately 1.2 times the reciprocal of the transmitted pulse width or, in this design, 1.2 MHz. However, to minimize phase dispersion across the filter

bandpass in the class of filters known as planar filters (Chebishev, Butterworth, and elliptic), a half-power IF bandwidth of 4 MHz is required.

The importance of filter skirt selectivity cannot be overstressed; many designs do not extend filter specifications beyond the bandwidth of the halfpower points which fails to specify the attenuation at frequencies further from the center frequency. If thought is given to the frequency sideband energy of the transmitted channel opposite to the receiver channel under consideration, then a moderate degree of data corruption may be caused by many factors such as the range, type of hydrometeors observed, and spectral distribution of the transmitter pulse. A moderate skirt selectivity requirement exists as some of the spurious frequencies generated within the LNA and given by Equation (2), which are the result of the two transmitted signals, are only 10 MHz removed from the anticipated received signal.

This condition exists when both the Doppler channel and the reflectivity channel return pulses are received simultaneously. We calculate that two -39 dBm signals into the low noise amplifier are required to generate an IMP at the receiver noise floor. Since a 1 dB increase in input level will cause a 3 dB increase in output level for third order IMP, returns greater than -36 dBm into the receiver will begin to degrade the data. We calculate that returns exceeding this level are expected infrequently. The elimination of this IMP then depends upon the filter skirt selectivity chosen so that the interfering pulse "sidebands" are attenuated into the noise. This condition may not be possible, as good skirt selectivity and phase dispersion are divergent from one another in planar filters.

4.5 LOCAL OSCILLATOR AND MIXER

While all of the present components are retained in the local oscillator chain, additional components are added to provide increased intra-channel isolation, phase balance, and amplitude balance. The increased losses of these items require a slight amplification of the local oscillator signal level so that the mixers may be operated in a lower distortion region. By further increasing this amplification, high intercept point mixers can be employed with the result that the overall receiver 1 dB compression point is sufficiently increased to be wholly determined by the RF amplifier. The original radar utilized phase locked loop oscillators. A filter following each oscillator is required to prevent the high spurious output of the oscillator from entering the mixer as these spurious components will allow the receiver to capture unwanted signals. Since spurious signals occur within 600 kHz of the local oscillator frequency, a high Q, thermally stable, cavity filter is required.

5 CONCLUSION

In the foregoing discussion we have presented the key design elements of the antenna, microwave package and receiver. Although we have considered only the highlights,

we have concentrated on the antenna, as this appears to be the most critical component of the system. We have also shown that the radar, including all its components, must be considered as an entity.

Antenna cross-polarization
Depends on the waveguide location.

Is Cassegrain best?
Let's put it to test
To get us the most isolation.

The IF filter skirt selectivity
Should reduce the system proclivity
For frequencies spurious.
But don't let them worry us--
We'll cut down their net transmissivity.

Mother Nature, they say, is a bitch,
Always looking to find us a glitch.

And so, in the end,
Everything will depend
On the high power microwave switch.

6. ACKNOWLEDGEMENTS

The authors thank Mr. E. J. Wilkinson of GTE International Systems for insight into antenna cross-polarization. This effort was supported by AFGL Contract Nos. F19628-81-K-0027 and F19628-82-K-0038.

7. REFERENCES

- Dijk, J., van Diepenbeek, C. T. W., Maanders, E. J., and Thurlings, L. F. G., 1974; "The Polarization Losses of Offset Paraboloid Antennas," IEEE Trans. Ant. Prop., AP-22, pp. 513-520.
- Ghobrial, S. I. and Futuh, M. M., 1976; "Cross-Polarization in Front-Fed and Cassegrain Antennas with Equal f/D Ratio," 1976 Region V IEEE Conf. Digest, p. 277.
- Ghobrial, S. I., 1979; "Off-axis Cross-Polarization and Polarization Efficiencies of Reflector Antennas," IEEE Trans. Ant. Prop., AP-27, 4, p. 460-466.
- Glover, K. A., Armstrong, G. M., Bishop, A. W., and Banis, K.J., 1981; "A Dual Frequency 10 CM Doppler Weather Radar," preprints 20th Conference on Radar Meteorology, Boston, MA.
- Hollis, J. S., Hickman, T. G., and Lyon, T. J., 1970; "Polarization Theory," Microwave Antenna Measurements Handbook, Chapter 3, Scientific Atlanta, Atlanta, Ga.
- Jones, E. M. T., 1954; "Paraboloid Reflector and Hyperboloid Lens Antennas," IRE Trans. Ant. Prop., AP-2, pp. 119-127.
- Ludwig, A. C., 1973; "The Definition of Cross-Polarization," IEEE Trans. Ant. Prop., AP-21, 1, p. 116-119.
- Ming Hui Chen and Tsandoulas, G. N., 1973; "A Wide-Band Square-Waveguide Array Polarizer," IEEE Trans. Ant. Prop., AP-21, 5, pp. 389-391.
- McCormick, G. C., 1981; National Research Council of Canada (retired) Granville Ferry, Nova Scotia, Canada, personal communication.
- McVay, F. C., 1967; "Don't Guess the Spurious Level," Electronic Design, 3, February 1, pp. 70-73.

- Nelson, E. A., 1972; "Polarization Diversity Array Design (PDAD)," General Electric Co., Aerospace Electronic Systems Dept., Utica, NY.
- Potter, P. D., 1967; "Application of Spherical Wave Theory in Cassegrainian-Fed Paraboloids," IEEE Trans. Ant. Prop., AP-15, pp. 727-736.
- Riblet, H. J., 1952; "The Short Slot Hybrid Junction," Proc. IRE, 40, 2, pp. 180-184.
- Saltzberg, E., 1978; "Microwave Hybrid Polarizer," U.S. Patent No. 4,122,406.
- Silver, S., Ed., 1949; Microwave Antenna Theory and Design, New York, NY: McGraw-Hill, pp. 417-423.
- Watson, P. A. and Ghobrial, S. I., 1972; "Off-Axis Polarization Characteristics of Cassegrain and Front-Fed Paraboloidal Antennas," IEEE Trans. Ant. Prop., AP-20, 6, pp. 691-698.
- Wilkinson, E. J., and Burdine, B. H., 1980; "A Low Sidelobe Earth Station Antenna for the 4/6 GHz Band," GTE International Systems Corp. Report.
- Wood, P. J., 1980; Reflector Antenna Analysis and Design, IEE, London and New York.

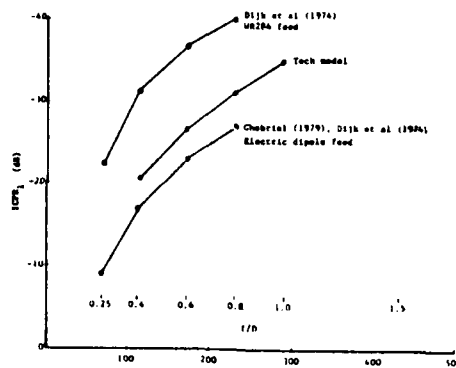


Figure 1. ICPR, for various feeds and f/D for an axisymmetric parabolic reflector antenna.

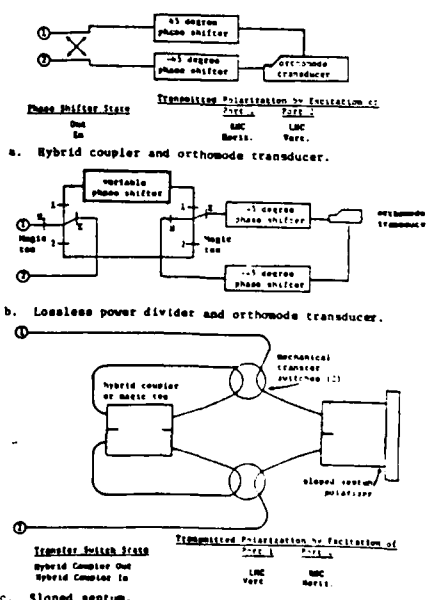


Figure 2. Candidate polarizer configurations.

APPENDIX B

ANTENNA STATIC
AND
DYNAMIC STRUCTURAL ANALYSIS

ER - 100 - 1

DESIGN REVIEW

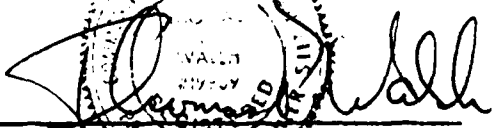
Prepared For

GEORGIA INSTITUTE OF TECHNOLOGY

Prepared By

H & W INDUSTRIES, INC.
COHASSET MASS.

Signed


Thomas P. Walsh, P.E.

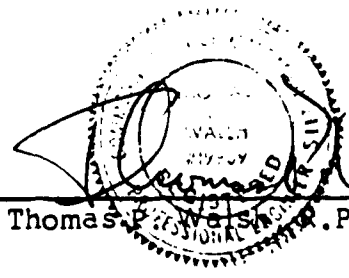


TABLE OF CONTENTS

1. Specification Review
2. Analysis Review
 - A. Static
 - B. Dynamic
3. Figures
 - A. The Math Model
 - a. Side Elevation View
 - b. Face View
 - c. Isometric
 - B. Static Deflections
 - a. Due to Elevation Rotation from 90° to 60°
 - b. Due to Elevation Rotation from 90° to 30°
 - c. Due to Elevation Rotation from 90° to 0°
 - d. Due to Temperature Change of 20°F
 - e. Due to 30 MPH frontal wind at elev = 0°
 - f. Due to 30 MPH Wind, 120° off boresite, at elev. = 0°
 - C. Dynamic Mode Shape
 - a. Face View
 - b. Side Elevation View
 - c. Plan View
4. Computer Readout
 - A. Final Static Run
 - B. Initial Static Run Output
 - C. Dynamic Output
5. Drawings
 - A. Subreflector #40166
 - B. Subreflector Support Assembly #40170
 - C. Feed Support Assembly #40171

1.0 Specification Review

Paragraphs 2.2, 2.3 and 2.4 of the Contract Statement of Work comprise the specification for the work to be performed under the present contract. Those paragraphs are copied below.

2.2 STATIC AND DYNAMIC STRUCTURAL ANALYSIS

Upon receipt of initiation letter, contractor shall determine the reflector deformations that may occur as a result of various natural and operational effects upon the reflector, subreflector, subreflector support assembly, and feed support assembly. Contractor shall also determine deformations, if any, that may occur within the support spars and subreflector. The effects shall include, but not be limited to:

1. dead weight distortion as a function of elevation angle,
2. seasonal thermal charges both with and without the radome,
3. wind loading distortion,
4. thermal charges due to shadowing, (out)
5. inertial loading distortion in both azimuth and elevation planes and
6. vibrational characteristics including those of the spars created by vortex shedding.

Servo-Loop resonances shall also be considered. Contractor shall send a preliminary report of this information to Georgia Tech within 60 days of initiation. Georgia Tech shall determine the impact of such deformations upon antenna performance, and may at their opinion request further investigation should the present reflector appear unsuitable. Such further investigation may include, but not be limited to, consideration of different spar support systems, or the addition of strengthening members to the reflector support assembly.

2.3 FEED SUPPORT AND SUBREFLECTOR SUPPORT

Upon receipt of initiation letter, contractor shall design and construct a structure to support a multi-taper circular horn feed antenna whose exterior length is approximately 60" and maximum outside diameter approximately 32". Adjustment and adjustment locking devices shall be incorporated within the design to allow precise location of the feed horn. The exterior of the horn and support structure shall be surrounded by a concentric, axisymmetric shroud assembly.

The contractor shall also design and construct a quadrapod subreflector support assembly. This assembly shall attach as closely to the perimeter of the main reflector as practicable and shall be designed to minimize resonances due to vortex shedding and other effects. This assembly shall allow for a six (6) inch axial adjustment range and a three (3) inch radial adjustment range as well as adjustment locking devices so that one sub-reflector can be precisely located and locked in position. For the purposes of these designs, the contractor shall consider both the condition with, and the condition without a radome enclosure surrounding the antenna assembly.

Prior to design finalization of these assemblies, Georgia Tech shall supply the exact dimensions of the feed horn assembly as well as the exact size, shape, and location of the subreflector assembly.

2.4 SUBREFLECTOR

Upon receipt of initiation letter, contractor shall construct a hyperbolic subreflector of a size not to exceed three feet in diameter. The subreflector shall contain a VSWR reduction button; the subreflector shall interface with, and mount upon the subreflector support assembly. Georgia Tech shall determine the shape and size of the subreflector.

2.0 Analysis Review

The reflector structure from the base of the hub to the apex of the subreflector support was modeled and analyzed via the finite element computer program, "Star-dyne". Both static and dynamic analyses were performed.

A. Static Analysis

The Static Analysis evaluated the following cases:

<u>Case</u>	<u>Subject</u>
1	Horizon Point, Dead Load Deflections & Stresses
2	Elevation = 30°, Dead Load Deflections
3	Elevation = 60°, Dead Load Deflections
4	Elevation = 90°, Dead Load Deflections
5	Elevation Rotation from 90° to 60°
6	Elevation Rotation from 90° to 30°
7	Elevation Rotation from 90° to 0°
8	Seasonal Temperature Change of 20°
9	Effects of a 30 MPH Frontal Wind
10	Effects of a 30 MPH Quartering Wind (120° off boresite)
11	Effects of a 10°/sec Rotational Acceleration

The input and output of the final run of the Static Analysis is included in Section 4. The output of this run was limited to deflections only. The output of the initial run is also included in Section 4. That run computed deflections for all cases and stresses for Cases 1, 8, 9, 10, and 11. The maximum stresses for those cases are listed below:

Case 1	1448 psi	due to dead load
Case 8	2750 psi	due to thermal effects
Case 9	192 psi	due to 30 mph frontal wind
Case 10	Negligible	due to 30 mph quartering wind
Case 11	Negligible	due to 100/sec rotational inertia

Considering the Aluminum Association Specification, allowable stress for 6063-T5 Aluminum (lowest strength alloy in the reflector) is 6500 psi, we can consider the stress levels acceptable. Further considerations relative to stress levels are:

1. The spar cross-sectional area has increased from 2 x 2 x 1/8 wall square tube in the initial run to 4" OD x 3/16 wall round tube in the final run. This change was implemented to lower the subreflector support deflections. An attendant stress effect is to halve the Case 1 stress of 1448 psi.

2. The math model assumed the base of the reflector hub to be fixed. In fact, the hub is attached to a steel structure. The thermal effects, therefore, are based on an aluminum structure with a coefficient of thermal expansion of 13×10^{-6} in/in/deg, expanding relative to a base interface with an expansion of zero. This analysis has utilized the most conservative possible end condition. In fact, the end condition could be either a continuous steel structure with a coefficient of thermal expansion of 8.6×10^{-6} in/in/deg or a steel structure with one end attached to a floating bearing. That is, the continuous structure would be one where both elevation bearings react loads parallel to the elevation shaft vs. one where one bearing takes radial load only. In the first case, the deflections and stresses of Case 8 would become $(1 - \frac{8.6}{13})$ or 34% of the calculated values; and in the second case, they would approach zero.

The above calculations and observations result in reflector stresses which are acceptable for all combinations of position, wind and thermal effects.

The significant reflector deflections of Cases 5 through 11 are plotted in Figures B.a. through B.f. These topographic plots are made joining points of equal deflections. Plots B.a., B.b., B.c. and B.f. are characteristically horizontal plot lines indicating the reflector is deflecting so as to generate an elevation pointing error. Plots B.d. and B.e. are characteristically polar deflection plots indicating a defocusing effect. We have RMS(ed) the nodal deflections

parallel to the boresight for the reflecting surface and tabulated the results below:

<u>Case</u>	<u>RMS (Nodes 1 - 96, Deflection X3)</u>
5	.0035"
6	.0062"
7	.0074"
8	.0031"
9	.0019"
10	< .001
11	< .001

All the above can be decreased by best fitting the data. Cases 5, 6, and 7 can be improved by rotating the coordinate system about the elevation axis and Cases 8 and 9 can be improved by calculating a change in the best fitting focal length. The magnitude of the tabulated data precludes the necessity of best fitting.

The sub.reflector support deflections due to elevation rotation can be obtained by reviewing deflections for Nodes 211, 222, 233 and 244.

<u>Case</u>	<u>X₂ Deflection - Final Run</u>
5	-.022
6	-.037
7	-.041

These deflections are approximately 1/2 the magnitude of their values for the initial run. The deflections appear acceptable in all cases.

B. Dynamic Analysis

The Dynamic Analysis extracted the first seven modes of vibration. See Section 4C. Since vibrations above 10HZ will have little or no effect on the servo band pass, the computer was programmed to extract and define all mode shapes with a frequency of 10HZ or less. Only one mode was found less than 10HZ at 7.799 HZ. The mode shape is defined in figures C.a., C.b. and C.c. In addition, the next six modal frequencies were calculated, (between 13 and 24 HZ). A review of the fundamental frequency mode shape shows it to be the torsional mode with the reflector structural components rotating around the hub. It is interesting to note that for this case, the spars do not depart greatly from their undeformed straight line shape. We can therefore expect the spars not to vibrate until at least 13 CPS.

The calculated individual spar resonant frequency is 27 HZ. Given a Strouhal number of .2 (tubes) the vortex street shedding frequency will coincide with the spar natural frequency at wind velocities about 30 MPH. The forces transmitted to the structure at this wind velocity will be sufficient to cause problems. We recommend that if the unit is to be used without the radome, a helical wind of small dia tube (approx. 5/8 dia) be wound along each spar at a pitch of approximately 2 feet.

The dynamic characteristics in all other respects are acceptable.

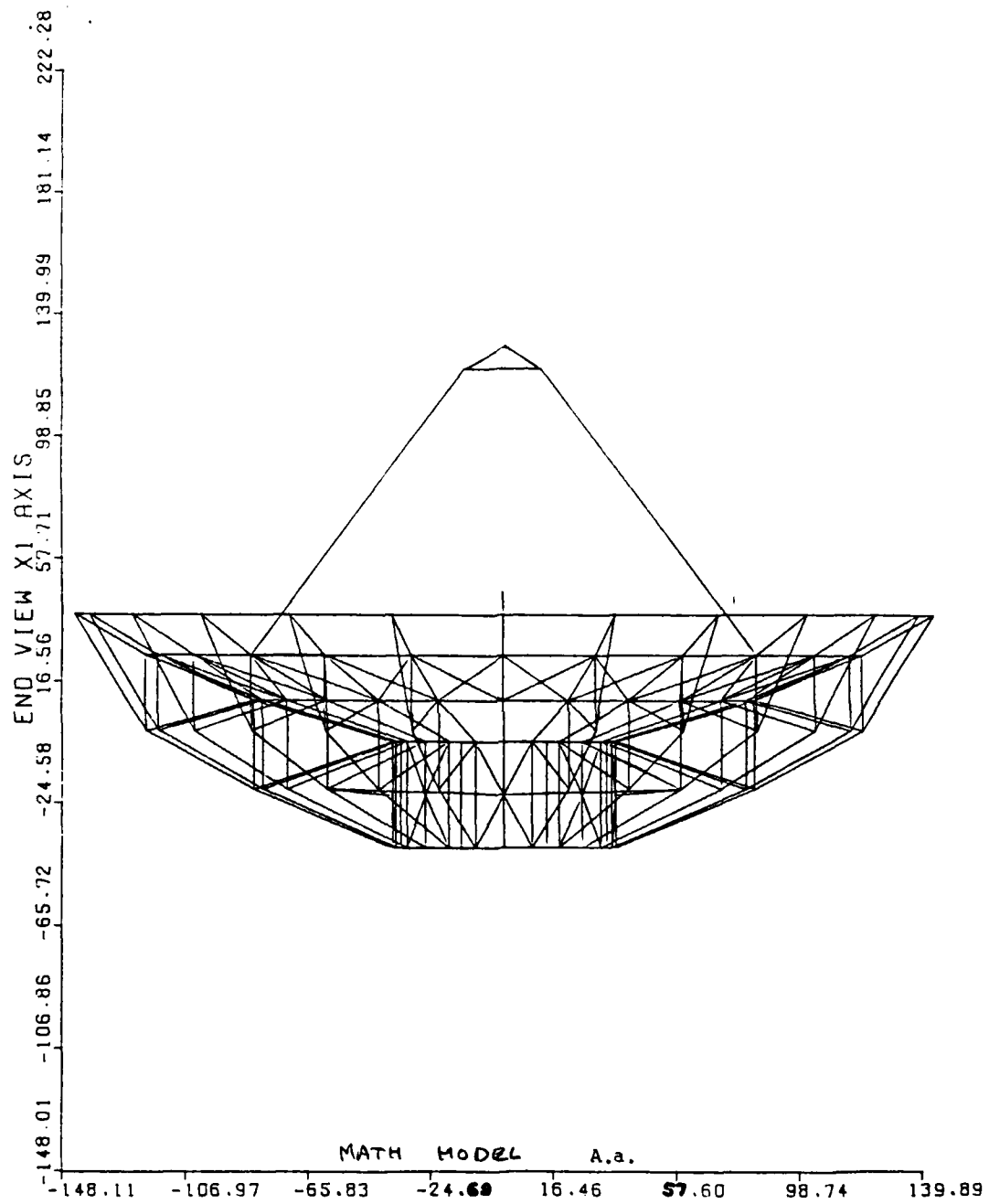


Figure A.a. The mathematical model, side elevation view.

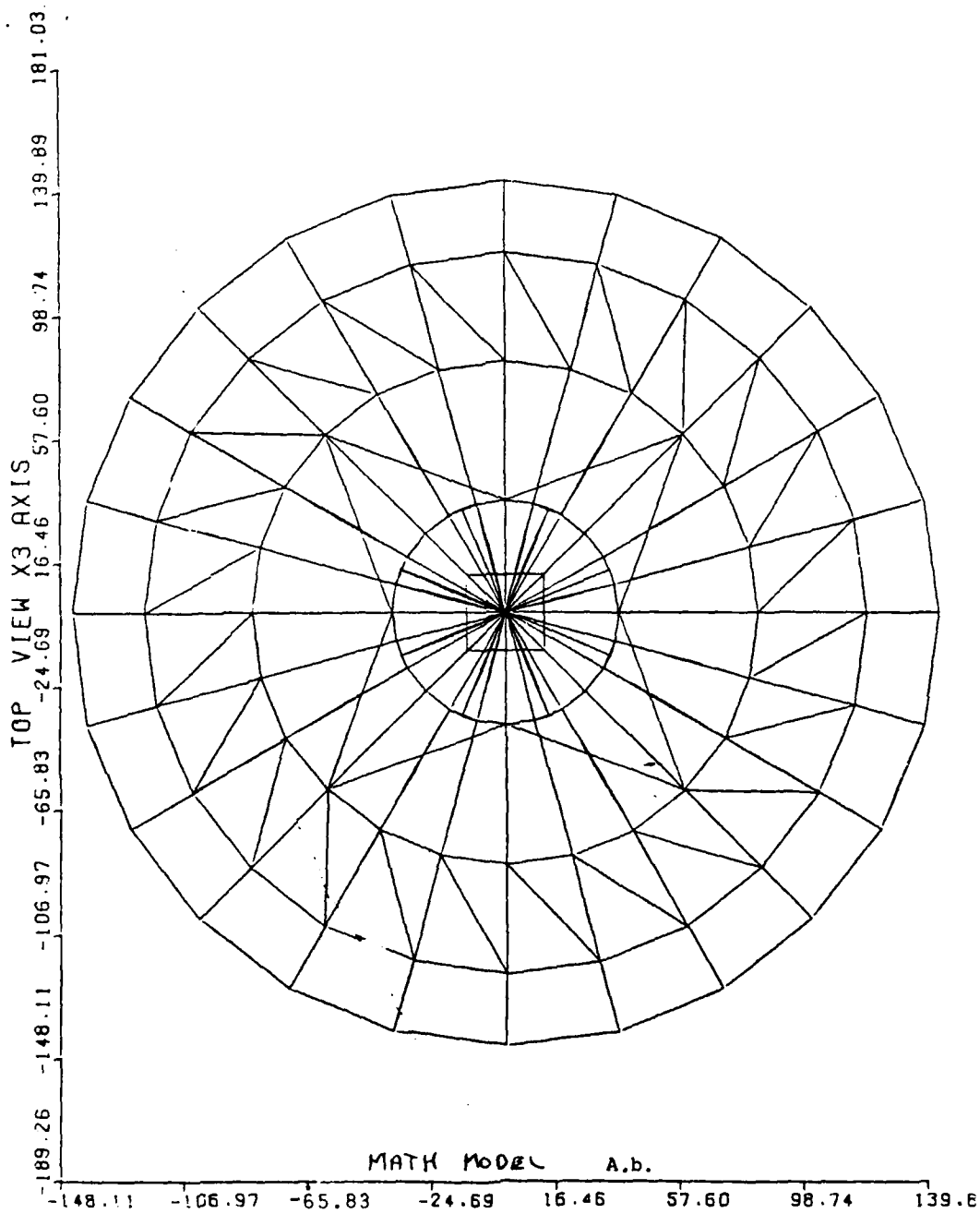


Figure A.b. The mathematical model, face view.

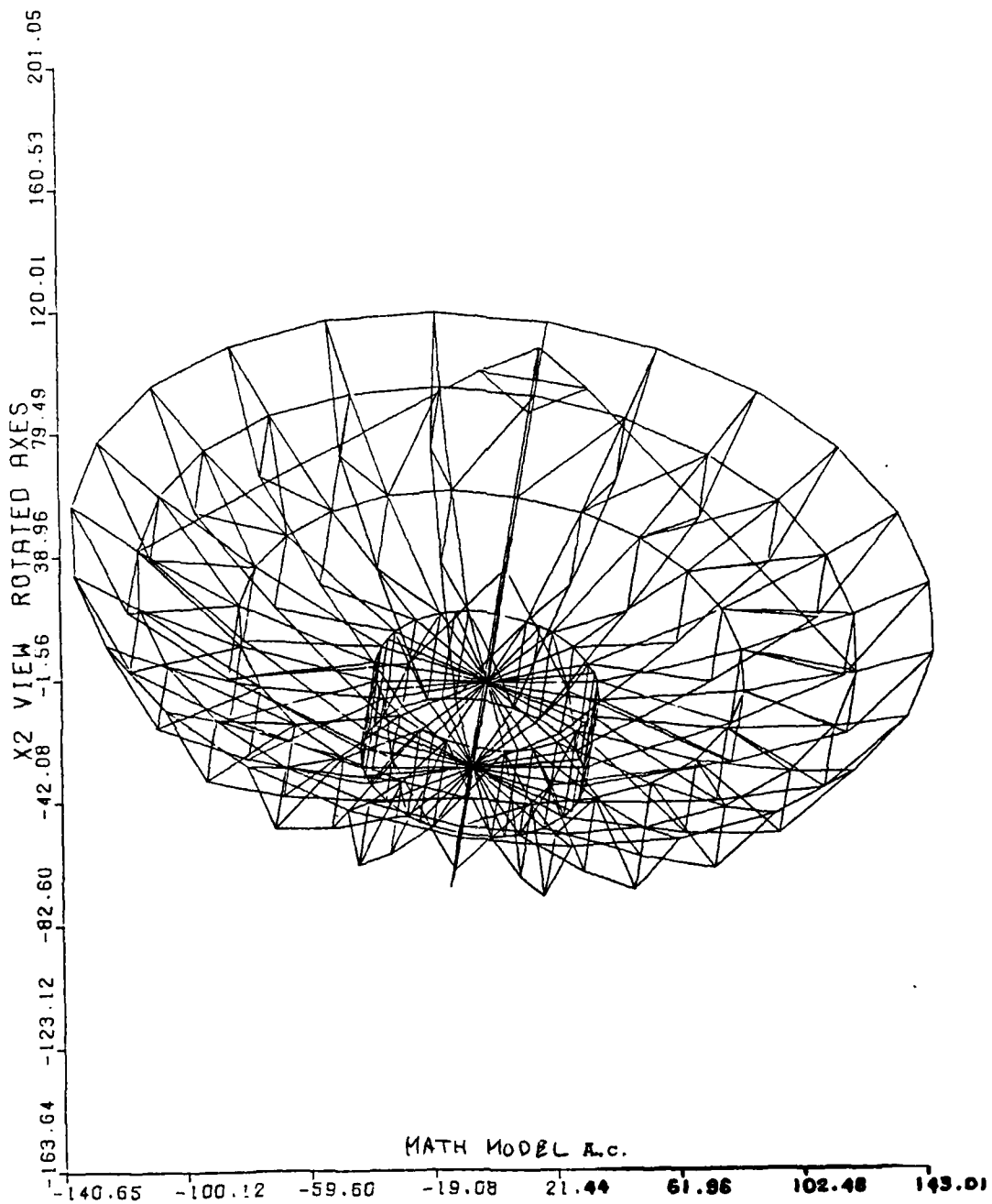
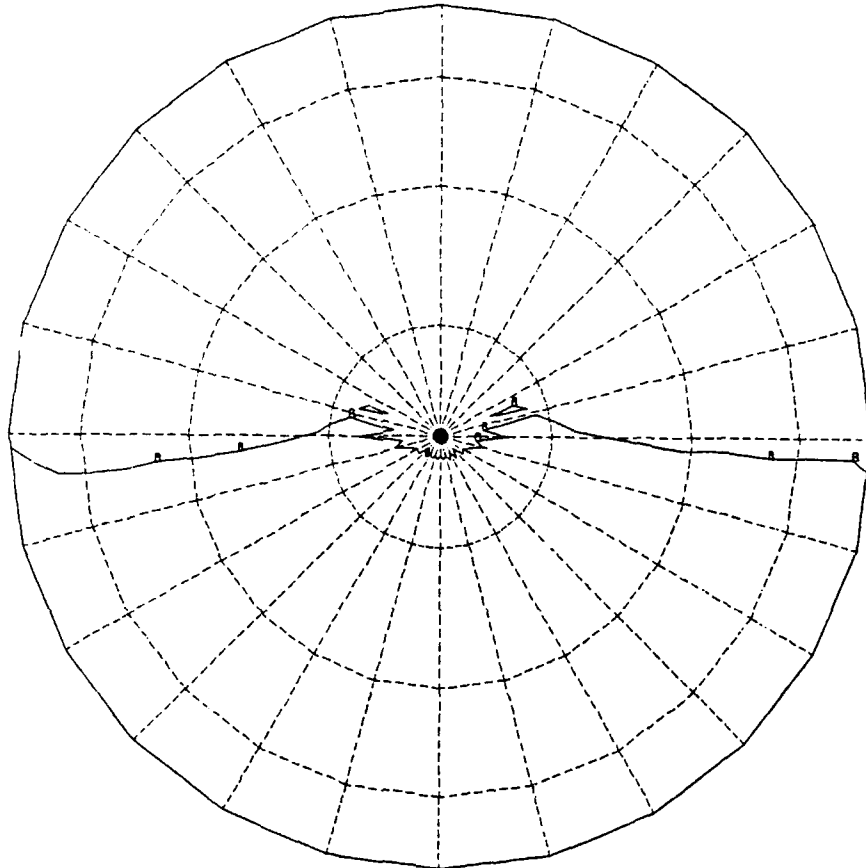


Figure A.c. The mathematical model, isometric view.

DEFLECTIONS NORMAL TO SURFACE



CONTOUR LEVELS
MIN -.80386E-02
A -.80386E-02
B .13391E-03
C .83064E-02
MAX .83064E-02

PLOT OF NORMAL DISPLACEMENT DUE TO EL. ROTATION FROM 90° TO 60°
STAR TAPE4 VECTOR NO 5
B.a. SCALE = 33.682

Figure B.a. Static Deflection, Plot of Normal Displacement due to Elevation Rotation 90° to 60°.

DEFLECTIONS NORMAL TO SURFACE

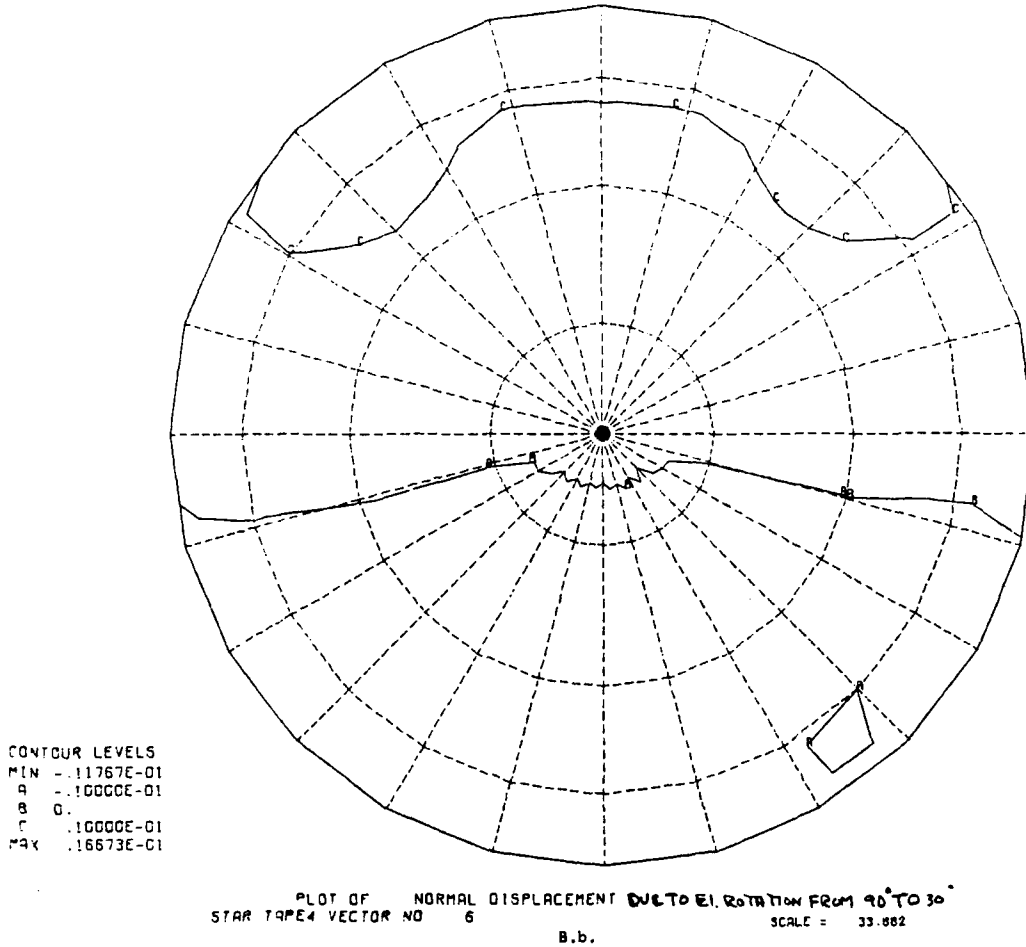


Figure B.b. Static Deflection, Plot of Normal Displacement due to Elevation Rotation from 90° to 30°.

DEFLECTIONS NORMAL TO SURFACE

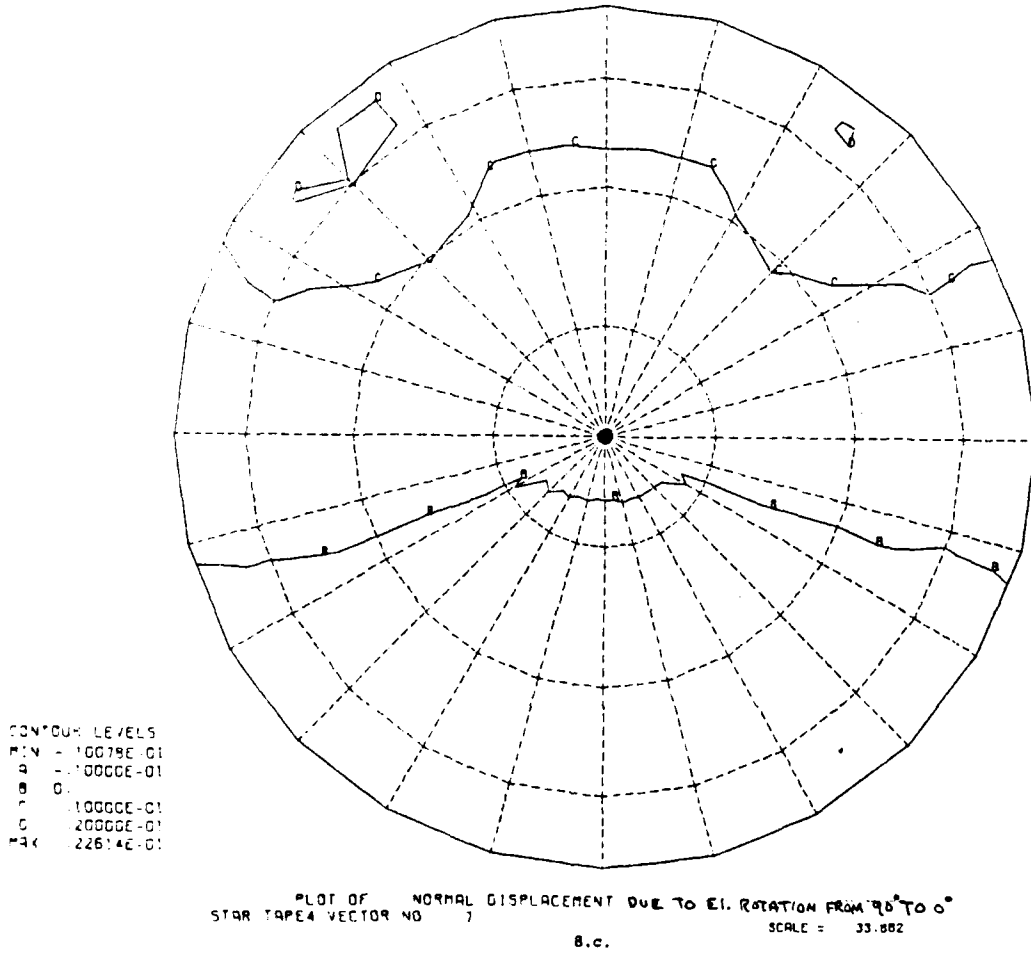
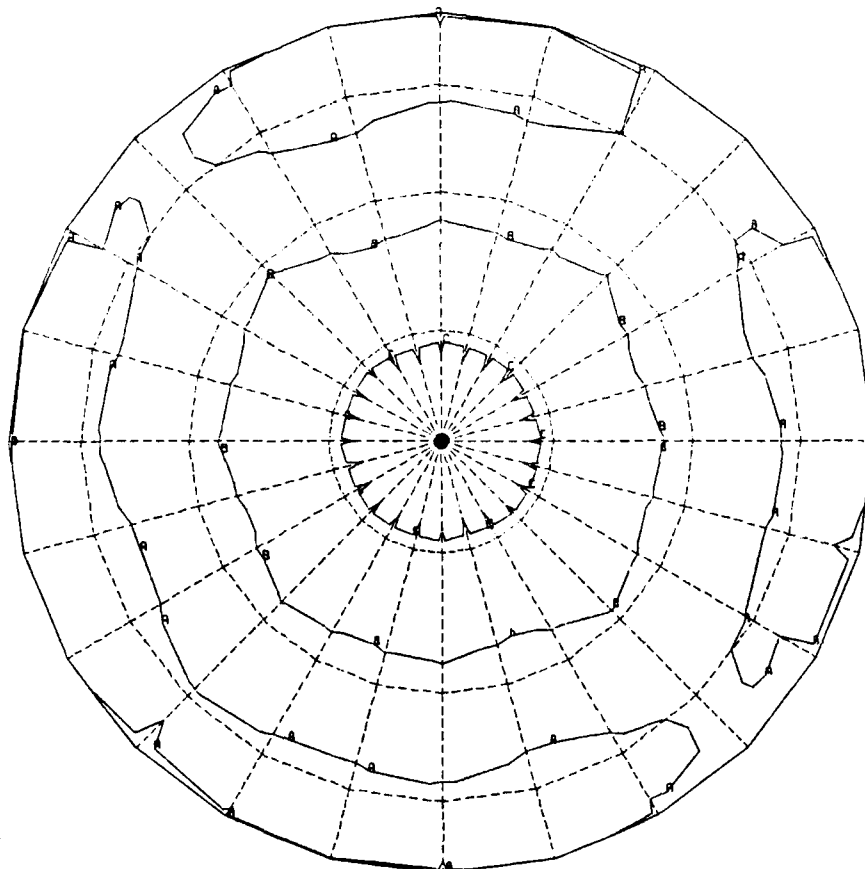


Figure B.c. Static Deflection, Plot of Normal Displacement due to Elevation Rotation from 90° to 0°.

DEFLECTIONS NORMAL TO SURFACE

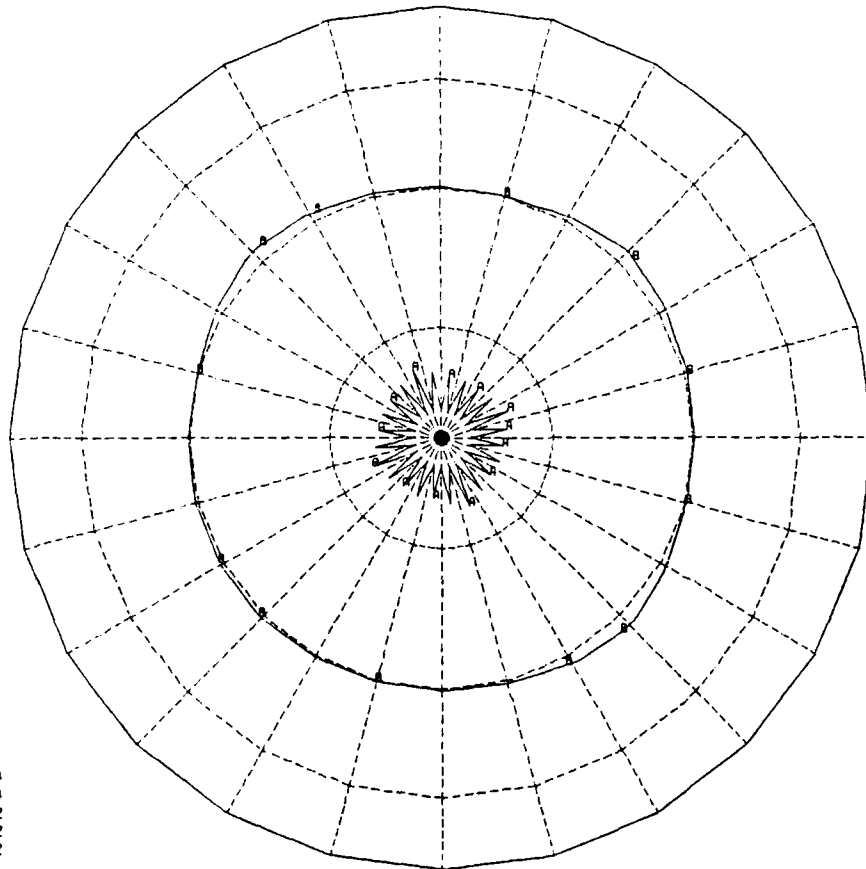


CONTOUR LEVELS
MIN -.16891E-01
A -.10000E-01
B 0.
C .10000E-01
MAX .12117E-01

PLOT OF NORMAL DISPLACEMENT DUE TO Δ TEMP = 20°F
STAR TAPE4 VECTOR NO 8 B.d. SCALE = 33.882

Figure B.d. Static Deflection, Plot of Normal Displacement due to Δ Temperature = 20°F.

DEFLECTIONS NORMAL TO SURFACE

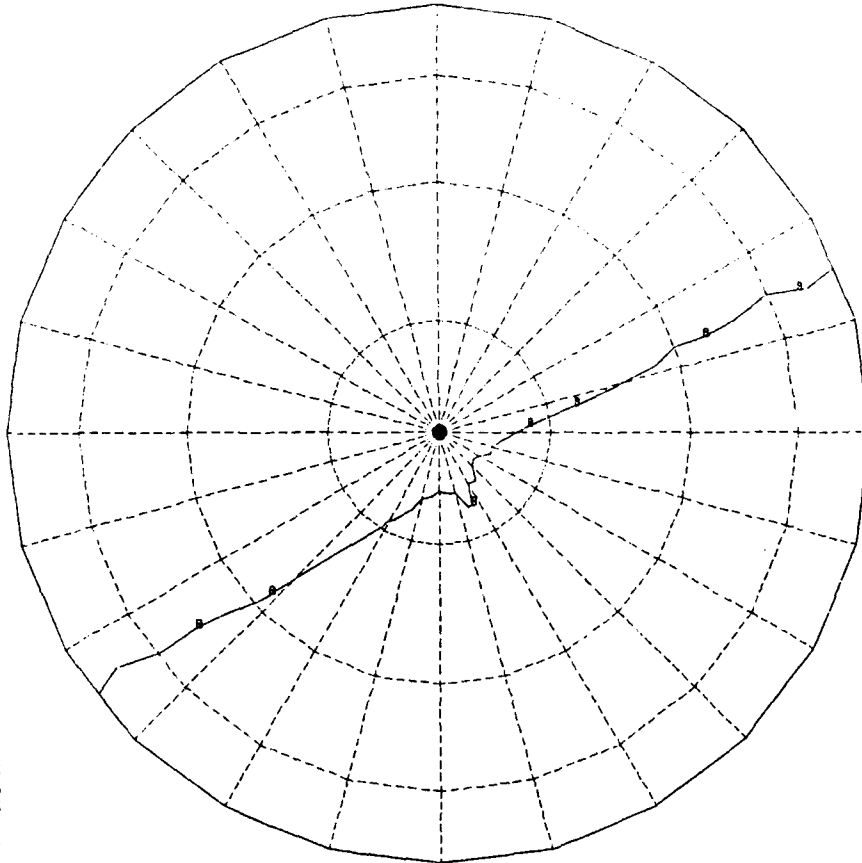


CONTOUR LEVELS
MIN .83570E-04
A .83570E-04
B .24903E-02
C .48971E-02
MAX .48971E-02

PLOT OF NORMAL DISPLACEMENT DUE TO 30 MPH FRONTAL WIND
STAR TAPE4 VECTOR NO 9
B.e. SCALE = 33.882

Figure B.e. Static Deflection, Plot of Normal Displacement due to 30 MPH Frontal Wind.

DEFLECTIONS NORMAL TO SURFACE



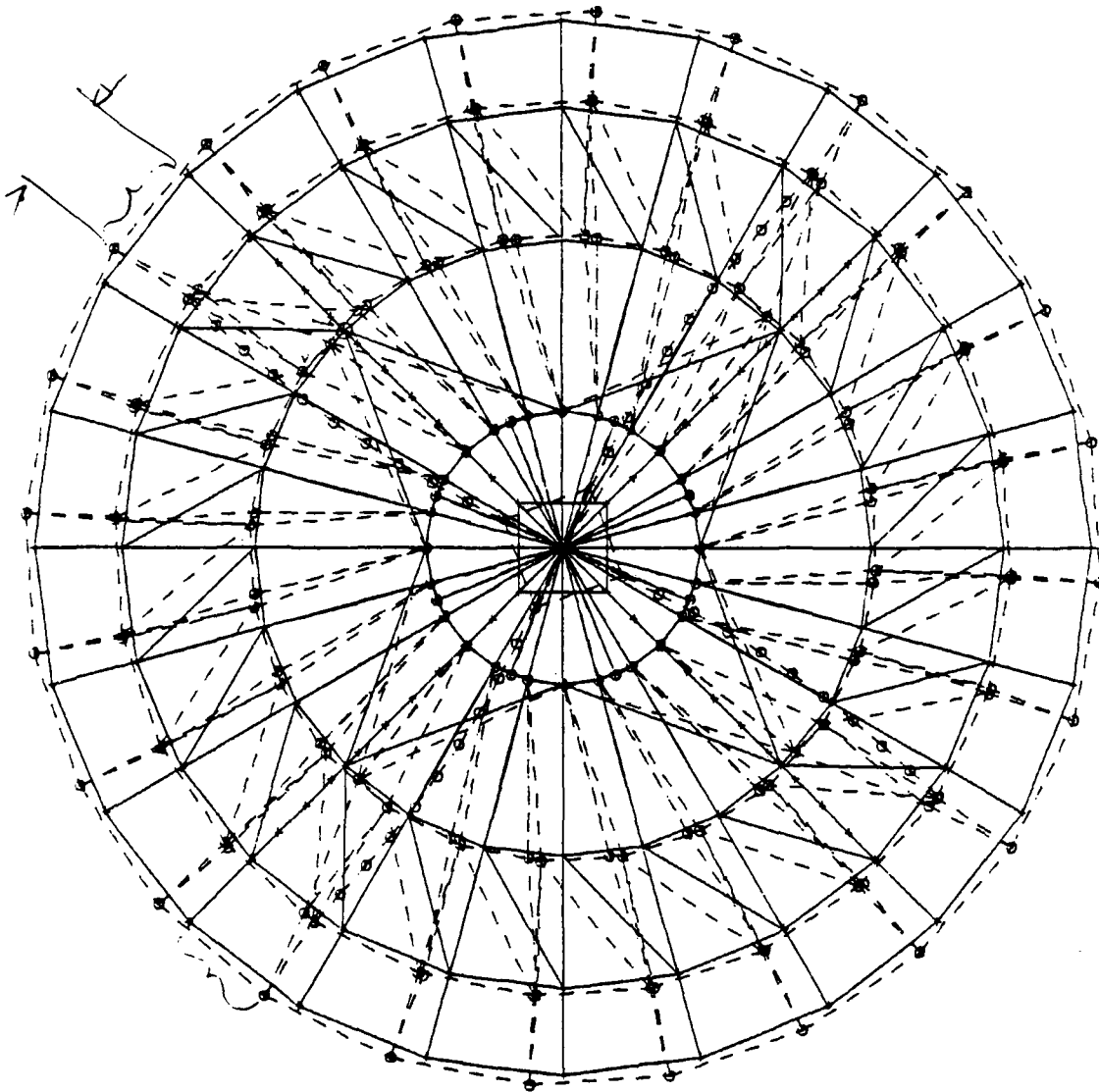
CONTOUR LEVELS
MIN - .31321E-05
A - .31321E-05
B .43222E-05
C .11779E-04
MAX .11779E-04

PLOT OF NORMAL DISPLACEMENT DUE TO 30MPH QUARTERING WIND
STAR TAPE4 VECTOR NO 10 SCALE = 33.882
B.f.

Figure B.f. Static Deflection, Plot of Normal Displacement due to 30 MPH Quartering Wind.

MODE SHAPE NO 1 FREQ=7.799HZ.

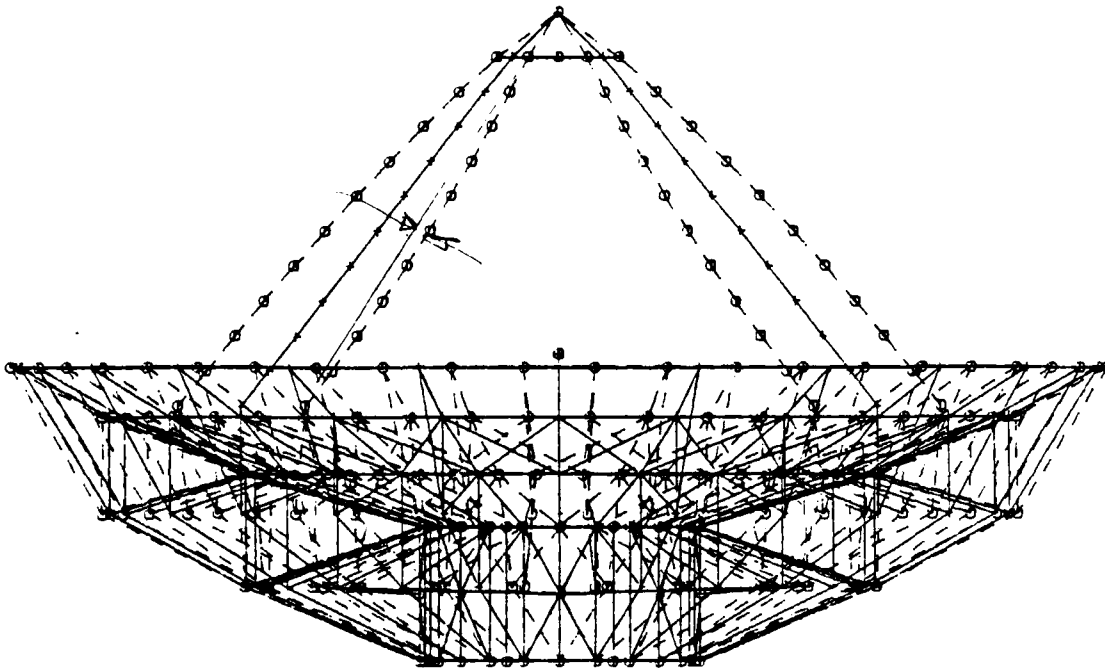
DISPLACEMENT CASE 1



STARBYNE FINITE ELEMENT MODEL PROJECTION ON X1-X2 PLANE CASE NO. 1

Figure C.a. Dynamic mode shape, face view.

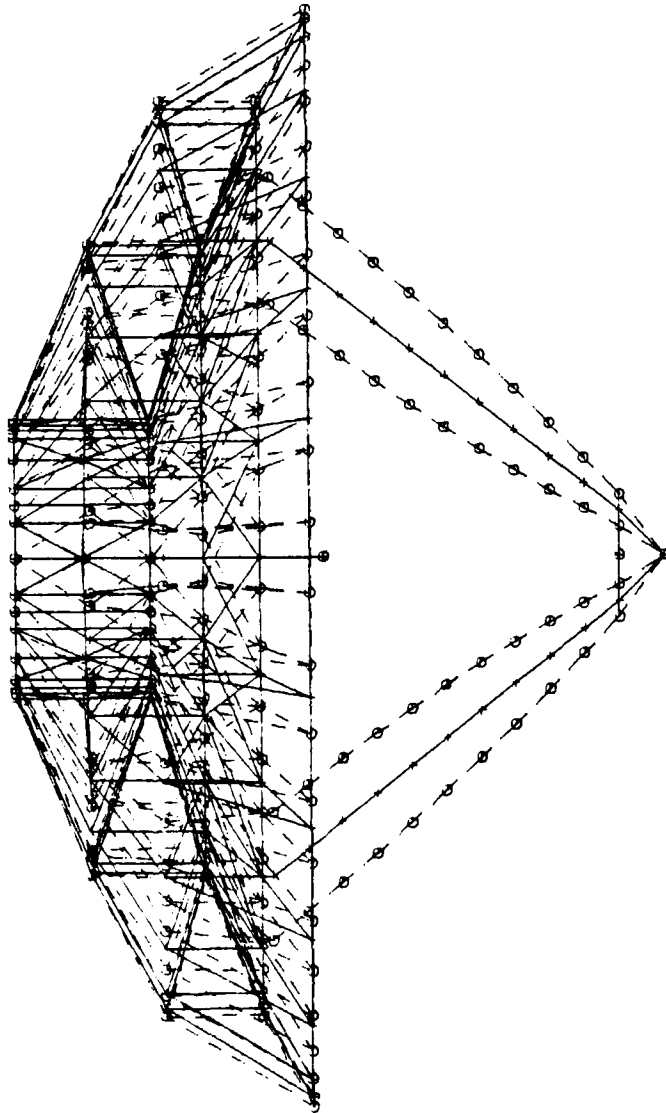
MODE SHAPE NO 1 FREQ=7.799HZ.
DISPLACEMENT CASE 1



STAROYNE FINITE ELEMENT MODEL PROJECTION ON X2-X3 PLANE CASE NO. 1

Figure C.b. Dynamic mode shape, side view.

MODE SHAPE NO 1 FREQ=7.799HZ.
DISPLACEMENT CASE 1



STARBYNE FINITE ELEMENT MODEL PROJECTION ON X3-X1 PLANE CASE NO. 1
C.c.

Figure C.c. Dynamic Mode Shape, Plan View.

END

FILMED

8-85

DTIC